AD-A171 489 FERROIC SHAPE MEMORY MATERIALS & PIEZO:PYRO-ELECTRIC ORIENTED RECRYSTALLI..(U) PENNSYLVANIA STATE UNIV UNIVERSITY PARK MATERIALS RESEARCH LA.. 1/2

UNCLASSIFIED R E NEWNHAM ET AL. JUL 86 ARO-18953.15-PH F/G 11/2 NL

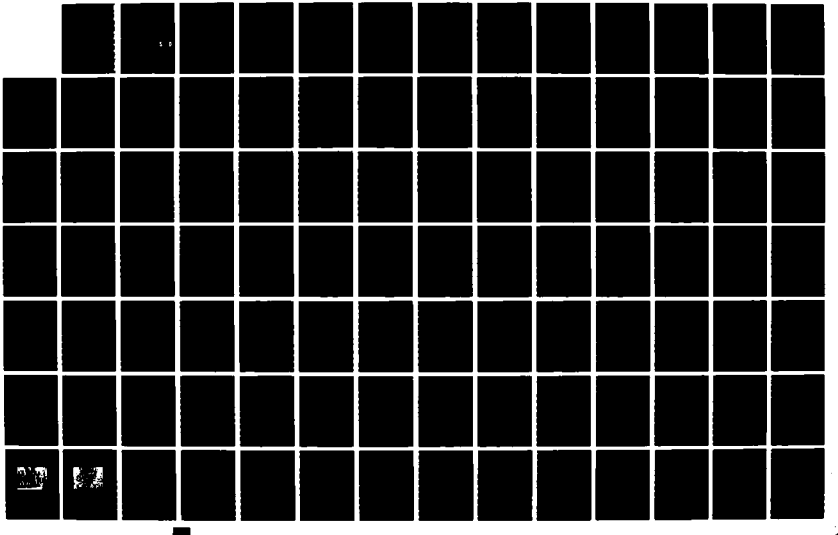

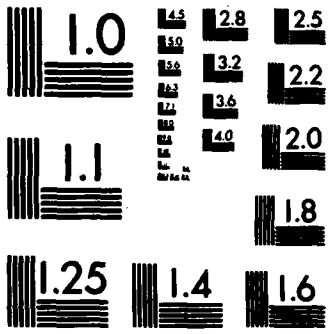

MICROCOPY RESOLUTION TEST CHART
NATIONAL BUREAU OF STANDARDS-1963-A

- FOR REPRODUCTION PURPOSES

(2)

SECUR **AD-A171 409** tered)

1. RE ARO 18953.15-PH	GOVT ACCESSION NO. N/A
	READ INSTRUCTIONS BEFORE COMPLETING FORM
	3. RECIPIENT'S CATALOG NUMBER N/A
4. TITLE (and Subtitle) Ferroic Shape Memory Materials & Piezo:Pyro-Electric Oriented Recrystallized Glasses	5. TYPE OF REPORT & PERIOD COVERED 1 Apr 83 - 31 Mar 86 Final Report
	6. PERFORMING ORG. REPORT NUMBER
7. AUTHOR(s) R. E. Newnham, A. S. Bhalla and A. Halliyal	8. CONTRACT OR GRANT NUMBER(s) DAAG29-83-K-0062
9. PERFORMING ORGANIZATION NAME AND ADDRESS Pennsylvania State University University Park, PA	10. PROGRAM ELEMENT, PROJECT, TASK AREA & WORK UNIT NUMBERS
11. CONTROLLING OFFICE NAME AND ADDRESS U. S. Army Research Office Post Office Box 12211 Research Triangle Park, NC 27709	12. REPORT DATE July 1986 13. NUMBER OF PAGES 6 +
14. MONITORING AGENCY NAME & ADDRESS(if different from Controlling Office)	15. SECURITY CLASS. (of this report) Unclassified 15a. DECLASSIFICATION/DOWNGRADING SCHEDULE

16. DISTRIBUTION STATEMENT (of this Report)

Approved for public release; distribution unlimited.

DTIC ELECTE AUG 2 8 1986 S D

17. DISTRIBUTION STATEMENT (of the abstract entered in Block 20, if different from Report)

NA

18. SUPPLEMENTARY NOTES

The view, opinions, and/or findings contained in this report are those of the author(s) and should not be construed as an official Department of the Army position, policy, or decision, unless so designated by other documentation.

19. KEY WORDS (Continue on reverse side if necessary and identify by block number)

Electroceramic Materials
Polar Glass-Ceramics
Piezoelectric Properties
Pyroelectric Properties
Hydrophones
Memory Materials
Pyroelectric Detectors

20. ABSTRACT (Continue on reverse side if necessary and identify by block number)

This final report summarizes the work on "Ferroic Shape Memory Materials, and Piezo:Pyro Electric Oriented Recrystallized Glasses". In this program a new family of electroceramic materials--grain oriented "polar Glass-ceramics" were developed. An extensive study of piezoelectric and pyroelectric propetties of a number of polar glass-ceramics was carried out. From the work carried out in this contract period, several polar glass-cermaic compositions useful for pyroelectric detectors and hydrophones have been identified.

DTIC FILE COPY

DD FORM 1 JAN 73 1473 EDITION OF 1 NOV 65 IS OBSOLETE

UNCLASSIFIED

ARO 18953.15-PH

FERROIC SHAPE MEMORY MATERIALS & PIEZO:PYRO-ELECTRIC ORIENTED RECRYSTALLIZED GLASSES

FINAL TECHNICAL REPORT

April 1, 1983 to March 31, 1986

Contract Grant Number DAAG29-83-K-0062

by

R.E. Newnham, A.S. Bhalla and A. Halliyal

Materials Research Laboratory
The Pennsylvania State University
University Park, Pennsylvania 16802

(814)865-1612

MATERIALS RESEARCH LABORATORY
THE PENNSYLVANIA STATE UNIVERSITY
UNIVERSITY PARK, PENNSYLVANIA 16802

FINAL REPORT

FIFTY COPIES REQUIRED

1. ARO PROPOSAL NUMBER: 18953-PH

3. PERIOD COVERED BY REPORT: April 1, 1983 to March 31, 1986 Final Report

3. TITLE OF PROPOSAL: FERROIC SHAPE MEMORY MATERIALS & PIEZO:PYRO-ELECTRIC ORIENTED RECRYSTALLIZED GLASSES

4. CONTRACT OR GRANT NUMBER: DAAG29-83-K-0062/DAAG46-84-K-0002

5. NAME OF INSTITUTION: The Pennsylvania State University

6. AUTHORS OF REPORT: R.E. Newnham, A. Halliyal, A.S. Bhalla, E. Ylo, S.A. Markgraf, M. Wheeler, L.E. Cross

7. LIST OF MANUSCRIPTS SUBMITTED OR PUBLISHED UNDER ARO SPONSORSHIP DURING THIS REPORTING PERIOD, INCLUDING JOURNAL REFERENCES:

New Glass-Ceramics for Piezoelectric and Pyroelectric devices. A. Hallilyal, A.S. Bhalla, R.E. Newnham and L.E. Cross. (To be published in P. McMillan Memorial Book on Glass-Ceramics, Edited by H. Lewis).

New Glass Ceramics for Pyroelectric Devices. A. Halliyal, A.S. Bhalla, L.E. Cross and R.E. Newnham. (Submitted to J. Am. Cer. Soc.)

Unusual Pyroelectric and Piezoelectric Properties of Fresnoite ($Ba_2TiSi_2O_8$) Single Crystal and Polar Glass-Ceramics. A. Halliyal, A.S. Bhalla, S.A. Markgraf, L.E. Cross and R.E. Newnham. Ferroelectrics 62, 27 (1985).

X-Ray Structure Refinement and Pyroelectric Investigation of Fresnoite, $Ba_2TiSi_2O_8$. S.A. Markgraf, A. Halliyal, A.S. Bhalla, R.E. Newnham and C.T. Prewitt. Ferroelectrics 62, 17 (1985).

Dielectric, Piezoelectric and Pyroelectric Properties of $Sr_2TiSi_2O_8$ A. Halliyal, A.S. Bhalla, L.E. Cross, R.E. Newnham. J. of Mat. Sci. 20, 3745-3749 (1985).

Phase Transitions, Dielectric, Piezoelectric and Pyroelectric Properties of Barium Titanium Germanate $Ba_2TiGe_2O_8$ Single Crystals. A. Halliyal, A.S. Bhalla and L.E. Cross. Ferroelectrics, 62, 3 (1985).

Piezoelectric Properties and Mircrostructure of Glass-Ceramics in the $BaO-SrO-SiO_2-TiO_2$ System. E.E. Ylo III, M. Wheeler, Halliyal, A.S. Bhalla and R.E. Newnham. (To be published in IEEE Proc. of International Symposium on Applications of Ferroelectrics, Bethlehem, 1986).

SCIENTIFIC PERSONNEL SUPPORTED BY THIS PROJECT AND DEGREES AWARDED DURING THIS REPORTING PERIOD:

R.E. Newnham, L.E. Cross, A.S. Bhalla, A. Halliyal, E.E. Ylo III, S.A. Markgraf, M. Wheeler.

BRIEF OUTLINE OF RESEARCH FINDINGS

This final report summarizes the work on "Ferroic Shape Memory Materials, and Piezo:Pyro Electric Oriented Recrystallized Glasses" carried out at the Materials Research Laboratory of The Pennsylvania State University under ARO Contract No. DAAG46-84-K-0002.

In this program a new family of electroceramic materials--grain oriented "polar glass-ceramics" were developed. An extensive study of piezoelectric and pyroelectric properties of a number of polar glass-ceramics was carried out. From the work carried out in this contract period, several polar glass-ceramic compositions useful for pyroelectric detectors and hydrophones have been identified. This report includes the papers published or submitted for publication in 1985 and 1986 (Appendices 1 to 7) and a copy of the Ph.D. thesis entitled "Study of the Piezoelectric and Pyroelectric Properties of Polar Glass-Ceramics". A brief description of the work done is given in this introductory section.

The preparation and properties of polar glass-ceramics were investigated in this work. Polar glass-ceramics consist of well-oriented crystallites of a polar but nonferroelectric crystalline phase. From the work carried out in this program it is clear that glass-ceramics offer several advantages for use in piezoelectric and pyroelectric devices. In this work, glasses were prepared from Li_2O-SiO_2-B_2O_3, BaO-GeO_2-TiO_2, BaO-SiO_2-TiO_2 and SrO-SiO_2-TiO_2 systems and were recrystallized to obtain polar glass-ceramics with crystallites of $Li_2Si_2O_5$, Li_2SiO_3, $Li_2B_4O_7$, $Ba_2TiGe_2O_8$, $Ba_2TiSi_2O_8$ or $Sr_2TiSi_2O_8$

oriented along their polar c-axes. The oriented region of the crystallites was 200-500 μm from the surface of glass-ceramics. Dielectric, piezoelectric and pyroelectric properties of glass-ceramics are in close agreement with the respective single crystal properties. Glass-ceramics in the fresnoite family are excellent candidate materials for hydrophones. Magnitudes of hydrostatic piezoelectric coefficient d_h ($\sim 100 \times 10^{-3}$ Vm/n) and dielectric constant (~10) of fresnoite glass-ceramics are comparable to the corresponding values of polyvinylidene fluoride. The electro-mechanical coupling coefficients k_p and k_t were in the range 15 to 20% (Appendix 1).

The polar growth behavior of cyrstallites from glass matrix depends on the original composition of glass. This property can be exploited to tailor the piezoelectric and pyroelectric properties of polar glass-ceramics. A connectivity model, based on the principles of series and parallel connectivity models has been described to predict the piezoelectric and pyroelectric properties of polar glass-ceramics (Appendix 1).

Pyroelectric properties of a number of polar glass ceramics were studied. The dielectric and pyroelectric properties of several compositions in the systems Li_2O-SiO_2-B_2O_3, BaO-SiO_2-TiO_2, and SrO-SiO_2-TiO_2 were investigated. The pyroelectric figures of merit of polar glass-ceramics are approximately 40 to 60% of those of $LiTaO_3$, and look very promising for pyroelectric devices (Appendix 2).

Since the piezoelectric and pyroelectric properties of glass-ceramics in the fresnoite family were promising, a detailed study of properties of $Ba_2TiSi_2O_8$ and $Ba_2TiGe_2O_8$ single crystals was carried out. Single crystal x-ray work was done to refine the crystal structure

parameters of $Ba_2TiSi_2O_8$ to investigate the origin of unusual properties of $Ba_2TiSi_2O_8$.

The dielectric, piezoelectric and pyroelectric properties of fresnoite ($Ba_2TiSi_2O_8$) single crystal and polar glass-ceramics were studied in the temperature range -150 to 200°C. The sign of pyroelectric coefficient is positive at room temperature and becomes negative at 190°C. The dielectric constant, pyroelectric coefficient and planar coupling coefficient show a maximum value at 160°C and the frequency constant shows a minimum at the same temperature. The probable reasons for the anomaly in these properties were investigated (Appendix 3).

Crystal structure parameters were refined from single crystal x-ray intensity data collected on $Ba_2TiSi_2O_8$ at 24 and 300°C. Anisotropic refinements in space group P4*bm* yielded residuals of 0.035 and 0.042 at 24 and 300°C, respectively. Pyroelectric measurements give a room temperature pyroelectric coefficient of +10 $\mu Cm^{-2} K^{-1}$. A structural mechanism for the pyroelectric effect is proposed in terms of large oxygen displacements. A sign reversal in the pyroelectric coefficient occurs at 160°C, perhaps caused by the cancellation of primary and secondary effects (Appendix 4).

Polar $Sr_2TiSi_2O_8$ glass-ceramics were prepared by recrystallizing glasses in a steep temperature gradient. The dielectric, piezoelectric and pyroelectric properties were studied as a function of temperature in the temperature range -150 to 200°C. The sign of the pyroelectric coefficient is positive at room temperature and is attributed to the dominance of the secondary pyroelectric effect over the primary effect. Anomalies were observed in the dielectric, pyroelectric and piezo-

electric properties and a large hysteresis was observed in all these properties. Probable causes for the anomalies were investigated (Appendix 5).

Measurement of the dielectric permittivity ε_{33}, the pyroelectric coefficient p_3 and the piezoelectric planar coupling k_p and frequency constant N_p in single crystal $Ba_2TiGe_2O_8$ show clear evidence of a heretofore unobserved first order phase change which occurs at -50°C on cooling and near 0°C on heating. The balance of evidence suggests that the transition is to a reorientable but irreversible ferroelectric phase, involving a tilt of the prototypic polar c axis. The inversion of the sign of the pyroelectric effect reported earlier near 135°C was confirmed and is attributed to the changing balance between primary and secondary components in the pyroelectric coefficient (Appendix 6).

Our earlier studies showed that fresnoite ($Ba_2TiSi_2O_8$) glass-ceramics with oriented crystallites are promising candidate materials for pyroelectric detectors and surface acoustic wave devices. A detailed investigation of the properties and microstructure of glass-ceramics in the $Ba_{2-x}Sr_xTiSi_2O_8$ solid solution was carried out. Glasses of several compositions were prepared and recrystallized through a heating schedule to produce an oriented region of crystallites perpendicular to the surface, 100-500 μm in depth. Their dielectric and piezoelectric properties were studied (Appencix 7).

APPENDIX 1

New Glass-Ceramics for Piezoelectric and Pyroelectric Devices

A. Halliyal, A.S. Bhalla, R.E. Newnham and L.E. Cross

(To be published in P. McMillan Memorial Book on Glass-Ceramics,
Edited by H. Lewis)

NEW GLASS-CERAMICS FOR PIEZOELECTRIC AND PYROELECTRIC DEVICES

Arvind Halliyal, Amar S. Bhalla, Robert E. Newnham

and Leslie E. Cross

Materials Research Laboratory

The Pennsylvania State University

University Park, Pennsylvania 16802

TABLE OF CONTENTS

1. Introduction

The advantages of glass-ceramics for preparing large, complex, pore free bodies have been exploited in the electronics industry for a variety of applications. New glass forming techniques which utilize fast quenching techniques have expanded the range of glass forming materials and the number of their applications (McMillan 1979).

Recently, mainly through the work in our laboratory, it has been realized that glasses with suitably selected composition can be recrystallized into a polar glass-ceramic form, which can then be used as a thermal or a pressure sensing element (Gardopee et al. 1980, 1981). In these glass-ceramics the crystalline phase is polar and the crystallites are aligned in a polar parallel array. The macroscopic polarity thus developed gives rise to both pyroelectric and piezoelectric activity with characteristics markedly different from those which are realized in poled ferroelectric ceramics. Extensive investigations have been carried out to evaluate the properties of these glass-ceramics for pyroelectric and piezoelectric devices (Halliyal et al. 1984a, 1984b) and they seem to be promising candidate materials for such devices as pyroelectric detectors (Halliyal et al. 1986) hydrophones and surface acoustic wave devices (Lee et al. 1984). In this article, the work done in the last decade on polar glass-ceramics is reviewed. Merits and demerits of ferroelectric and non-ferroelectric materials are briefly discussed in the next section. The earlier work done on ferroelectric glass-ceramics is also described. The advantages of preparing polar materials by

glass-ceramic route are described and guidelines for selection of glass compositions are presented. Later sections describe the preparation conditions, some useful glass compositions, heat treatment methods and microstructure. The dielectric and pyroelectric properties are described in sections 7 and 8. The piezoelectric properties of glass-ceramics and their evaluation for hydrophones are given in section 10. A connectivity model to predict and tailor the properties of polar glass-ceramics is discussed in section 11.

2. Ferroelectric and Non Ferroelectric Materials

A large number of ferroelectric single crystals and ceramics are available at present for use in piezoelectric and pyroelectric devices (Herbert 1982). In polycrystalline form, the polar axes in individual crystallites are normally oriented at random. An essential feature of ferroelectric ceramics which makes them usable for piezoelectric and pyroelectric applications is the ability to reorient the polar axes in individual crystallites under a strong electric field so as to impart long-range remnant polar order (the process called poling). In polar but non-ferroelectric ceramics this orientability is not possible, so that randomly axed ceramics of these materials do not exhibit piezo-electric or pyroelectric properties. In non-ferroelectric single crystals also, if there are polar twins, it is not possible to switch the twins to a single domain pattern and they cannot be used in devices. Quartz is used extensively in frequency control devices. A number of non-ferroelectric but polar single crystals

($Li_2B_4O_7$ (Shorrochs et al. 1981), $Ba_2TiGe_2O_8$ (Kimura et al. 1973), $Ba_2TiSi_2O_8$ (Ito et al. 1981, Yamauchi 1978, Kimura 1977)) show excellent piezoelectric properties and look promising for surface acoustic wave (SAW) devices.

Although electrical polability makes the ferroelectric materials usable in ceramic form, it also carries several disadvantages. Since there is by definition a family of equivalent orientations in each crystallite, the material can also depole, either spontaneously with time, giving rise to the well-known aging phenomenon or under high electrical or mechanical drive fields leading to instability in response and drift in sample dimensions. Engineers must necessarily put up with these inconveniences for the advantages of low expense, simple formability and large size which are available in conventional ceramics.

The present work on polar glass-ceramics was started with the intention of exploring the possibilities of preparing non-ferroelectric ceramics with polar properties. The glass-ceramic route provided an interesting possibility of developing polar order in a ceramic, as discussed in the next section.

2.1 Ferroelectric Glass-Ceramics

In the last two decades research workers at Corning, Bell Telephone Laboratory and in Japan have investigated a number of ferroelectric glass-ceramic systems in which ferroelectric crystallline phases were $BaTiO_3$, $LiTaO_3$, $NaNbO_3$, $Pb_5Ge_3O_{11}$, $PbTiO_3$, etc. (Herczog 1964, 1973; Borrelli 1967; Borrelli and

Layton 1969, 1971; Layton and Herczog 1969; Layton and Smith 1975; Glass et al. 1977(a), 1977(b); Takashige et al. 1981). The main emphasis in this work was on the study of dielectric and electro-optic properties as a function of composition, heat treatment and grain size. By controlling the crystallite size to values below 0.2 μm transparent ferroelectric glass-ceramics have been prepared which show a large electro-optic effect. Weak pyroelectric responses have been measured in glass-ceramics containing either $LiTaO_3$, $LiNbO_3$ (Glass et al. 1977a) or $NaNbO_3$ crystalline phases. Takahashi and co-workers (Takahashi et al. 1975, 1979) demonstrated a simple method of preparing $Pb_5Ge_3O_{11}$ single crystals from a glass of similar composition. They first prepared a glass of composition $Pb_5Ge_{3-x}Si_xO_{11-}(0 \leq x \leq 1.5)$ by melting. A few pieces of glass were then remelted and annealed to obtain thin plate-like crystals with the polar c-axis oriented perpendicular to the surface. They showed that the pyroelectric figure of merit of these monocrystals was comparable to $LiTaO_3$. It should be noted, however, that the material obtained after recrystallization was more like a single crystal than a glass-ceramic.

Apart from the papers referenced above there have been very few studies of the dielectric and electro-optic properties, and no detailed work seems to have been done on the piezoelectric and pyroelectric properties of ferroelectric glass-ceramics. One of the reasons for this is the difficulty in electrical poling of glass-ceramics. Very few ferroelectric materials are good glass formers. This necessitates the incorporation of a large percentage of a network former in the composition for glass formation.

After recrystallization, if there is a glassy phase of low dielectric constant between the crystallites, electrical poling is generally very difficult. For this reason, it is often much simpler to prepare ferroelectric ceramic materials by powder processing and sintering methods.

2.2 Polar But Nonferroelectric Glass-Ceramics

In nonferroelectric ceramics the domain configuration cannot be changed by externally applied electric field. The polar order must be built in during the processing stage. Gardopee and co-workers (Gardopee et al. 1980, 1981) demonstrated the possibility of preparing a polar but nonferroelectric material through the glass-ceramic route. This was achieved by crystallizing a glass in such a manner that the crystallites had both crystallographic and polar orientation. The system chosen was $Li_2O.2SiO_2$ and the polar phase obtained after the recrystallization was $Li_2Si_2O_5$ (orthorhombic point group mm2). It had previously been shown by Rindone (Rindone 1962a, 1962b) that in lithium silicate glasses $Li_2Si_2O_5$ crystals grow with a high degree of orientation with respect to the surface of glass. Needle like crystals forming a thin layer near the surface have their c-axes perpendicular to the sample surface. X-ray diffractometer patterns taken on surfaces of recrystallized samples, confirmed a high degree of preferred orientation. If all or most of the $Li_2Si_2O_5$ crystallites in the glass-ceramic show similar polar orientation, it is obvious that we obtain a glass-ceramic which will exhibit the polar properties of single crystals. It was demonstrated by Gardopee (Gardopee et

al. 1981) that the degree of orientation of crystallites can be improved remarkably if well-polished glass samples are crystallized in a large temperature gradient. These grain-oriented glass-ceramics showed substantial pyroelectric responses, thus confirming the polar orientation of the crystallites. The piezoelectric properties of these glass-ceramics were, however, very weak. We call such a glass-ceramic with pyroelectric properties, a polar glass-ceramic. A schematic which defines a route to obtain polar glass-ceramics is shown in Fig. 1. It is clear that the above procedure provides an interesting and novel technique to prepare grain oriented polar but nonferroelectric glass-ceramics. In this technique, the poling problems encountered in ferroelectric glass-ceramics are avoided. In addition the problem of depoling and aging do not arise because polar glass-ceramics are nonferroelectric and since they do not have a Curie temperature, they can be used at high temperature also. All the glass-ceramics described in this paper are polar but not ferroelectric.

2.3 Tensor Properties of Grain-Oriented Polar Glass-Ceramics

The domains in an unpoled ferroelectric ceramic are randomly oriented with polarization vectors pointing in all directions as shown schematically in Fig. 2, where all the grains are assumed to be single domain grains for simplicity. Application of a voltage across the ceramic causes most of the domains to line up with their polarization vectors more nearly parallel to the field (Fig. 1b). The grain structure of grain-oriented glass-ceramic is

similar to that of a poled ceramic (Fig. 1c). Thus a poled ferroelectric ceramic and grain-oriented polar glass-ceramic belong to the same conical point group, ∞m. For piezoelectric, dielectric, and elastic phenomena, this is equivalent to hexagonal symmetry 6mm. For this symmetry there are five independent elastic coefficients, (s_{11}, s_{12}, s_{13}, s_{33}, s_{44}); three independent piezoelectric constants (d_{33}, d_{31}, d_{15}); two independent dielectric constants (K_{11}, K_{33}) and one pyroelectric coefficient (p_3) (Nye 1957). By convention, the X_3 direction is chosen to be the polar axis, normal to the surface of the recrystallized polar glass-ceramic. Additional nonzero coefficients are related to these by symmetry. In order to evaluate the usefulness of polar glass-ceramics in devices, it is necessary to measure the above properties and compare them with other commonly used materials.

3. Selection of Glass Compositions

Several factors had to be considered before making a proper choice of the systems for the present study. The system chosen should satisfy the following criteria.

(1) The crystalline phase must belong to one of the polar point groups.

(2) It should form a glass easily.

(3) The crystallites in the glass-ceramic should show both crystallographic and polar orientation after processing.

(4) The glass-ceramic should have good mechanical strength.

Each of these four criteria are discussed in detail in the following sections.

3.1 Polar Systems

Of the 32 crystallographic point groups, only 20 show piezoelectric properties and 10 of these 20 piezoelectric classes are pyroelectric (or polar). The ten polar point groups are 1, 2, 3, 4, 6, m, mm2, 3m, 4mm, and 6mm (Nye 1957). For the present study only crystalline phases belonging to one of the above polar point groups are considered so that both pyroelectric and piezoelectric properties could be studied.

3.2 Glass Formation

For ease in processing, only compositions which form glasses readily by air quenching were considered. This places a major restriction on the number of systems that can be studied since the glass composition must then contain at least one glass former such as SiO_2, GeO_2, B_2O_3, or P_2O_5. If new fast-quenching methods like splat cooling or twin roller quenching are used for preparation of glasses, the number of polar systems that can be studied will be much larger.

3.3 Crystallographic and Polar Orientation

All the systems examined in the present work were non-ferroelectric. To achieve glass-ceramics with polar properties, the crystallization must be carried out in such a way that the individual crystallites possess both crystallographic and polar orientation. This requirement limits the number of systems that can be studied since many of the polar systems might form glasses

easily but they may not yield glass-ceramics with crystallographic and polar orientation.

To satisfy this criterion a logical approach would be to select polar glass-forming systems which are known to re-crystallize along a preferred direction. Even if a glass crystallizes along a preferred direction, but fails to show any polar orientation, it will not exhibit either pyroelectric or piezoelectric properties. Since information concerning the crystallographic or polar orientation of polar glass forming systems is lacking, a number of systems were tested in order to select a few which satisfy this requirement. If the crystal structure is highly anisotropic with molecular chains of layers, there is a strong possibility that the crystallites may grow along a preferred direction. But it is difficult to predict apriori whether the crystallites will show polar orientation or not. Polarity must be determined by experiment.

3.4 Physical Properties of Recrystallized Glass-Ceramics

Once the chosen polar system satisfies the criteria for glass formation together with crystallographic and polar orientation, the last but equally important criterion is the recrystallization behavior of the system. If the glass-ceramic shows both crystallographic and polar orientation, but the individual crystallites are not bonded together by the glass matrix as in the case of $Li_2Si_2O_5$ (Gardopee et al. 1981) again the system is not of much use for practical devices. This is particularly true in the present study since the objective of the work was to prepare large

area glass-ceramics with uniform properties. The glass-ceramics should have reasonably good mechanical strength to prepare samples for measurement.

3.5 Selection of Polar Glass Forming Systems

Polar glass forming systems that were tested during the course of the present work are listed in Table 1. The systems that were examined fall into four groups. The systems in group A did not form glass when stoichiometric compositions were melted. Group B systems formed glasses, but the recrystallized glass-ceramics lacked good mechanical strength. Glasses of group C were hygroscopic. Systems of group D formed good glasses, but the recrystallized glass-ceramics did not show crystallographic or polar orientation.

Hence the first task was to prepare optimized glass compositions which formed glasses easily and recrystallized uniformly with maximum crystallographic and polar orientation. Among the systems listed in Table 1, the systems that partially satisfied the criteria are $Ba_2TiSi_2O_8$, $Ba_2TiGe_2O_8$, $Li_2Si_2O_5$, Li_2SiO_3, and $Li_2B_4O_7$. However, acceptable glass-ceramics were not obtained from glasses of stoichiometric compositions in any of these systems. Hence a wide range in compositions was investigated for each system to arrive at compositions which satisfied all four requirements. Further, various modifying oxides such as PbO, CaO, ZnO and SrO were added to optimize both the electrical and mechanical properties.

Data concerning crystal structure, melting point, point group symmetry and polar axes of the above materials are given in Table 2.

4. Preparation of Glass-Ceramics

4.1 Glass Melting

Reagent grade chemicals (silicic acid $SiO_2.nH_2O$, GeO_2, Li_2CO_3, $BaCO_3$, $CaCO_3$, TiO_2, H_3BO_3, PbO) were weighed and mixed by ball milling in alcohol for 8 to 10 hours and then dried. Glass batches of approximately 50 gms were melted in a platinum crucible in an open atmosphere using an electric globar furnace. Melting temperatures for different compositions were in the range 1200 to 1450°C. The melt was retained in the furnace for 4 to 8 hours for fining and homogenization.

The fined glass melt was air quenched by pouring it into graphite molds to form cylinders of approximately 0.8 to 1 cm in diameter and 1 to 1.5 cm in length. The cylinders were cooled to room temperature and examined for cracking, devitrification and other defects using the optical microscope. If the glass samples contained small air bubbles, the batch was remelted and further fining was carried out to remove the bubbles from the melt. Thermal stresses were partially relieved by annealing the glasses for 12 hours well below the nucleation temperature to avoid bulk nucleation in glasses. (Li_2O-SiO_2-B_2O_3 glasses were annealed at 400°C and BaO-TiO_2-GeO_2 and BaO-TiO_2-SiO_2 glasses were annealed at 500°C and 600°C respectively).

For crystallization studies, glass samples were prepared by grinding and polishing one surface of the glass cylinders. The samples were ground using an abrasive diamond wheel, followed by polishing with 400 and 600 grit silicon carbide powder, and later with 12 and 3 μm alumina powder. The final polishing was done using 1 μm diamond polishing paste. The polished samples for crystallization studies were disks approximately 1 cm in diameter and 1 cm in length.

4.2 Crystallization of Glasses

Differential thermal analysis (DTA) runs were made with glass powders to determine the crystallization temperature.

Two types of crystallization treatments were used in the present study. Heat treatments in which the entire sample was uniformly heated to the crystallization temperature are termed "isothermal crystallization." Heat treatments in which the glass samples were recrystallized in a temperature gradient are called "temperature gradient crystallization." To obtain polar glass-ceramics with well orientated crystallites and good mechanical strength, many different heat treatment cycles were carried out. The effect of nucleation on oriented growth of crystallites was studied by crystallizing glasses after heating through a nucleation step.

Recrystallization in a temperature gradient was carried out by positioning the polished glass samples on a microcope hot stage. The direction of crystallization was parallel to the direction of temperature gradient. The crystalline phases in the glass-

ceramics were identified by powder x-ray diffraction (XRD) patterns. The degree of preferred orientation of crystallites in the glass-ceramic was evaluated from XRD patterns recorded on surfaces normal to the direction of temperature gradient. The surface XRD patterns were compared with powder diffraction patterns obtained from randomly oriented crystallites to determine the relative degree of orientation.

5. Compositions of Glasses

The systems selected for detailed study were $Ba_2TiSi_2O_8$, $Ba_2TiGe_2O_8$, $Si_2TiSi_2O_8$, $Li_2Si_2O_5$ and $Li_2B_4O_7$. A wide range in composition and additives were tested for each system to obtain glass-ceramics with optimized properties. A list of compositions tested is given in Table 3. The glass formation characteristics, mechanical strength, and approximate pyroelectric coefficients are also listed in the table. Out of several compositions tested, only those which yielded polar glass-ceramics with desired quality and substantial pyroelectric activity were selected for carrying out detailed study.

In the fresnoite system, for example, the melting point of stoichiometric composition is very high (>1450°C) and hence it was not easy to prepare glass of stoichiometric composition. In addition the recrystallization of the glasses was not uniform and the mechanical strength was poor. To overcome these problems, different ratios of BaO, SiO_2 and TiO_2 were tested to improve the crystallization. The composition which gave reasonably good glass-ceramics was $2BaO-3SiO_2-TiO_2$. However, for this compoisiton

also, it was necessary to further improve the physical properties. Several different substituents were tried for BaO and TiO_2 to improve the properties (Table 3). Addition of a small amount of PbO, CaO or SrO helped in obtaining glass-ceramics with good physical properties. With most of the other substituents, there was no problem with glass formation but there was no improvement in crystallization behavior. Additions of Al_2O_3, K_2O or MnO_2 helped in obtaining well-crystallized glass-ceramics, but the measured d_{33} coefficient was zero for these glass ceramics, indicating very poor polar orientation of the crystallites.

Similar studies were carried out for other compositions listed in Table 3. Optimized compositions are listed in Table 4. The crystallization temperatures as determined by DTA runs and the crystalline phases identified from powder XRD patterns are also presented in the table.

6. Heat treatment and Microstructure

The ideal microstructure of polar glass-ceramics would consist of well-oriented crystallites extending between both sides of the glass-ceramic. Different heat treatment schedules were tried to achieve this goal.

Generally nucleation and crystallization begins first at the surface of glasses because of the imperfect nature of the surface structure (McMillan 1979). The bulk nucleation process does not begin until later. The ideal way to obtain polar glass-ceramics with oriented crystallites would be to start nucleation on the surface of the glass and allow the crystallites to grow into the

bulk of the sample, thereby avoiding as far as possible bulk nucleation and the growth of spherulites.

It is clear that the following factors should be considered in order to obtain glass-ceramics with oriented crystallites.

(1) The glasses should not contain nucleating agents which stimulate bulk nucleation.

(2) The surface finish of glasses should be as flat as possible.

(3) The heat treatment process should be such that the crystallization takes place primarily by surface nucleation since this promotes oriented growth.

(4) Bulk nucleation and crystallization produces randomly oriented spherulites and should be avoided; this may be possible if the bulk nucleation step is completely avoided.

It is obvious that if the glass is heat treated under isothermal conditions, both surface and bulk crystallization can start simultaneously and hence the oriented growth of crystallites will stop when crystallites growing from the surface encounter randomly growing crystallites in the bulk of the sample.

It has been shown by several workers that directional crystallization is possible in amorphous materials if the crystallization is carried out in a temperature gradient. Gardopee (Gardopee et. al 1980, 1981) crystallized Li_2O-$2SiO_2$ glasses in both isothermal and temperature gradient environments and showed that temperature gradient crystallization produces glass-ceramics in which the oriented region of crystallites is larger. Thermal gradient

crystallization technique has been used to produce oriented crystallites of $CdGeAs_2$ (Sekhar and Risbud 1981, Risbud 1979), and Na_2SiO_3 (Melling and Duncan 1980).

XRD patterns were taken on as crystallized surfaces of glass-ceramics listed in Table 4. The ratio of I_{002}/I_{211} (for fresnoite glass-ceramics) or I_{002}/I_{040} (for lithium silicate and lithium borosilicate glass-cseramics) was taken as a measure of the preferred degree of orientation of crystallites. The ratio was greater than 100 for all glass-ceramics indicating highly oriented growth of crystallites. In all cases the polar c axis of the crystallites was perpendicular to the initial crystallizing surface.

Glass samples were crystallized in both isothermal and temperature gradient environments and x-ray and microstructure studies were carried out to assess the degree of preferred orientation of crystallites carried out as a function of depth from the initial crystallizing surface.

The glass composition selected for detailed study was Li_2O-$2SiO_2$-0.2ZnO, for which the nucleation and crystallization temperatures were 480° and 600°C, respectively. The isothermal heating cycles used are shown in Fig. 3. Heating cycles A, B and C did not include any nucleation step whereas heating cycle D included a nucleation step. The only difference between heating cycles A, B and C is the different upper crystallization temperature. In cycle E, the sample was heated slowly at a uniform rate up to the upper crystallization temperature. Glasses were crystallized by following one of the heating cycles similar

to those shown in Fig. 3. The ratio of I_{002}/I_{040} was determined as a function of depth and plotted for different heat treatment cycles (Fig. 4). Several obsservations were made from this study.

(1) The degree of orientation of crystallites was high ($I_{002}/I_{040} > 100$) up to a depth of about 50 μm for both temperature gradient and isothermal crystallization, for all heating cycles.

(2) In the case of heating cycles in which there was enough time for nucleation (cycles D, E) the orientation of crystallites decreases very fast with depth from the initial crystallizing surface. Typically, the orientation becomes completely random at a depth of about 200 μm. The orientation of crystallites is worse for the isothermally crystallized samples. The reason for this is clear from the discussion given in the previous section. The nucleation step tends to promote bulk crystallization in the case of isothermally crystallized samples. The bulk crystallization is spherulitic and thus there is no preferred orientation of crystallites. The oriented surface crystallization will continue until the crystallites encounter spherulites at which point further growth of oriented crystallites stops.

(3) In the case of heating cycles (both isothermal and temperature gradient) in which there was not enough time for nucleation (cycles A, B, C), the orientation of crystallites was reasonably good even at a depth of 300 μm.

For the present study, all the glass-ceramics were prepared in a temperature gradient.

The microstructures of glass-ceramics of selected compositions were examined using optical and electron microscopes. Typically the microstructure consisted of needle-like crystallites growing from the initial crystallizing surface into the bulk of the samples.

A vertical cross-sectional view (parallel to the temperature gradient) of Li_2O-$2SiO_2$-0.2ZnO glass-ceramic is shown in Fig. 5(a), in which the oriented growth of $Li_2Si_2O_5$ crystallites from the surface and also spherulites resulting from bulk nucleation and crystallization can be seen. The oriented region extends to a depth varying from 200 to 500 μm. Fig. 5(b) shows a horizontal cross-sectional view of the same sample cut perpendicular to temperature gradient. The diameter of the crystallites is generally in the range 1-3 μm.

7. Dielectric Properties

For dielectric, pyroelectric and piezoelectric measurements, disks of approximately 1 cm diameter and 0.4 to 0.8 mm thick were prepared by sectioning the oriented region of the glass-ceramics near the surface. The length of the crystallites was 200-500 μm extending from surface into the interior of the glass-ceramic. The remainder of the glass-ceramic consisted of randomly oriented crystallites. The samples were lightly polished with 3 μm alumina powder and electroded with sputtered gold films.

Dielectric constant and dissipation factors were measured over a temperature range from 150 to 200°C and at frequencies from 10^2 to 10^7 Hz using a multifrequency LCR meter* and a desk top computer.** The physical and dielectric properties of glass-ceramics are listed in Table 5. Dielectric constants lie in the range 5-15, comparable to the values obtained in the corresponding single crystals. The variation of dielectric constant and dissipation factor with temperature is shown in Fig. 6 for Li_2O-$1.8SiO_2$-$0.2B_2O_3$ glass-ceramics. This is typical of all lithium borosilicate glass-ceramics. The general trend is that both the dielectric constant and losses increase as the temperature is raised, with the temperature dependence becoming less marked at higher frequencies. At lower frequencies the dielectric losses increase with temperature, due to the increasing contribution from ionic mobility. This trend is typical of alkali silicate glass-ceramics (McMillan 1979).

The temperature variation of the dielectric constant of fresnoite glass ($2BaO$-$3SiO_2$-TiO_2), shown in Fig. 7 is featureless in the temperature range -60°C to 220°C. The dielectric constant increases slightly with temperature. In the case of glass-ceramics of the same composition, a broad peak is observed in the dielectric constant curve at around 140°C (Fig. 8a). Both the dielectric constant and losses (Fig. 8b) begin increasing with temperature at about 300°C. The broad peak in the dielectric

---

*Model 4274A and Model 4275A, Hewlett-Packard, Palo Alto, CA.

**Model 9825A, Hewlett-Packard, Palo Alto, CA.

constant at 140°C was observed in all glass-ceramics in which $Ba_2TiSi_2O_8$ was the major phase. The cause of the dielectric maximum at 140°C in fresnoite based glass-ceramics has been discussed previously (Hallilyal et al. 1985a).

8. Pyroelectric Properties

A direct method (Byer and Roundy 1972) was used for measuring pyroelectric coefficients. The measurement was carried out using a desk top computer with instrument control and data transfer provided by a multiprogrammer interface.† The computer controlled the heating or cooling rate through the multiprogrammer and the interface. Pyroelectric current was measured with a pico-ammeter.†† The typical heating or cooling rate was 3-4°/min. Pyroelectric coefficients were calculated in the temperature range -150 to 220°C in both the heating and cooling cycles.

An evaluation of pyroelectric properties and pyroelectric figures of merit of glass-ceramics for different applications is given in this section.

Pyroelectric effect is quite frequently used for the detection of infrared radiation. Even though the detectivities (D*) of pyroelectric materials are two to three orders of magnitude smaller than those of cooled photoconductive detectors, the

---

†Model 59500A, Hewlett-Packard, Palo Alto, CA.

††Model 41140B, Hewlett-Packard, Palo Alto, CA.

advantage of operating at low temperature together with lower cost makes the pyroelectric detectors more versatile. This has led to an extensive use of pyroelectric detectors for military and commercial applications including intruder alarms, forest fire mapping and thermal imaging devices (vidicons) (Porter 1981). Optimum property requirements for a pyroelectric target material have been reviewed in detail by a number of authors (Herbert 1982; Putley 1970; Liu 1976, 1980; Whatmore et al 1980). Properties of both single crystals (such as triglycine sulfate, $LiTaO_3$, $Pb_5Ge_3O_{11}$, $Sr_{0.5}Ba_{0.5}O_6$) and ceramics (such as $PbZr_{0.5}Ti_{0.5}O_3$, modified $PbTiO_3$ and $PbZrO_3$) have been evaluated for pyroelectric devices (Whatmore et al 1980).

It is desirable, when comparing the properties of pyroelectric materials, to define appropriate figures of merit for the particular application of interest. A few of the commonly used figures of merit are listed in Table 6 (Herbert 1982, Whatmore et al. 1980). In general to achieve high detectivity, it is desirable to use a material which has a high pyroelectric coefficient, low dielectric constant, low dissipation factor, low density, low specific heat and low thermal diffusivity.

Currently triglycine sulfate [TGS = $(NH_2CH_2COOH)_3H_2SO_4$] or $LiTaO_3$ single crystals are used in pyroelectric devices. TGS has a high figure of merit but it is water soluble and hygroscopic. The lower Curie temperature of TGS (49°C) is also a disadvantage. The figures of merit of $LiTaO_3$ are lower than TGS but it has advantages of a high Curie temperature and insolubility in water.

The variation of pyroelectric coefficient p, with temperature for a few polar glass-ceramic compositions is shown in Fig. 9 and 10. The following trends in the pyroelectric properties of glass-ceramics are evident.

(1) The room temperature pyroelectric coefficients are in the range 5 to 10 $\mu C/m^2{}^\circ K$.

(2) For lithium borosilicate (Li_2O-B_2O_3-SiO_2), the sign of pyroelectric coefficient at room temperature is negative and remains practically constant up to 100°C. Above 100°C, the pyroelectric current is masked by large thermal currents.

(3) For $Ba_2TiGe_2O_8$ glass-ceramics, the sign of p_3 is negative at room temperature and increases sharply at lower temperatures. The magnitude of p_3 is about 8 $\mu m\ C/m^2{}^\circ K$ at -140°C. There is a change in the sign of p_3 at about 130°C. Above 130°C, p_3 is positive and increases with temperature.

(4) In glass-ceramics containing either $Ba_2TiSi_2O_8$ or $Sr_2TiSi_2O_8$ crystallites, the sign of p_3 is positive at room temperature and its magnitude increases slightly with increasing temperature. The sign of p_3 becomes negative at about 180°C, and its magnitude increases with temperature.

Pyroelectric properties of $Ba_2TiGe_2O_8$ (Halliyal et al. 1985b), $Ba_2TiSi_2O_8$ (Halliyal et al. 1985a) and $Li_2B_4O_7$ (Bhalla et al. 1986) single crystals have been studied extensively. Room temperature pyroelectric properties of these single crystals are

also listed in Table 7. It is difficult to grow defect free $Li_2Si_2O_5$ and $Sr_2TiSi_2O_8$ (Halliyal et al. 1985c) single crystals and there are no reports about the pyroelectric properties of these materials. It is clear that the values of pyroelectric coefficient (p_3) of glass-ceramics are about 80 to 90% of their respective single crystal values.

The characteristic variation of p_3 with temperature and the reversal of its sign in $Ba_2TiGe_2O_8$ (at 130°C) (Halliyal et al. 1985b) and in $Ba_2TiSi_2O_8$ (at 190°C) (Halliyal et al. 1985a) single crystals has been attributed to the changing balance between primary and secondary pyroelectric effects with temperature in these crystals. The positive value of p_3 at room temperature in $Ba_2TiSi_2O_8$ and $Sr_2TiSi_2O_8$ may be due to the dominance of secondary pyroelectric effect. The above argument also applies to glass-ceramics since the pyroelectric properties of glass-ceramics are due to the oriented crystallites of these phases.

The pyroelectric figures of merit of glass-ceramics and single crystals are given in Table 7. The figure of merit M_4 was not calculated because data on thermal diffusivity are not available. A comparison of the figures of merit of glass-ceramics with those of commonly used pyroelectric materials is given below.

The figure of merit M_1 is highest for lithium borosilicate glass-ceramics and is about one-third of $LiTaO_3$. For glass-ceramics in the fresnoite family M_1 is about one-fourth of $LiTaO_3$. The figure of merit M_2 of glass-ceramics is much lower than that of $LiTaO_3$ and other pyroelectric materials, because dielectric constant does not enter in the calculation of M_2. Lithium

borosilicate glass-ceramics have higher M_3 (almost half of $LiTaO_3$) than fresnoite glass-ceramics because of their low density and dielectric constants. In the calculation of M_5, both the dielectric constant and tan δ are considered. Tan δ values are very high for lithium borosilicate glass-ceramics (~0.05) whereas for fresnoite glass-ceramics tan δ values are very small (<0.001). For calculation of M_5, the highest value of tan δ (0.001) was taken for all fresnoite glass-ceramics. M_5 of lithium borosilicate glass-ceramics is very low because of high dielectric losses and those of fresnoite glass-ceramics are about 25% of $LiTaO_3$. Actual values of M_5 of fresnoite glass-ceramics will be slightly higher than the values listed in Table 7, if smaller tan δ values are taken for the calculation.

The pyroelectric figures of merit of most of the glass-ceramics are in the range of 40 to 60% of those of $LiTaO_3$. Further improvement in the figures of merit of glass-ceramics can be achieved either by fine tuning the composition or by improved preparation techniques. Studies in our laboratory have shown that an oriented region up to 500 μm in length near the surface can be achieved even by isothermal recrystallization of glasses. This suggests the possibility of preparing large area targets by heating large glass sheets in a furnace. This technique can be applied only to materials which form glass easily. This, however, limits the choice of materials to silicates, germanates and borates if conventional glass melting techniques are followed. If alternative techniques for glass formation (e.g., sputtered glassy

films, roller quenching, sol-gel method) are used, it may be possible to synthesize additional polar glass-ceramics.

9. Piezoelectric Properties

An evaluation of piezoelectric and electromechanical properties of polar glass-ceramics is given in this section, along with the temperature variation of the electromechanical properties of piezoelectric coefficients. Hydrostatic piezoelectric coefficients of glass-ceramics in the fresnoite family are presented and an evaluation of glass-ceramics for hydrophone applications is made by comparing their properties with those of lead zirconate titanate (PZT) and polyvinylidene fluoride (PVF_2).

Piezoelectric constant d_{33} parallel to the crystallization direction was measured using a Berlincourt d_{33} meter*. Resonance behavior in the thickness mode and planar mode were investigated using a spectrum analyzer.† The resonance frequency constants, electromechanical coupling factors and mechanical quality factor Q were determined by measuring the resonance and anti resonance frequencies. From these values, some of the elastic and piezoelectric coefficients were calculated. The temperature coefficient of resonance (TCR) was evaluated by measuring the resonance frequency as a function of temperature.

---

*Model CPDT 3300, Channel Products, Chesterland, OH.

†Model 3585A, Hewlett-Packard, Inc., Loveland, CO.

9.1 Electromechanical Properties

The electromechanical properties of glass-ceramics resonating in the radial and thickness modes, the piezoelectric coefficients d_{33} (measured by d_{33}-meter) and d_{31} (measured by resonance technique) are listed in Table 8.

The coupling coefficients k_p and k_t of glass-ceramics range between 10 and 15% and 20 to 30%, respectively. In the temperature range -20° to 60°C, the temperature coefficient of resonance lie between 50 to 100 ppm/°C.

In most of the piezoelectric devices, high coupling coefficients and low TCR are desirable. For glass-ceramics, the coupling coefficients are small compared to commonly used piezoelectric materials (such as PZT or $LiNbO_3$) but the TCR of some compositions are low (50 to 60 ppm/°C). The strong dependence of TCR on composition for glass-ceramics suggests the possibility of obtaining temperature-compensated resonators by compositional modification.

9.2 Hydrostatic Measurements

The hydrostatic voltage coefficient g_h was measured by the method described by Safari (Safari 1984). The value of g_h for lithium borosilicate glass-ceramics was almost zero whereas that of glass-ceramics in the fresnoite system was comparable to the g_h values of PVF_2. Values of dielectric constant K_{33}, d_{33} and g_h of glass-ceramics in the fresnoite family are listed in Table 9 along with the calculated values of g_{33}, d_h and $d_h g_h$. A comparison of

the dielectric and hydrostatic properties of glass-ceramics is given in Table 10.

The values of g_h and $d_h g_h$ of glass-ceramics are comparable to PVF_2 and much higher than PZT. Although the values of d_{33} and d_h of glass-ceramics are comparatively low, the magnitudes of g_{33} and g_h of glass-ceramics are high because of their low dielectric constant. The unusually high values of g_h in fresnoite glass-ceramics can be attributed to the positive d_{31} coefficient in these materials. A composite model has been proposed (Halliyal et al. 19984b) to explain the positive sign of d_{31} in fresnoite based on the crystal structure of fresnoite and internal Poisson's ratio stress. A discussion of the advantages of these glass-ceramics in hydrophone applications will be given in the next section.

9.3 Application in Hydrophones

A hydrophone is a passive device used as a hydrostatic pressure sensor (Safari 1984). For hydrophone applications, the commonly used figure of merits are the hydrostatic voltage coefficient g_h and the product $d_h g_h$. Among the desirable properties of the transducer material are:

1. High d_h and g_h.
2. A density suited for acoustic matching with the pressure transmitting medium, usually water.
3. High compliance and flexibility such that the transducer can withstand mechanical shock, and can conform to any surface.
4. No variation of g_h with static pressure.

Acoustic impedance Z can be calculated from the relation $Z = \rho c$ where ρ is the density of the material and c is the velocity of sound in the medium. By measuring the thickness mode frequency constant N_t of the material, the velocity c can be calculated from the relation $c = 2N_t$. The acoustic impedances of glass-ceramics, PZT and PVF_2 are listed in Table 10.

PZT ceramics are used extensively as piezoelectric transducers despite having several disadvantages. The values of g_h and $d_h g_h$ of PZT are low because of its high dielectric constant (~1800). In addition the high density of PZT (~7900 kg/m^3) makes it difficult to obtain a good impedance match with water. PZT is also a brittle ceramic, whereas for hydrophone applications, a more compliant material with better shock resistance would be desirable (Safari 1984). PVF_2 offers several advantages over PZT ceramic for hydrophone applications. It has low density (1760 kg/m^3) and is a flexible material, and although it has low d_{33} and d_h, the dielectric constant of PVF_2 is low enough that large values of piezoelectric voltage coefficients g_{33} and g_h are possible. Overall, this combination of properties is very attractive and PVF_2 transducers are under intensive development (Sessler 1981). However, a major problem in the use of PVF_2 is the difficulty in poling PVF_2 sheets. A very high voltage is necessary to pole PVF_2 (about 10 to 100 MV/m) and this places a limitation on the thickness of PVF_2 transducers.

To overcome these problems, a number of composites of PZT and polymer have been studied in recent years. A detailed description of different kinds of composites and the principles involved can

be found elsewhere (Newnham et al. 1980, Safari et al. 1985). In a composite the polymer phase lowers density and dielectric constant and increases elastic compliance. Very high values of g_h and $d_h g_h$ have been achieved with the composite approach.

From Table 10 it is clear that the piezoelectric coefficient d_{33} and d_h of glass-ceramics are comparable to PVF_2, but much lower than that of PZT. However, because of the low dielectric constant of glass-ceramics, the g_{33} and g_h values of glass-ceramics are considerably higher than PZT. Hence, these glass-ceramics will be useful in passive devices such as hydrostatic pressure sensors where g_h is more important than d_h. The variation of g_h with pressure was measured for glass-ceramics up to 8 MPa. There was no significant variation of g_h with pressure (Ting et al 1984, 1986).

In practice glass-ceramics offer several possible advantages over PVF_2 and other ferroelectric materials for application in piezoelectric devices. Since the polar glass-ceramics are nonferroelectric, no poling step is involved, which is a major problem with PVF_2. Thus there will be no problem of depoling or aging which are encountered in many ferroelectric materials. Hence, glass-ceramics can be used in devices operating at high temperatures. Large area devices can be prepared by routine glass preparation techniques, which reduces the cost of the device significantly. Since acoustic impedances of glass-ceramics are in the range 18-20 x 10^6 rayls, good acoustic matching can be obtained with metals like aluminum. Non-destructive testing of aircraft metals over a wide temperature range is a possibility.

These glass-ceramics also look attractive for use in devices in which glass fibers are used because of the good impedance matching.

10. Surface Acoustic Wave Properties

In recent years piezoelectric materials have become of increasing importance for SAW devices (Whatmore 1980, Mathews 1978). High electromechanical coupling coefficient (k_s^2) and low temperature coefficient of surface wave velocity are desirable material properties for SAW devices. Only a few piezoelectric materials are useful for SAW applications because an undesirable trade off between temperature coefficient of delay (TCD) and k_s^2 is observed in most of the materials presently used for SAW devices (Whatmore 1980). For example, ST-cut quartz exhibits zero TCD but shows only weak electromechanical coupling. On the other hand, Y-cut Z-propagating $LiNbO_3$ shows strong electromechanical coupling, but exhibits a high TCD (94 ppm/°C). Other piezoelectric materials which exhibit good piezoelectric properties for SAW devices present severe crystal growth problems (Whatmore 1980).

Attempts have been made to use piezoelectric ceramic materials for SAW devices (Ito et al 1981(a), 1981(b); Jyomura 1981, Tamura 1974). Unfortunately, in ceramic materials the SAW propagation losses are very high, presenting a major problem in device fabrication (Tamura 1974). Lead titanate ceramics modified with additives of Nd_2O_3, MnO_2 and In_2O_3 have been developed which have zero TCD, low propagation losses and an electromechanical coupling

of about 2% (Ito et al 1981a). However, variation in the properties of ceramics makes it difficult to use lead titanate ceramics for SAW devices.

Since surface wave propagation in SAW devices is generally limited to within a few wavelengths of the surface it is possible that polar glass-ceramics with oriented crystallites near the surface might exhibit useful SAW properties. To test this possibility, polar glass-ceramics of modified fresnoite compositions were prepared and their SAW properties were evaluated on polished surfaces perpendicular to the oriented crystallites.

For SAW measurements a number of uniform overlapping interdigital transducer pairs, in either single or double electrode format, were fabricated on polished surfaces of glass-ceramics. The transducer structure had the following characteristics: periods = 19.5, aperture = 1 mm and wavelength = 30 μm. With this arrangement several odd harmonics were detectable. At higher frequencies SAW response was masked by excessive electromagnetic feed through.

Figure 11 shows the SAW response for fresnoite glass-ceramics having single finger electrodes of 30 μm wavelength. Essential features of this response are the clean $(\text{Sin } x/x)^2$ response with very little interference from bulk wave coupling. It was shown that bulk wave coupling was almost entirely absent within the SAW passband. For the response shown in Fig. 11, the insertion loss was 30 dB and the measured center frequency was 87.96 MHz.

For modified fresnoite glass-ceramics the SAW coupling was about 0.8 to 1.2% and the temperature coefficient of delay was in

the range 10 to 60 ppm/°C. However, propagation losses were high. Work is now in progress to prepare glass-ceramics with optimized composition and microstructure to reduce the SAW propagation loss (Ylo 1986).

Based on preliminary results, polar glass-ceramics look promising for SAW devices. A particularly attractive feature of the glass-ceramic processing route is the ease of fabrication of large area piezoelectric substrates. Although large area lithium niobate single crystals are available, they are expensive. In principle, the glass ceramic process could be used to advantage for planar processing on a much larger scale than is possible for lithium niobate SAW fabrication. This might also help in fabricating SAW devices with more reproducible properties than ceramics.

A further advantage of the glass-ceramic processing is that piezoelectric properties of glass-ceramics can be tailored by modification of the parent glass-composition. The possibility of further reducing temperature coefficient of delay and SAW attenuation in fresnoite glass-ceramics by strontium doping is being explored (Ylo 1986).

11. Connectivity Model for Piezoelectric and Pyroelectric Properties of Polar Glass-Ceramics and Tailoring the Properties

Polar glass-ceramics consist of needle-like crystallites oriented along the c-axis in a glassy matrix phase. The excellent piezoelectric and pyroelectric properties of glass-ceramics (approaching the single crystal properties) indicate that the

glass-ceramics possess a high degree of both crystallographic and polar orientation. In this section, the growth behavior of crystallites in glass-ceramics of different composition will be discussed. An attempt will be made to analyze the properties of the glass-ceramics by considering it as a composite of a crystalline phase and a glass phase. Several interesting combinations of piezoelectric and pyroelectric properties can be achieved by adjusting the composition and degree of crystallinity.

11.1 Growth Behavior of Crystallites in Glass-Ceramics

All the glass-ceramics studied in the present work were nonferroelectric. Hence, unlike ferroelectric materials, the electrical twin configuration of the nonferroelectric crystalline phases in these glass-ceramics cannot be switched by an externally applied electric field. Thus both crystallographic and polar orientation must be achieved during the nucleation stage of the recrystallization process, and must remain unaltered during subsequent growth of crystallites. Since the recrystallization process takes place through surface nucleation and crystallization, the initial stage of recrystallization at the surface and its influence on the crystallographic and polar orientation of crystallites during subsequent growth are extremely important. It is clear that the initial crystallographic and polar orientation are retained as the crystallization progresses from the surface into the bulk.

During the present work an interesting effect occurred in the polar orientation of different crystalline phases in glass-

case of glass-ceramics belonging to the systems $Ba_2TiSi_2O_8$, $Ba_2TiGe_2O_8$, $Sr_2TiSi_2O_8$, LiO-B_2O_3 and Li_2O-SiO_2-B_2O_3 the sign of d_{33} is positive, indicating that the positive end of the dipoles point towards the high temperature end of the sample. For Li_2O-$2SiO_2$, Li_2O-SiO_2-ZnO and Li_2O-SiO_2-Fe_2O_3 glass-ceramics, the sign of d_{33} is negative, indicating that the negative end of the dipoles point towards the high temperature end. There are several possible reasons for this characteristic growth behavior in the above systems.

For glass-ceramics in the fresnoite system ($Ba_2TiSi_2O_8$, $Ba_2TiGe_2O_8$ and $Sr_2TiSi_2O_8$) there is only one crystalline phase present in the glass-ceramic, and d_{33} is positive for all the phases. Hence this growth behavior or polar orientation (positive d_{33}) seems to be characteristic of fresnoite glass-ceramics. On the other hand, for glass-ceramics in the system Li_2O-$2SiO_2$, Li_2O-SiO_2-ZnO, Li_2O-SiO_2-Fe_2O_3 and Li_2O-SiO_2-B_2O_3 the major phase is $Li_2Si_2O_5$. Minor amounts of Li_2ZnSiO_4 and quartz were present in Li_2O-SiO_2-ZnO system and $Li_2B_4O_7$ and Li_2SiO_3 in Li_2O-SiO_2-B_2O_3 system. The presence of Zno, B_2O_3 or Fe_2O_3 appears to influence the growth habit of $Li_2Si_2O_5$ crystallites, possibly by controlling the surface nucleation sites. The presence of Li_2SiO_3 or $Li_2B_4O_7$ as separate phases, which are also polar phases, may be influencing the growth habit of $Li_2Si_2O_5$. In any case the present study indicates clearly that the polar orientation of crystallites and the resulting piezoelectric and pyroelectric properties depend on the composition of the initial glass (Halliyal et al. 1983).

11.2 Diphasic Glass-Ceramic Composites

A polar glass-ceramic is essentially a composite of a glassy phase and one or more crystalline phases. If there is only one crystalline phase, it can be considered a diphasic system consisting of a crystalline phase embedded in an amorphous matrix. X-ray diffraction and microstructure studies of glass-ceramics indicate that the oriented region of crystallites extends deep into the sample and then tapers off. However, not all the crystallites extend throughout the thickness of the samples. The crystalline and glassy phases are partly in series and partly in parallel connection. As the grain orientation is improved, the length of the crystallites increases and the composite approaches pure parallel connectivity. In the present section equations will be derived for piezoelectric and pyroelectric properties of a diphasic glass-ceramic composite.

For a composite consisting of two phases, one-dimensional solutions for dielectric, piezoelectric and pyroelectric properties have been presented for both series and parallel connectivity (Newnham et al. 1978, Skinner et al 1978). If the dielectric constant, piezoelectric coefficient, pyroelectric coefficient and volume fraction of the crystalline and glass phases are designated as ${}^1K_3$, ${}^1d_{33}$, ${}^1p_3$, ${}^1v$ and ${}^2K_3$, ${}^2d_{33}$, ${}^2p_3$, ${}^2v$, respectively, expressions for K_3, d_{33} and p_3 of the glass-ceramic can be derived by making certain simplifying assumptions.

For the glass phase, ${}^2d_{33}$ and ${}^2p_3$ are equal to zero. In many nonferroelectric glass-ceramics, the dielectric constants of

crystalline and glass phases are roughly the same. With this assumption it is obvious that the dielectric constant of the composite is the same for both series and parallel connections.

Further, if we assume that the elastic compliance of crystalline and glassy phases are the same ($^1s_{33} = {}^2s_{33}$), the expressions for d_{33} and p_3 reduce to the following expressions for both series and parallel connectivity (Halliyal et al. 1983)

$$d_{33} = {}^1d_{33}\ {}^1v \tag{1}$$

and

$$p_3 = {}^1p_3\ {}^1v \tag{2}$$

The magnitudes of $^1d_{33}$ and $^1p_3$ of the crystalline phase itself depend upon the degree of both crystallographic and polar orientation of the crystallites, which is not accounted for in equations (1) and (2). We conclude that in the ideal case of complete crystallographic and polar orientation of the crystallites, the magnitudes of d_{33} and p_3 of the composite are directly proportional to the percentage of crystalline phase, irrespective of whether the crystallites are connected in series or parallel. In addition, for this ideal case, if the glass-ceramics contain a very high percentage of crystalline phase, the values of d_{33} and p_3 approach the single crystal values of the crystalline phase. The pyroelectric coefficient p_3 of fresnoite ($Ba_2TiSi_2O_8$) and $Ba_2TiGe_2O_8$ glass-ceramics are 75 to 80% of the

single crystal values. The lower value of p_3 of glass-ceramics can be accounted for by the lack of perfect orientation of the crystallites. The piezoelectric d_{33} coefficient of the glass-ceramics is also about 75 to 80% of the single crystal values.

11.3 Multicomponent Glass-Ceramic Composites

Most of the compositions listed in Table 12 result in glass-ceramics with several crystalline phases after recrystallization. In such cases, the polar vectors in different crystalline phases may be oriented parallel (or antiparallel) to the temperature gradient. If we assume that the crystallites of two or more phases preserve their characteristic growth habit in relation to the direction of temperature gradient, then the piezoelectric and pyroelectric properties of polar glass-ceramic containing several phases can be predicted by the analysis discussed below. For simplicity, an analysis for glass-ceramic composites containing only two crystalline phases will be given here, recognizing however, that the analysis can be extended to more than two phases. For the signs of d_{33} and p_3, the same convention will be followed as defined in the previous section.

Consider a polar glass-ceramic containing two crystalline phases. Let the dielectric constant, piezoelectric coefficient, and the volume fraction of the two phases be ${}^1K_3$, ${}^1d_{33}$, ${}^1p_3$, ${}^1v$ and ${}^2K_3$, ${}^2d_{33}$, ${}^2p_3$, ${}^2v$, respectively. Let us assume that both the phases have similar elastic compliances (${}^1s_{33} = {}^2s_{33}$) and thermal expansion coefficients, thereby eliminating any secondary contributions to the pyroelectric effect. To further simplify the

analysis, let us assume that the properties of glass-ceramic are not influenced by the glassy phase ($^3v = 0$). Irrespective of whether the crystalline phases are connected in series or parallel, we get the following equations for the properties of the composite (Halliyal et al. 1983).

$$K_3 = {}^1v\,{}^1K_3 + {}^2v\,{}^2K_3$$

$$d_{33} = {}^1v\,{}^1d_{33} \pm {}^2v\,{}^2d_{33}$$

$$p3 = {}^1v\,{}^1p_3 \pm {}^2v\,{}^2p_3$$

The resultant values of d_{33} and p_3 of the composite depend upon the sign and magnitude of the properties of individual phases, and also upon the volume fraction of the individual phases. Since $^1d_{33}$ and $^2d_{33}$ can be positive or negative at the growth end and $^1p_3$ and $^2p_3$ can be positive or negative, there are 16 possible cases of d_{33} and p_3, eight of which are listed in Table 13. If we consider the resulting piezoelectric and pyroelectric properties of the glass-cseramic, these 16 cases can be grouped into four classes.

The crystalline phases have the same growth behavior in the case of glass-ceramics belonging to class (a) and (b) and opposite growth behavior in cases (c) and (d). Depending on the signs of pyroelectric coefficients $^1p_3$ and $^2p_3$ of the two phases, we obtain glass-ceramic composites with completely different piezoelectric and pyroelectric properties. Glass-ceramics of class (a) are fully piezoelectric as well as pyroelectric and in the ideal case their properties can be expected to approach those of single

domain single crystal materials. Glass-ceramics of class (b) are fully piezoelectric but only partially pyroelectric (or non-pyroelectric) because of the opposite signs of $^1p_3$ and $^2p_3$. Glass-ceramics of class (c) are both non-piezoelectric and non-pyroelectric and hence are not of much interest for devices. Class (d) glass-ceramics are fully pyroelectric but non-piezoelectric. Glass-ceramics of classes (b) and (d) are interesting for piezoelectric and pyroelectric device applications where the interference of the two properties may be a problem, as will be discussed below.

11.4 Examples of the Four Classes

The growth habit and the signs of pyroelectric coefficients of the crystalline phases can be exploited to design compositions which give glass-ceramics with properties of any one of the four classes just described.

Glass-ceramics in the system Li_2O-SiO_2-ZnO, Li_2O-SiO_2-Fe_2O_3, and Li_2O-SiO_2-B_2O_3 have negative pyroelectric coefficient, but exhibit opposite growth behavior (case c). Compositions in the quaternary system Li_2O-SiO_2-ZnO-B_2O_3 illustrate the reduced pyroelectric and piezoelectric effect characteristic of glass-ceramics of class (c). $Ba_2TiSi_2O_8$ and $Ba_2TiGe_2O_8$ phases crystallized from glasses of composition 2BaO-3SiO_2-TiO_2 and BaO-GeO_2-TiO_2 respectively showed similar growth habit, but opposite signs for pyroelectric coefficients. A glass-ceramic of composition 2BaO-2SiO_2-GeO_2-TiO_2 which gave a solid solution phase after recrystallization had almost zero pyroelectric coefficient,

but piezoelectric properties remained the same (Fig. 13). In this case, there is no appreciable change in the piezoelectric properties, whereas the pyroelectric property reduced substantially over a wide temperature range.

11.5 Optimizing the Piezoelectric and Pyroelectric Properties

From the examples just presented, it is clear that glass-ceramics with tailored piezoelectric or pyroelectric properties can be prepared by crystallizing multicomponent glasses of suitable composition. The growth habit of the crystalline phases provides a means to tailor the piezoelectric and pyroelectric properties of the final glass-ceramic composite. Two of the cases look especially interesting for device applications; piezoelectric glass-ceramics which are non-pyroelectric (case b) and pyroelectric glass-ceramics which are non-piezoelectric (case d).

In piezoelectric devices used in ambient conditions, pyroelectric noise is usually undesirable. In hydrophone elements fabricated from PZT-polymer composites, for instance, pyroelectric noise can be reduced only within a relatively narrow working temperature range (Lynn 1982).

In a similar way, piezoelectric noise interferes with the high frequency IR pyroelectric signals. In some cases alternate methods are used to elminate the interfering piezoelectric voltages developed in such devices. In the case of $LiTaO_3$ detectors, piezoelectric oscillations are damped by embedding the pyroelectric element in epoxy (Glass and Abrams 1970); and in PLZT detectors, piezoelectric noise is eliminated by modifying the

electronics (Simhony and Bass, 1979). Piezoelectric oscillations superimposed on the pyroelectric response have been shown to have an incubation time of 40-60 nsec, and occur after the onset of pyroelectric signals (<40 nsec). Thus the piezoelectric oscillations occur in the tail of the pyroelectric response, and can be eliminated with suitable electronics.

Piezoelectric glass-ceramics which are non-pyroelectric should satisfy the relation $\pm {}^{1}v^{1}p_3 + {}^{2}v^{2}p_3 = 0$ (case b). Referring to Table 13 candidate compositions can be found in the solid solution of $Ba_2Si_2TiO_8$ and $Ba_2Ge_2TiO_8$. Piezoelectric glass-ceramics which are not pyroelectric would be useful as pressure sensors that are insensitive to temperature changes. (Quartz is piezoelectric and non-pyroelectric, but cannot be used to measure pressure changes because $d_{11} + d_{22} + d_{33} = 0$. This is generally true for all piezoelectric crystals belonging to non-pyroelectric point groups.)

The second case of interest is pyroelectric glass-ceramics which are not piezoelectric (case d). Here the requirement is that ${}^{1}v^{1}d_{33} - {}^{2}v^{2}d_{33} = 0$ should be satisfied. Candidate compositions may exist in the Li_2O-B_2O_3-SiO_2-ZnO quaternary system containing different amounts of ZnO_3. Such pyroelectric materials will not be sensitive to mechanical oscillations.

12. Summary

The preparation and properties of polar glass-ceramics were described in this article. Polar glass-ceramics consist of well-

oriented crystallites of a polar but nonferroelectric crystalline phase.

Glasses were prepared from Li_2O-SiO_2-B_2O_3, BaO-GeO_2-TiO_2, Bao-SiO_2-TiO_2 and SrO-SiO_2-TiO_2 systems and were recrystallized to obtain polar glass-ceramics with crystallites of $Li_2Si_2O_5$, Li_2SiO_3, $Li_2B_4O_7$, $Ba_2TiGe_2O_8$, $Ba_2TiSi_2O_8$ or $Sr_2TiSi_2O_8$ oriented along their polar c-axes. The oriented region of the crystallites was 200-500 μm from the surface of glass-ceramics. Dielectric, piezoelectric and pyroelectric properties of glass-ceramics are in close agreement with the respective single crystal properties. Glass-ceramics in the fresnoite family are excellent candidate materials for hydrophones. Magnitudes of hydrostatic piezoelectric coefficient d_h ($\sim 100 \times 10^{-3}$ Vm/N) and dielectric constant ($\sim$10) of fresnoite glass-ceramics are comparable to the corresponding values of polyvinylidene fluoride. The electromechanical coupling coefficients k_p and k_t were in the range 15 to 20%. Several glass-ceramics showed pyroelectric figures of merit up to 60% of those obtained on $LiTaO_3$ single crystal. Surface acoustic wave properties of glass-ceramics in the fresnoite family are promising.

The polar growth behavior of crystallites from glass matrix depends on the original composition of glass. This property can be exploited to tailor the piezoelectric and pyroelectric properties of polar glass-ceramics. A connectivity model, based on the principles of series and parallel connectivity models has been described to predict the piezoelectric and pyroelectric properties of polar glass-ceramics.

Acknowledgements

It is a pleasure to thank our colleagues at the Materials Research Laboratory for their help in this work. This work was supported by the Army Research Office through contract #DAAG29-83-K-0062 and the National Science Foundation through contract #DMR-8010811.

References

Bhalla, A.S., Cross, L.E., and Whatmore, R.W. (1986), J. Phys. Soc. Jap. (accepted).

Blasse, G., (1968), J. Inorg. Nucl. Chem., 30, 2283.

Borrelli, N.F., (1967), J. Appl. Phys. 38, 4243.

Borrelli, N.F., and Layton, M.M., (1969), IEEE Trans. on Electron Devices, Vol. ED-16, 19.

Borrelli, N.F., and Layton, M.M., (1971), J. Noncryst. Solids, 6, 37.

Brun, M.K., Bhalla, A.S., Spear, K.E., Cross, L.E., and Berger, R.S., (1979), J. Cryst. Growth, 47, 335.

Byer, R.L. and Roundy, C.B., (1972), Ferroelectrics, 3, 333.

Gabelica-Robert, M. and Tarte, P., (1981), Phys. Chem. Minerals, 7:26, 30.

Gardopee, G., Newnham, R.E., Halliyal, A., and Bhalla, A.S., (1980), Appl. Phys. Lett., 36, 817.

Gardopee, G., Newnham, R.E. and Bhalla, A.S. (1981), Ferroelectrics, 33, 155.

Glass, A.M., and Abrams, R.L., (1970), J. Appl. Phys., 41, 4455.

Glass, A.M., Lines, M.E., Nassau, K., and Shiver, J.W. (1977a), Appl. Phys. Lett., 31, 249.

Glass, A.M., Nassau, K. and Shiever, J.W. (1977b), J. Appl. Phys., 48, 5213.

Halliyal, A., Bhalla, A.S. and Newnham, R.E., (1983), Mat. Res. Bull., 18, 1007.

Halliyal, A. (1984a), Ph.D. Thesis, The Pennsylvania State University.

Halliyal, A., Safari, A., Bhalla, A.S., Newnham, R.E. and Cross, L.E. (1984b), J. Am. Cer. Soc. 67, 331.

Halliyal, A., Bhalla, A., Markgraf, S.A., Cross, L.E., and Newnham, R.E., (1985a), Ferroelectrics, 62, 27.

Halliyal, A., Bhalla, A.S. and Cross, L.E., (1985b), Ferroelectrics, 62, 3.

Halliyal, A., Bhalla, A.S., Cross, L.E. and Newnham, R.E., (1985c), J. Mater. Sci., 20, 3745.

Halliyal, A., Bhalla, A.S., Newnham, R.E. and Cross, L.E., (1986), J. Am. Cer. Soc. (submitted).

Herczog, A., (1964), J. Am. Cer. Soc. 47, 107.

Herczog, A., (1973), IEEE Trans. on Parts Hybrids and Packaging, Vol. PHP-9, 247.

Herbert, J.M., (1982), "Ferroelectric Transducers and Sensors", Gordon and Breach, NY.

"IRE Standards on Piezoelectric Crystals" (1949), Proc. IRE, 37, 1378.

Ito, Y., Nagatsuma, K., and Ashida, S., (1981a) Jap. J. Appl. Phys. 20, Suppl. 20-4, 163.

Ito, Y., Takeuchi, H., Nagatsuma, K., Jyomura, S. and Ashida, S., (1981b), J. Appl. Phys., 52, 3223.

Ito, Y., Nagatsuma, K., Takeuchi, H. and S. Jyomura (1981c), J. Appl. Phys. 52, 4479.

Jyomura, S., Nagatsuma, K. and Takeuchi, H., (1981), J. Appl. phys., 52, 4472.

Kimura, M., Doi, K., Nanamatsu, S., and Kawamura, T., (1973), Appl. Phys. Lett., 23, 531.

Kimura, M., (1977), J. Appl. Phys., 48, 2850 (1977).

Krog-Moe, J., (1962), Acta. Cryst. 15, 190.

Layton, M.M., and Herczog, A., (1969), Glass Technology, 10, 50.

Layton, M.M. and Smith, J.W., (1975), J. Am. Cer. Soc. 58, 435.

Lee, C.W., Bowen, L.J. Browne, J.M., Halliyal, A., Bhalla, A.S., and Ylo, E., (1984), IEEE Ultrasonic Symposium, 285.

Liebau, V.F. (1961), Acta. Cryst., 14, 389.

Liu, S.T., (1976), Ferroelectrics, 10, 83.

Lynn, S.Y., (1982), M.S. Thesis, The Pennsylvania State University (1982).

Mathews (1978), Ed. "Surface Wave Filters", John Wiley and Sons, New York.

McMillan, P.W. (1979), Glass-Ceramics, Academic Press, New York.

Melling, P.J. and Duncan, J.F., (1980), J. Am. Cer. Soc. 63, 264.

Moore, P.B. and Loinsnatham, J., (1969), Z. Kristallogr, 130, 438 (1969).

Newnham, R.E., Skinner, D.P. and Cross, L.E., (1978), Mat. Res. Bull., 13, 525.

Newnham, R.E., Bowen, L.J., Klicker, K.A. and Cross, L.E., (1980), Mat. Engg., 2, 93.

Nye, J.F., (1957) "Physical Properties of Crystals", Oxford University Press, London.

Porter, S.G., (1981), Ferroelectrics, 33, 193.

Putley, E.H. (1970), "Semiconductors and Semimetals Vol. 5", 259, Academic Press, NY.

Rindone, G.E., (1962a) in "Proc. of the Symposium on Nucleation and Crystallization in Glasses and Melts", Ed. by Roser, M.K., Smith, G. and Insley, H.; American Ceramic Society, Columbus, Ohio.

Rindone, G.E., (1962b), J. Am. Cer. Soc. 45, 7.

Risbud, S.H., (1979), Metall. Trans. 10A, 1953.

Safari, A., (1984), Ph.D. Thesis, The Pennsylvania State University.

Safari, A., Sa-gong, G., Giniewicz, J., and Newnham, R.E., (1985), "Proc. of Symposium on Tailoring Multiphase and Composite Ceramics" (in press).

Sekhar, J.A., and Risbud, S.H., (1981), Mat. Res. Bull., 16, 681.

Sessler, G.M., (1981), J. Acoust. Soc. Am. 70, 1596.

Shorrocks, N.M., Whatmore, R.W., Ainger, F.W., and I.M. Young, (1981), IEEE Ultrasonic Symposium, 337.

Simhony, M., and Bass, M., (1979), Appl. Phys. Lett., 34, 426.

Skinner, D.P., Newnham, R.E., and Cross, L.E., (1978), Mat. Res. Bull., 13, 599.

Takashige, M., Mitsiu, T., Nakamura, T., Aikawa, Y. and Jang, M. (1981), Jap. J. Appl. Phys. 20, L159.

Takahashi, K., Cross, L.E., and Newnham, R.E., (1975), Mat. Res. Bull., 10, 599.

Takahashi, K., Hardy, L.H., Newnham, R.E. and Cross, L.E., (1979), Proc. 2nd Meeting on ISAF, 257.

Tamura, M. and Yonezawa M. (1974, Proc. IEEE 62, 416.

Ting. R.Y., Halliyal, A., and Bhalla, A.S., (1984), Appl. Phys. Lett., 44, 852.

Ting, R.Y., Halliyal, A., and Bhalla, A.S., (1986), Jap. J. Appl. Phya. (accepted).

Whatmore, R.W., Herbert, J.M., and Ainger F.W. (1980), Phys. Stat. Sol.(a), 61, 73.

Whatmore, R.W., (1980), J. Cryst. Growth, 48, 530.

Yamauchi, H., (1978), J. Appl. Phys. 49, 6162.

Ylo, E., (1986), Private Communication.

Figure Caption

(1) Fig. 1. Glass-ceramic route for preparing polar glass-ceramics

(2) Fig. 2. Domain structure in (a) an unpoled ferroelectric ceramic and (b) poled ferroelectric ceramic and (c) polar glass-ceramic

(3) Fig. 3. Isothermal heat treatment cycles

(4) Fig. 4. The degree of preferred orientation as a function of depth for Li_2O-$2SiO_2$-0.2ZnO glass-ceramic for different isothermal heating cycles

(5) Fig. 5. Vertical (a) and horizontal (b) view of Li_2O-$2SiO_2$-0.2ZnO glass-ceramic

(6) Fig. 6. Dielectric constant (a) and dissipation factor (b) of Li_2O-$1.8SiO_2$-$0.2B_2O_3$ glass-ceramic as a function of temperature and frequency

(7) Fig. 7. Dielectric constant of 2BaO-$3SiO_2$-TiO_2 glass as a function of temperature and frequency

(8) Fig. 8. Dielectric constant (a) and dissipation factor (b) of 2BaO-$3SiO_2$-TiO_2 glass-ceramic as a function of temperature and frequency

(9) Fig. 9. Variation of pyroelectric coefficient with temperature for (a) Li_2O-$1.8SiO_2$-$0.2B_2O_3$ and (b) BaO-GeO_2-TiO_2 glass-ceramics

(10) Fig. 10. Pyroelectric coefficient as a function of temperature for (a) 2BaO-$3SiO_2$-TiO_2 and (b) 1.9BaO-0.1PbO-$3SiO_2$-TiO_2 glass-ceramics

(11) Fig. 11. Relative amplitude vs. frequency response of (a) surface wave and (b) bulk wave
Vertical scale 10dB/div
Horizontal = 72-203 MHz

(12) Fig. 12. Polar orientation--two types of growth behavior

(13) Fig. 13. Pyroelectric coefficients of glass-ceramics in the fresnoite system; (a) $2BaO-3SiO_2-TiO_2$ (b) $2BaO-2SiO_2-GeO_2-TiO_2$ (c) $BaO-GeO_2-TiO_2$

Table 1. Polar Glass-Forming Systems*

A	B
Li_2SiO_3	$Li_2Si_2O_5$
Li_2GeO_3	$Ba_2TiGe_2O_8$
$Li_2Ge_2O_5$	$Ba_2TiSi_2O_8$
$Li_2B_4O_7$	
Na_2SiO_3	
$Sr_2TiSi_2O_8$	
Li_3PO_4	
C	D
$Na_2Si_2O_5$	SrB_4O_7
ZnP_2O_6	PbB_4O_7

*All the systems are polar but nonferroelectric.

Table 2. Crystal System and Point Group Symmetry

Crystal	Melting Point (°C)	Crystal System	Point Group Symmetry	Polar Axis	Reference
$Ba_2TiSi_2O_8$	1440	tetragonal	4mm	c	Moore and Louisnathan 1959
$Ba_2TiGe_2O_8$	1260	orthorhombic	mm2	c	(Blasse (1968)
$Sr_2TiSi_2O_8$	1380	tetragonal	4mm	c	(Robert and Tarte 1981)
$Li_2Si_2O_5$	1200	orthorhombic	mm2	c	(Liebau 1961)
Li_2SiO_3	1201	orthorhombic	mm2	c	(Brun et al. 1979)
$Li_2B_4O_7$	917	tetragonal	4mm	c	(Krog-Moe 1962)

Table 3. Glass Formation and Recrystallization Behavior of Various Compositions of Glasses.

Composition	Glass Formation	Mechanical Strength of Glass-Ceramics	p_3 $\mu C/m^2 °K$	Detailed Study
$Ba_2TiSi_2O_8$ system				
*$2BaO-2SiO_2-TiO_2$	hmp	p	---	no
$0.64SiO_2-0.36BaTiO_3$	g	s	2	no
$BaO-SiO_2-TiO_2$	s	s	2	no
$2BaO-4SiO_2-TiO_2$	g	p	---	no
$2BaO-2.5SiO_2-1.5TiO_2$	s	s	4	no
$2BaO-2.8SiO_2-1.3TiO_2$	s	p	---	no
$2.3BaO-3.1SiO_2-0.7TiO_2$	s	s	(0)	no
$2BaO-3SiO_2-TiO_2$	g	s	8	yes
$2BaO-0.15CaO-2.9SiO_2-TiO_2$	g	g	6	yes
$1.6BaO-0.4CaO-2.8SiO_2-TiO_2$	g	g	6	yes
$1.8BaO-0.2CaO-2SiO_2-TiO_2$	g	p	---	no
$1.7BaO-0.3SrO-3SiO_2-TiO_2$	g	p	---	no
$1.6BaO-0.4SrO-3SiO_2-TiO_2-0.2CaO$	g	g	5	yes
$1.9BaO-0.1PbO-3SiO_2-TiO_2$	g	g	8	yes
$1.6BaO-0.4PbO-3SiO_2-TiO_2$	g	p	---	no
$1.4BaO-0.4SrO-0.2PbO-3SiO_2-1.1TiO_2$	g	s	---	no
$2BaO-3SiO_2-TiO_2-0.2K_2O$	s	s	(0)	no
$2BaO-3SiO_2-ZrO_2$	hmp	---	---	no
$2BaO-3SiO_2-0.8TiO_2-0.2ZrO_2$	g	p	---	no
$2BaO-2.2SiO_2-TiO_2-0.2Al_2O_3$	s	s	(0)	no
$2BaO-3SiO_2-0.8TiO_2-0.2MnO_2$	g	s	(0)	no
$2BaO-3SiO_2-0.9TiO_2-0.1SnO_2$	s	p	---	no
$1.85BaO-0.15BaF_2-3SiO_2-TiO_2$	g	p	---	no

Table 3. (Continued).

Composition	Glass Formation	Mechanical Strength of Glass-Ceramics	$p3_2$ $\mu C/m^2 °K$	Detailed Study
$Ba_2TiGe_2O_8$ system				
*$2BaO-2GeO_2-TiO_2$	h	---	---	no
$2BaO-3GeO_2-TiO_2$	s	p	---	no
$BaO-GeO_2-TiO_2$	g	g	-2	yes
$BaO-GeO_2-TiO_2-0.1CaO$	g	g	-1	no
$BaO-GeO_2-TiO_2-0.2CaO$	g	p	---	no
$BaO-GeO_2-0.9TiO_2-0.1ZrO_2$	g	p	---	---
$BaO-GeO_2-0.9TiO_2-0.05Nb_2O_5$	p	p	---	---
$BaO-GeO_2-0.8TiO_2-0.2ZnO$	p	p	---	---
$0.8BaO-0.2SrO-GeO_2-TiO_2$	g	p	---	no
$Sr_2TiSi_2O_8$ system				
*$2SrO-2SiO_2-TiO_2$	ps	---	---	---
$2SrO-3SiO_2-TiO_2$	g	g	8	yes
$1.8SrO-0.2BaO-2.8SiO_2-0.1CaO-TiO_2$	g	g	2	yes
$Li_2B_4O_7$ system				
*$Li_2O-2B_2O_3$	r	p	---	no
$Li_2O-2B_2O_3$	s	s	---	no
$Li_2O-0.5B_2O_3-0.5SiO_2$	g	p	---	no
$Li_2Si_2O_5$ system				
*$Li_2O-2SiO_2$	g	p	---	no
$Li_2O-xSiO_2$ (x = 3)	g	p	---	no

Table 3. (Continued).

Composition	Glass Formation	Mechanical Strength of Glass-Ceramics	p_{32} $\mu C/m^2 °K$	Detailed Study
Li_2O-$2SiO_2$-$xZnO$ (x = 0.1 to 0.4)	g	s	-2	no
Li_2O-$1.5SiO_2$-$0.5GeO_2$	g	p	---	no
Li_2O-$1.8SiO_2$-$0.2CaO$	g	p	---	no
Li_2O-$1.9SiO_2$-$0.1MO$ (MO = Ta_2O_5, PbO, Ba_2O_3, SnO_2, TiO_2, P_2O_5, Fe_2O_3)	g	p	---	---
<u>$(Li_2Si_2O_5 + Li_2B_4O_7)$ system</u>				
Li_2O-$(2-x)SiO_2$-xB_2O_3 (x = 0.1 to 0.7)	g	g	-6 to -11	yes
Li_2O-$1.5SiO_2$-$0.4B_2O_3$-$0.1Al_2O_3$	g	g	(0)	no
Li_2O-$1.6SiO_2$-$0.2B_2O_3$-$0.2WO_3$	g	s	(0)	no
Li_2O-$1.8SiO_2$-$0.1B_2O_3$-$0.1ZnO$	g	g	(0)	no
$0.85Li_2O$-$0.15Na_2O$-$1.8SiO_2$-$0.2B_2O_3$	g	p	---	no
$0.8Li_2O$-$0.2LiF$-$1.8SiO_2$-$0.2B_2O_3$	g	s	---	no
Li_2O-$1.8SiO_2$-$0.2B_2O_3$-$0.03Y_2O_3$	g	s	---	no
Li_2O-$1.8SiO_2$-$0.2B_2O_3$-$0.4P_2O_5$	g	s	(0)	no
Li_2O-$1.7SiO_2$-$0.2B_2O_3$-$0.06Si_3N_4$	g	p	---	no

* Stoichiometric compositions.

(0) Piezoelectric d_{33} coefficient, almost zero.

Table 3. (Continued).

Explanation of Symbols

(a) Glass Formation:

g - easy glass formation even by slow air quenching of the melt; no problem of recrystallization;

s - glass formation possible by air quenching, but some of the samples crystallized partially;

p - problem of recrystallization; fast quenching necessary;

r - the melt crystallizes completely on air quenching;

ps - the melt separates into two phases;

hmp - high melting point (<1450°C); difficult to get rid of air bubbles from the melt.

(b) Mechanical Strength of Glass-Ceramics

g - Glass-ceramics have good mechanical strength; possible to prepare thin sections (200 μm) by polishing;

s - glass-ceramics have reasonably good mechanical strength, but diffiuclt to prepare thin sections by polishing;

p - the mechanical strength of glass-ceramics not enough to polish and prepare thin sections.

Table 4. Compositions, Crystallization Temperature and Crystalline Phases.

Composition	Glass Melting Temp(°C)	Crystallization Temperature	Crystalline Phases
$Ba_2TiSi_2O_8$ system			
$2BaO-3SiO_2-TiO_2$	1450	930	$Ba_2TiSi_2O_8$
$1.9BaO-0.1PbO-3SiO_2-TiO_2$	1450	920	$Ba_2TiSi_2O_8$
$2BaO-0.15CaO-2.9SiO_2-TiO_2$	1450	920	$Ba_2TiSi_2O_8$
$1.6BaO-0.4CaO-2.8SiO_2-TiO_2$	1450	930	$Ba_2TiSi_2O_8$
$1.6BaO-0.4SrO-3SiO_2-TiO_20.2CaO$	1450	930	$Ba_2TiSi_2O_8$
$Ba_2TiGe_2O_8$ system			
$BaO-GeO_2-TiO_2$	1400	800	$Ba_2TiGe_2O_8$
$Sr_2TiSi_2O_8$ system			
$2SrO-3SiO_2-TiO_2$	1450	950	$Sr_2TiSi_2O_8$
$1.8SrO-0.2BaO-2.8SiO_2-0.1CaO-TiO_2$	1450	940	$Sr_2TiSi_2O_8$
$Li_2Si_2O_5$ system			
$Li_2O-2SiO_2$	1350	585	$Li_2Si_2O_5$
$Li_2O-2SiO_2-0.2ZnO$	1350	580	$Li_2Si_2O_5+Li_2ZnSiO_4+\alpha SiO_2$
$Li_2B_4O_7$ system			
$Li_2O-3B_2O_3$	1250	580	$Li_2B_4O_7+Li_2B_6O_{10}$
$Li_2Si_2O_5+Li_2B_4O_7$ system			
$Li_2O-1.8SiO_2-0.2B_2O_3$	1250	605,680	$Li_2Si_2O_5+Li_2B_4O_7+Li_2SiO_3$
$Li_2O-1.7SiO_2-0.3B_2O_3$	1250	595,670	$Li_2Si_2O_5+Li_2B_4O_7+Li_2SiO_3$
$Li_2O-1.6SiO_2-0.4B_2O_3$	1250	625,665	$Li_2Si_2O_5+Li_2B_4O_7+Li_2SiO_3$

Table 5. Dielectric and Physical Properties of Glass-Ceramics

Composition	Density g/cc	Specific Heat $J/cm^3°K$	K_3 1kHz	Tan δ 1kHz
$Li_2O-2SiO_2-0.2ZnO$	2.47	2.36	6.5	0.008
$Li_2O-1.8SiO_2-0.2B_2O_3$	2.34	2.39	7.0	0.05
$Li_2O-1.7SiO_2-0.3B_2O_3$	2.32	--	7.5	0.05
$Li_2O-1.6SiO_2-0.4B_2O_3$	2.35	--	7.0	0.05
$BaO-GeO_2-TiO_2$	4.78	--	15	--
$2BaO-3SiO_2-TiO_2$	4.01	2.04	9.0	0.001
$2BaO-0.15CaO-2.9SiO_2-TiO_2$	3.98	--	10	0.001
$1.6BaO-0.4CaO-2.8SiO_2-TiO_2$	--	--	10.5	0.001
$1.6BaO-0.4SrO-3SiO_2-0.2CaO-TiO_2$	3.87	--	9.8	0.001
$1.9BaO-0.1PbO-3SiO_2-TiO_2$	4.05	2.04	10.0	0.001
$2SrO-3SiO_2-TiO_2$	3.53	--	11.5	0.001
$1.8SrO-0.2BaO-2.8SiO_2-0.1CaO-TiO_2$	3.63	--	10.5	0.001

Table 6. Pyroelectric Figures of Merit*

Symbol	Expression	Application
M_1	p/K	For a quick evaluation of material.
M_2	$p/\rho c$	Current mode: a thin disc feeding current into a low impedance amplifier.
M_3	$p/\rho cK$	Voltage mode: a disc supplying voltage to a high impedance amplifier, the inherent noise of which limits the sensitivity of detector.
M_4	$p/\rho KD$	For vidicons
M_5	$p/\rho cK^{1/2}\tan\delta^{1/2}$	Voltage mode: for a high impedance amplifier when the pyroelectric element is the main source of noise.

*p = Pyroelectric coefficient
K = Dielectric constant
tan δ = Dissipation factor
ρ = Density
c = Specific heat per unit mass
c^1 = Specific heat per unit volume ($=\rho c$)
D = Thermal diffusivity

Table 7. Room Temperature Pyroelectric Figures of Merit of Glass-Ceramics

Composition	p $\mu C/m^2 °K$	p/K $\mu C/m^2 °K$ M_1	p/c^1 $(10^{-12}$ Cm/J) M_2	p/c^1K $(10^{-12}$ Cm/J) M_3	$\beta/c^1\sqrt{K \tan \delta}$ $(10^{-12}$ Cm/J) M_5
Li_2O-$2SiO_2$-0.2ZnO	- 3.0	0.46	1.27	0.20	5.6
Li_2O-$1.8SiO_2$-$0.2B_2O_3$	-11.0	1.57	4.60	0.66	7.8
Li_2O-$1.7SiO_2$-$0.3B_2O_3$	-10.0	1.33	4.18	0.56	6.8
Li_2O-$1.6SiO_2$-$0.4B_2O_3$	-10.0	1.43	4.18	0.60	7.1
BaO-GeO_2-TiO_2	- 2.0	0.13	0.98	0.07	8.0
2BaO-$3SiO_2$-TiO_2	+ 8.0	0.88	3.92	0.44	41.3
1.9BaO-0.1PbO-$3SiO_2$-TiO_2	+ 8.0	0.80	3.92	0.39	39.2
2BaO-0.15CaO-$2.9SiO_2$-TiO_2	+ 6.0	0.60	2.94	0.29	29.0
1.6BaO-0.4CaO-$2.8SiO_2$-TiO_2	+ 5.5	0.52	2.70	0.26	26.4
1.6BaO-0.4SrO-$3SiO_2$-TiO_2-0.2CaO	+ 4.5	0.46	2.21	0.23	22.3
2SrO-$3SiO_2$-TiO_2	+ 8.0	0.70	3.92	0.34	36.6
1.8SrO-0.2BaO-$2.8SiO_2$-0.1CaO-TiO_2	+ 7.0	0.66	3.43	0.32	33.3
$Li_2B_4O_7$ (single crystal)	-30.0	3.0	9.4	0.94	2.10
$Ba_2TiGe_2O_8$ (single crystal)	- 4.0	0.35	1.97	0.17	18.4
$Ba_2TiSi_2O_8$ (single crystal)	+10.0	0.91	4.90	0.45	46.7

Table 8. Electromechanical and Piezoelectric Properties of Glass-Ceramics

Composition	N_p m·Hz	k_p	N_t m·Hz	k_t	k_{31}	d_{33} pC/N	d_{31} pC/N	Q (Radial)	TCR (ppm/°C)
$2BaO-3SiO_2-TiO_2$	3500	0.14	2250	0.25	--	7	--	800	100
$1.9BaO-0.1PbO-3SiO_2-TiO_2$	3450	0.14	2300	0.20	--	7	--	800	120
$2BaO-0.15CaO-2.9SiO_2-TiO_2$	--	--	--	--	--	6	--	--	--
$1.6BaO-0.4CaO-2.8SiO_2-TiO_2$	--	--	2500	0.15	0.04	6	1.8	--	100
$1.6BaO-0.4SrO-3SiO_2-TiO_2-0.2CaO$	3450	0.10	2350	0.22	--	6	--	500	--
$BaO-GeO_2-TiO_2$	3300	0.06	2500	0.08	0.04	6	1.2	2000	65
$2SrO-3SiO_2-TiO_2$	3300	0.10	2550	0.08	0.03	14	1.6	700	50
$1.8SrO-0.2BaO-2.8SiO_2-0.1CaO-TiO_2$	--	--	2550	0.20	--	10	--	--	--
$Li_2O-2SiO_2-0.2ZnO$	--	--	--	--	--	4	--	--	--
$Li_2O-1.8SiO_2-0.2B_2O_3$	4500	0.15	3750	0.25	0.09	6	-2.4	800-1000	80-100
$Li_2O-1.7SiO_2-0.3B_2O_3$	4500	0.14	3700	0.2	--	5	--	500-1000	80-100
$Li_2O-1.6SiO_2-0.4B_2O_3$	4500	0.12	3700	low	--	5	--	500-1000	80-100
PZT 501A	2000	0.60	1860	0.50	0.35	400	-175	80	250
$LiNbO_3$	--	0.048*	--	--	0.02	6.0	0.9	--	95
Quartz	--	0.0014*	--	--	--	d_{11}=2.31 d_{14}=0.7		--	0

N_p, N_t = Frequency constants for radial and thickness mode of resonance

k_p, k_t = Electromechanical coupling coefficients for radial and thickness mode of resonance

Q = Mechanical quality factor; TCR = temperature coefficient of resoanance $\left(\frac{1}{f}\ \frac{\partial f}{\partial T}\right)$

* = Surface coupling coefficient k_s^2

Table 9. Hydrostatic Measurements

Composition	K_{33}	d_{33} pC/N	g_{33} (10^{-3} Vm/N)	g_h (10^{-3} Vm/N)	d_h (pC/N)	$d_h g_h$ (10^{-15} m^2/N)
$2BaO-3SiO_2-TiO_2$	9	7	88	110	8.8	970
$(1.9BaO-0.1PbO)-3SiO_2-TiO_2$	10	7	80	110	9.7	1070
$2BaO-0.15CaO-2.9SiO_2-TiO_2$	10	6	68	75	6.6	500
$(1.6BaO-0.4CaO)-2.8SiO_2-TiO_2$	10.5	6	65	85	7.9	670
$(1.6BaO-0.4SrO)-3SiO_2-TiO_2-0.2CaO$	9.8	6	70	100	8.7	870
$2SrO-3SiO_2-TiO_2$	11.5	14	138	85	8.7	740
$(1.8SrO-0.2BaO)-2.8SiO_2-0.1CaO-TiO_2$	10.6	10	107	100	9.4	940
$BaO-GeO_2-TiO_2$	15	6	45	70	9.3	650

Table 10. Comparison of Hydrostatic Properties

Property	Glass-Ceramics	PVF_2	PZT
K	10	13	1800
$d_{33}(10^{-12}$ C/N)	8-10	30	450
$d_{31}(10^{-12}$ C/N)	+1.5	-18	-205
$d_h(10^{-12}$ C/N)	8-10	10	40
$g_{33}(10^{-3}$ Vm/N)	100	250	28
$g_h(10^{-3}$ Vm/N)	100	100	2.5
$d_h g_h(10^{-15}$ m^2/N)	1000	1000	100
Z* (10^6 rayls)	15-25	2-3	30

*Z = Acoustic impedance units of rayl: $kg/m^2.sec$

Table 11. Saw Properties

Property \ Material	Fresnoite Glass Ceramic	ZX-Fresnoite Single Crystal	YZ-$LiNbO_3$	ST-Quartz	Lead Titanate
Coupling Coefficient K^2	0.008 to 0.012	0.016±0.003	0.0482	0.00116	0.022
Velocity m/sec	2600	2678±3	3488	3158	2610
TCD ppm/°C	10 to 60	51	94	0	<1

Table 12. Sign and Magnitude of d_{33} and p_3

Composition	d_{33} (10^{-12} pC/N)	p_3 ($\mu C/m^2 \cdot °K$)
$2BaO-3SiO_2-TiO_2$	+ 7	+ 8
$1.9BaO-0.1PbO-3SiO_2-TiO_2$	+ 7	+ 8
$2BaO-0.15CaO-2.9SiO_2-TiO_2$	+ 6	+ 6
$1.6BaO-0.4CaO-2.8SiO_2-TiO_2$	+ 6	+ 5.5
$1.6BaO-0.4SrO-3SiO_2-TiO_2-0.2$ CaO	+ 6	+ 4.5
$BaO-GeO_2-TiO_2$	+ 6	- 2
$2SrO-3SiO_2-TiO_2$	+14	+ 8
$1.8SrO-0.2BaO-2.8SiO_2-0.1CaO-TiO_2$	+10	+ 7
$Li_2O-2SiO_2$	- 1	--
$Li_2O-2SiO_2-0.2ZnO$	- 4	- 3.0
$Li_2O-1.95SiO_2-0.05Fe_2O_3$	- 3	--
$Li_2O-3B_2O_3$	+ 3	--
$Li_2O-1.8SiO_2-0.2B_2O_3$	+ 6	-11.0
$Li_2O-1.7SiO_2-0.3B_2O_3$	+ 5	-10.0
$Li_2O-1.6SiO_2-0.4B_2O_3$	+ 5	-10.0
$Li_2O-1.8SiO_2-0.1(ZnO,B_2O_3)$	- 2	--

Table 13. Eight Combinations of Piezoelectric and Pyroelectric Properties

Case	Growth habit* Sign of d_{33}		Sign of d_{33}	sign of p_3		d_{33} of Composite	p_3 of Composite	Resultant Properties
	Phase I	Phase II		Phase I	Phase II			
a	+	+	+	+	+	$^1v^1d_{33}+^2v^2d_{33}$	$+(^1v^1p_3+^2v^2p_3)$	piezo and pyro
	+	+		-	-	$^1v^1d_{33}+^2v^2d_{33}$	$-(^1v^1p_3+^2v^2p_3)$	
b	+	+	+	+	-	$^1v^1d_{33}+^2v^2d_{33}$	$+^1v^1p_3-^2v^2p_3$	piezo but nonpyro
	+	+		-	+	$^1v^1d_{33}+^2v^2d_{33}$	$-^1v^1p_3+^2v^2p_3$	
c	+	-	+	+	+	$^1v^1d_{33}-^2v^2d_{33}$	$+^1v^1p_3-^2v^2p_3$	nonpiezo and nonpyro
	+	-		-	-	$^1v^1d_{33}-^2v^2d_{33}$	$-^1v^1p_3+^2v^2p_3$	
d	+	-	+	+	-	$^1v^1d_{33}-^2v^2d_{33}$	$+(^1v^1p_3+^2v^2p_3)$	pyro but nonpiezo
	+	-		-	+	$^1v^1d_{33}-^2v^2d_{33}$	$-(^1v^1p_3+^2v^2p_3)$	

*Sign of d_{33} measured on the initial crystallizing surface. Eight more combinations can be obtained with a negative d_{33} sign for phase I.

fig 1

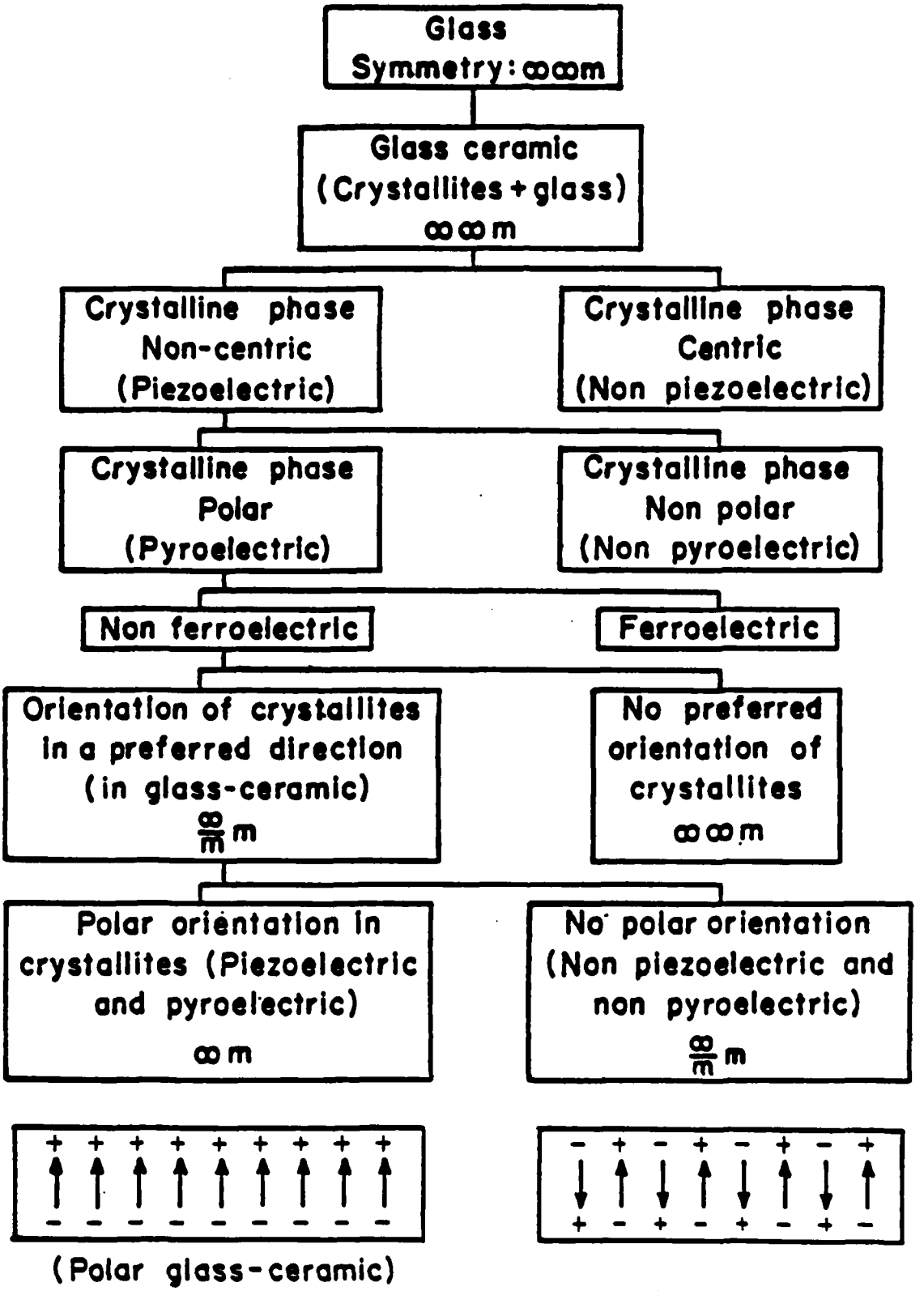
Glass
Symmetry: ∞∞m
Glass ceramic
(Crystallites + glass)
∞∞m
Crystalline phase
Non-centric
(Piezoelectric)
Crystalline phase
Centric
(Non piezoelectric)
Crystalline phase
Polar
(Pyroelectric)
Crystalline phase
Non polar
(Non pyroelectric)
Non ferroelectric
Ferroelectric
Orientation of crystallites
in a preferred direction
(in glass-ceramic)
∞/m m
No preferred
orientation of
crystallites
∞∞m
Polar orientation in
crystallites (Piezoelectric
and pyroelectric)
∞m
No polar orientation
(Non piezoelectric and
non pyroelectric)
∞/m m
(Polar glass-ceramic)

Fig 2

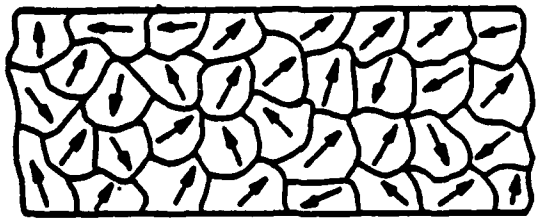

(a)

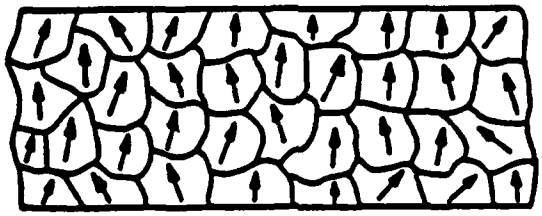

(b)

(c)

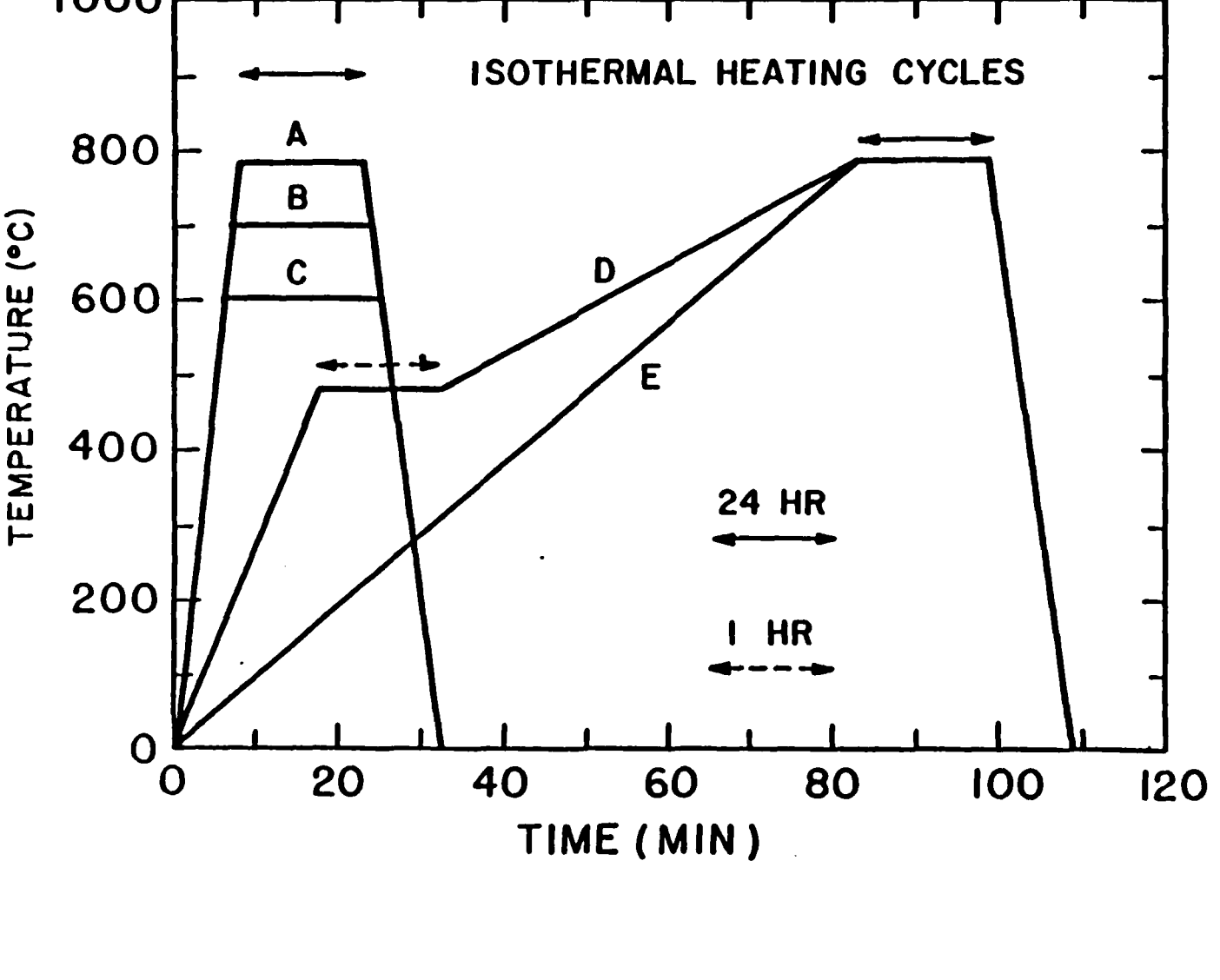
ISOTHERMAL HEATING CYCLES
A
B
C
D
E
24 HR
1 HR
TEMPERATURE (°C)
TIME (MIN)
0
200
400
600
800
1000
0
20
40
60
80
100
120

Fig 4

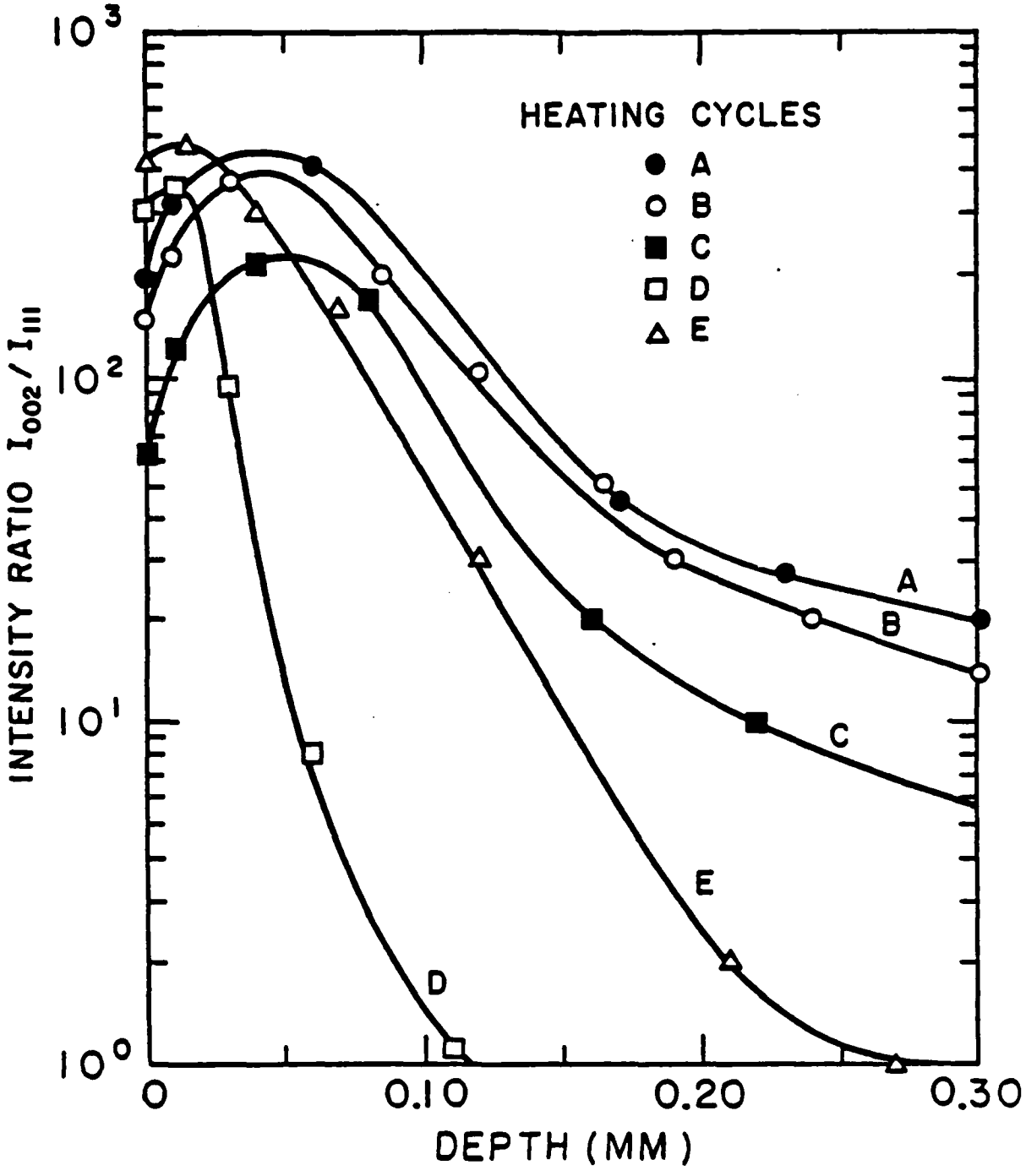
HEATING CYCLES
A
B
C
D
E
INTENSITY RATIO I_{002}/I_{111}
10^3
10^2
10^1
10^0
0
0.10
0.20
0.30
DEPTH (MM)

fig 5(a)

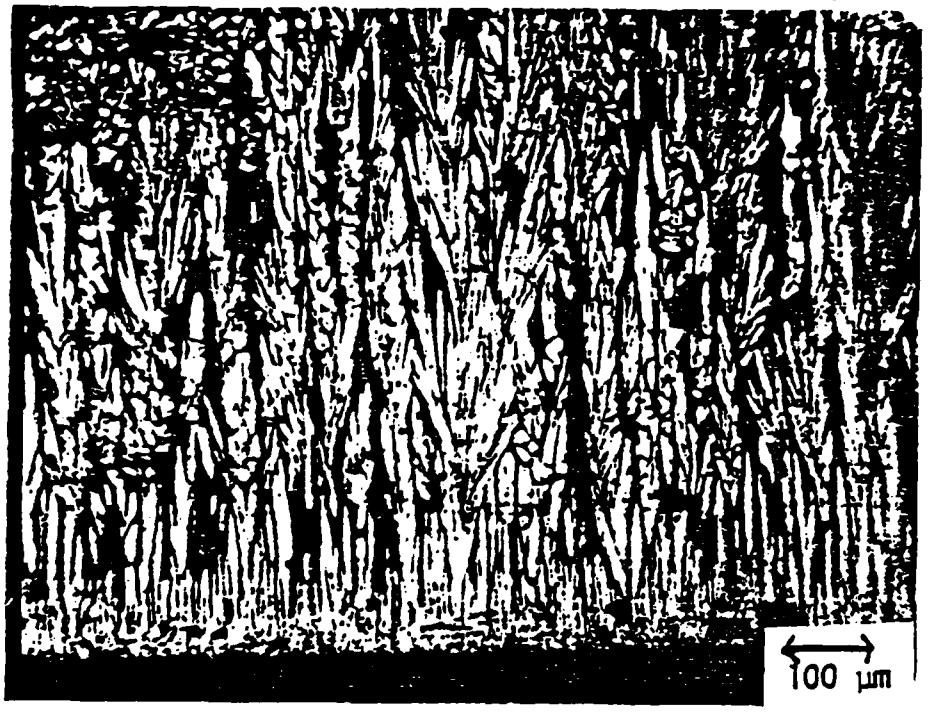

fig 5 (b)

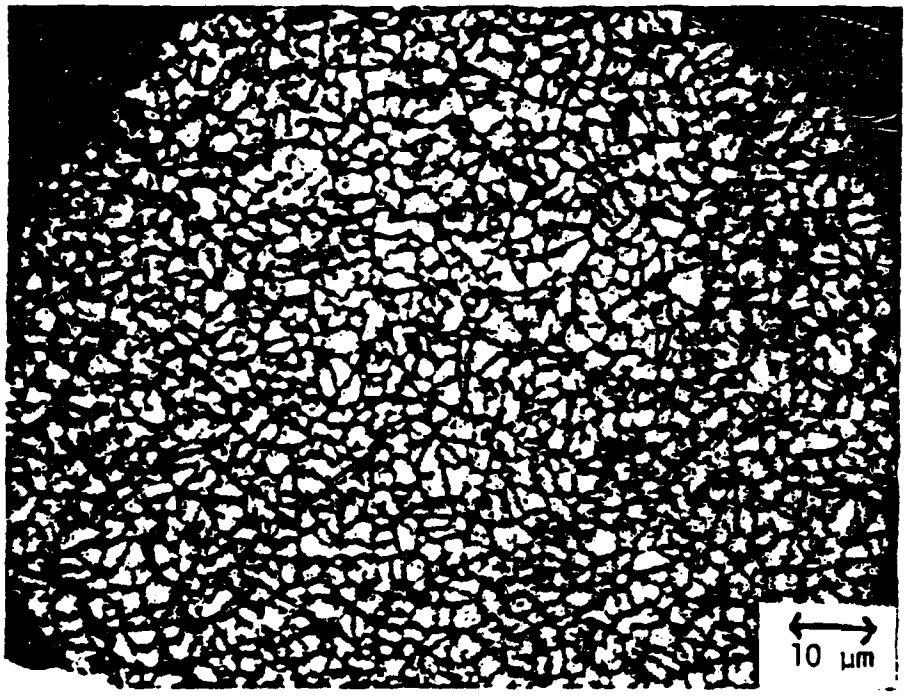

Fig 6

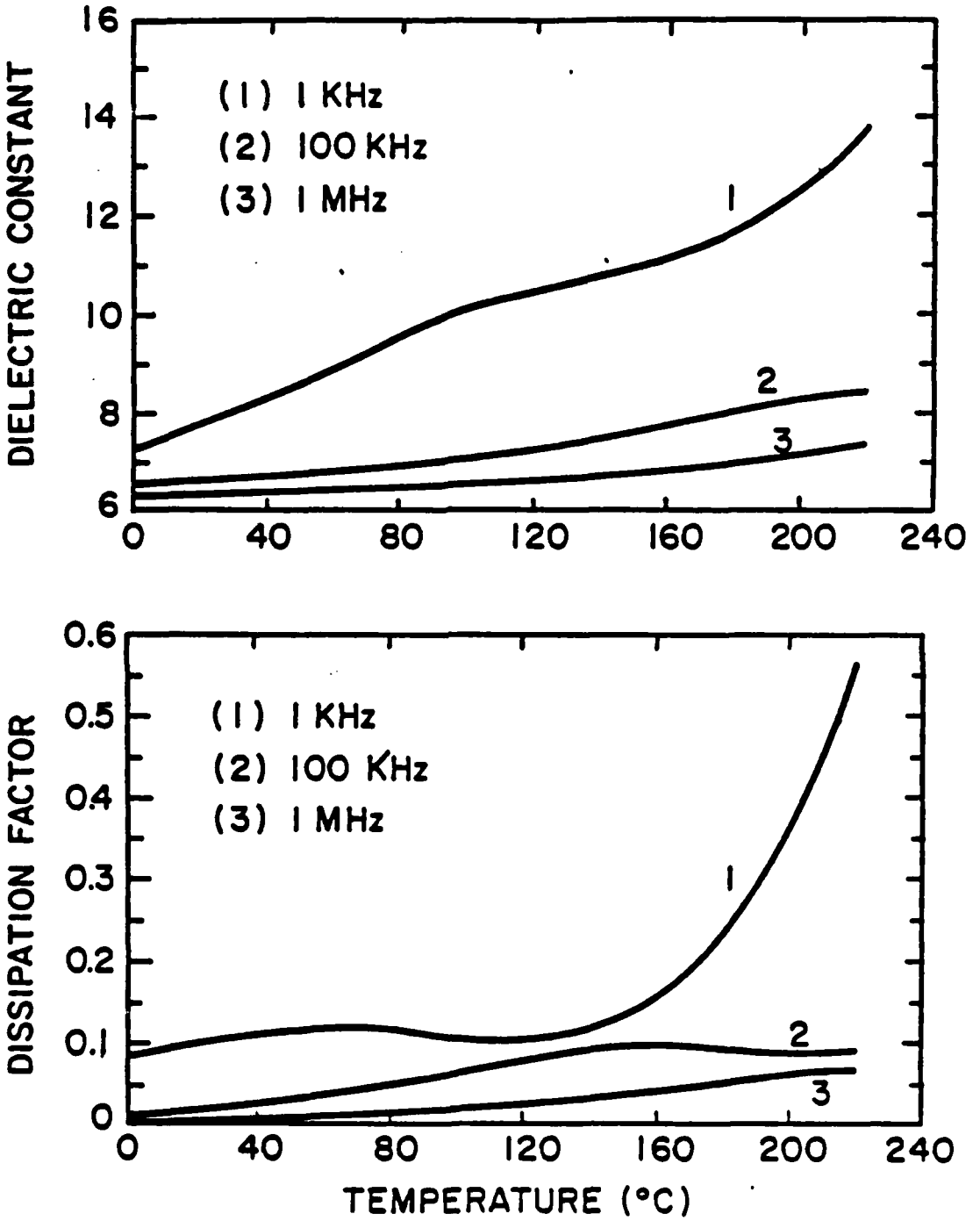
DIELECTRIC CONSTANT
16
14
12
10
8
6
(1) 1 KHz
(2) 100 KHz
(3) 1 MHz
1
2
3
0
40
80
120
160
200
240
DISSIPATION FACTOR
0.6
0.5
0.4
0.3
0.2
0.1
0
(1) 1 KHz
(2) 100 KHz
(3) 1 MHz
1
2
3
0
40
80
120
160
200
240
TEMPERATURE (°C)

fig 7

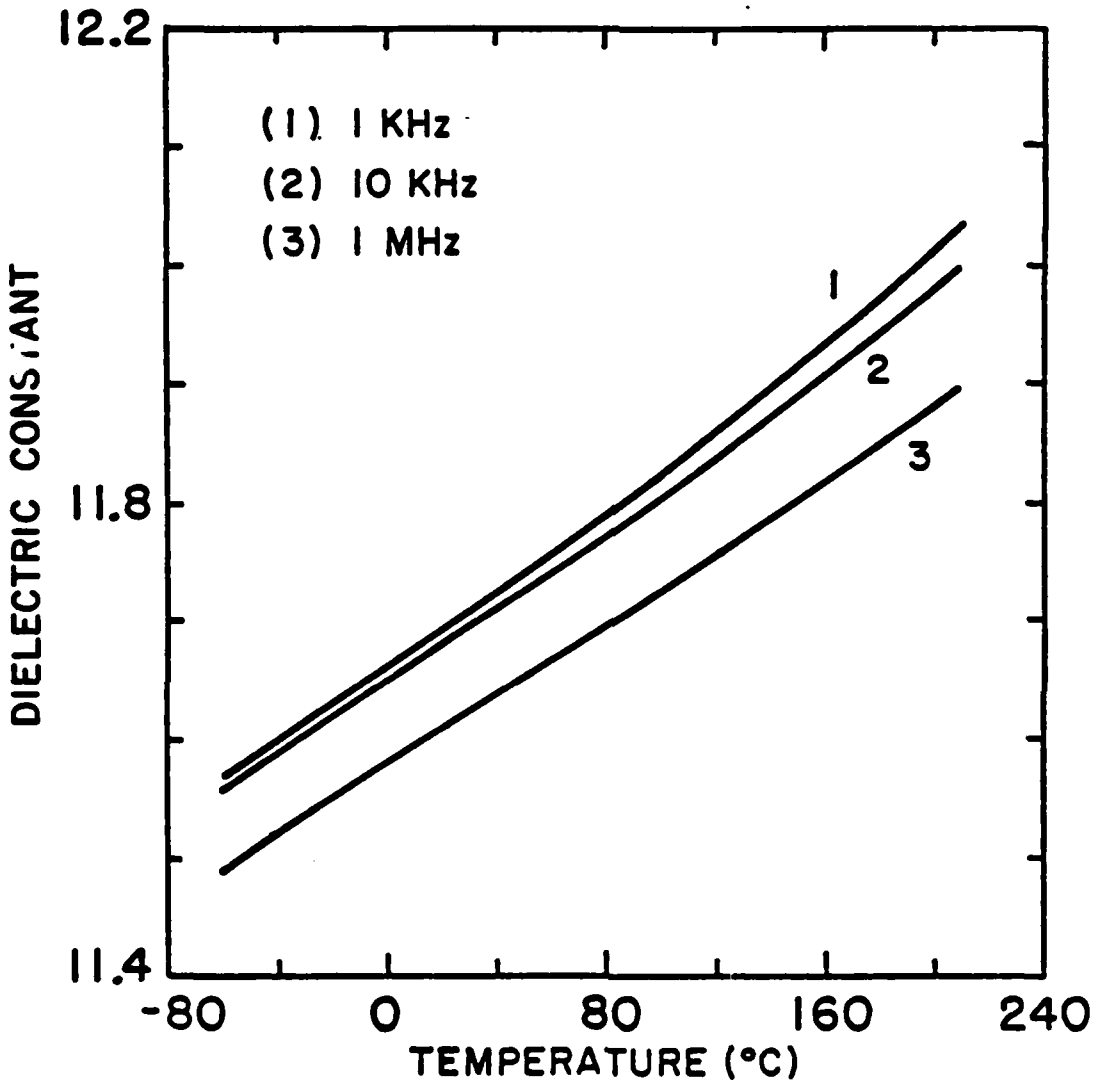
12.2
11.8
11.4
DIELECTRIC CONSTANT
(1) 1 KHz
(2) 10 KHz
(3) 1 MHz
1
2
3
-80
0
80
160
240
TEMPERATURE (°C)

fig 8

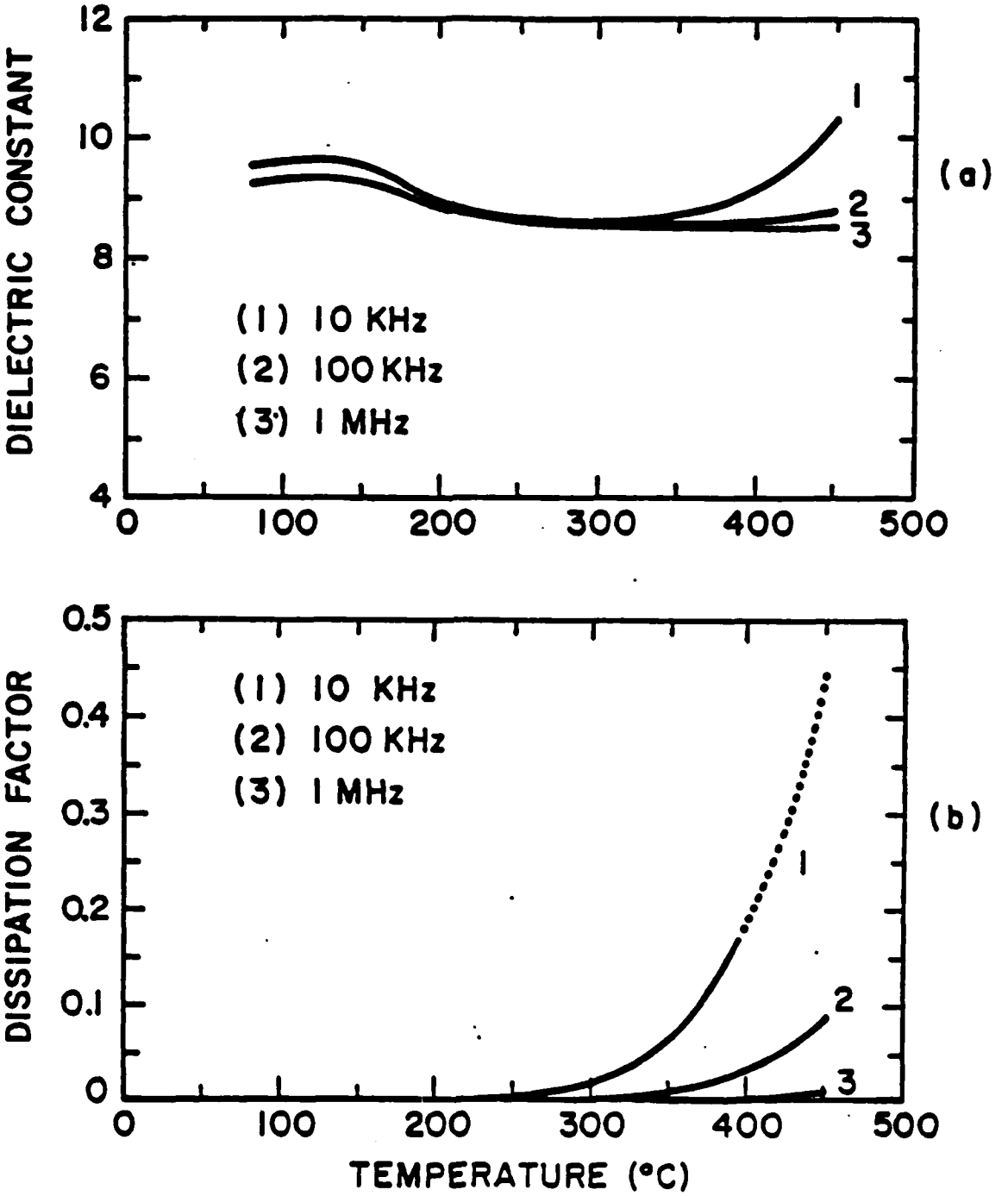
DIELECTRIC CONSTANT
12
10
8
6
4
0
100
200
300
400
500
1
2
3
(1) 10 KHz
(2) 100 KHz
(3) 1 MHz
(a)
DISSIPATION FACTOR
0.5
0.4
0.3
0.2
0.1
0
(1) 10 KHz
(2) 100 KHz
(3) 1 MHz
(b)
TEMPERATURE (°C)

Fig 9

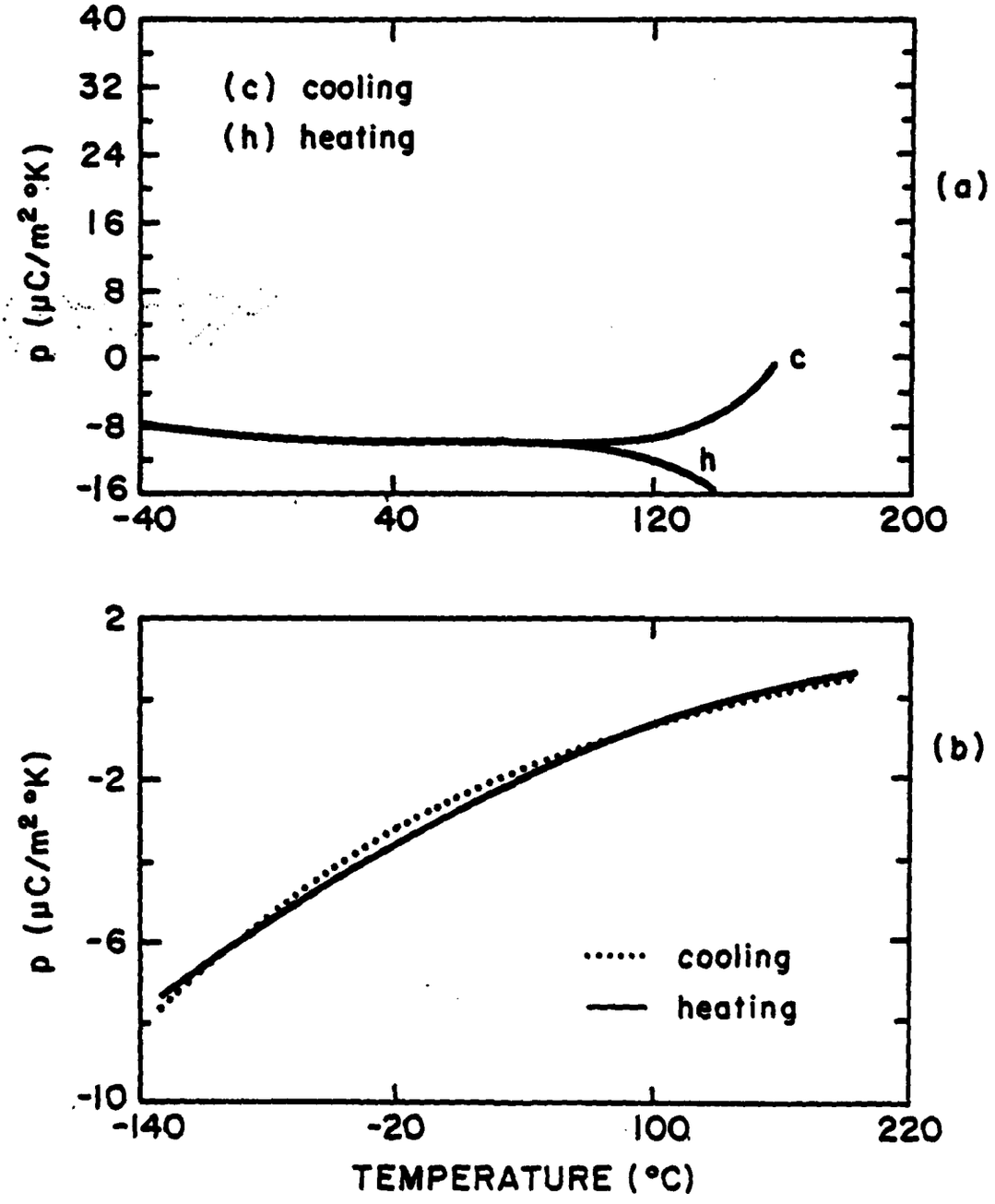
40
32
24
16
8
0
-8
-16
p (μC/m² °K)
(c) cooling
(h) heating
c
h
(a)
-40
40
120
200
2
-2
-6
-10
p (μC/m² °K)
cooling
heating
(b)
-140
-20
100
220
TEMPERATURE (°C)

fig 10

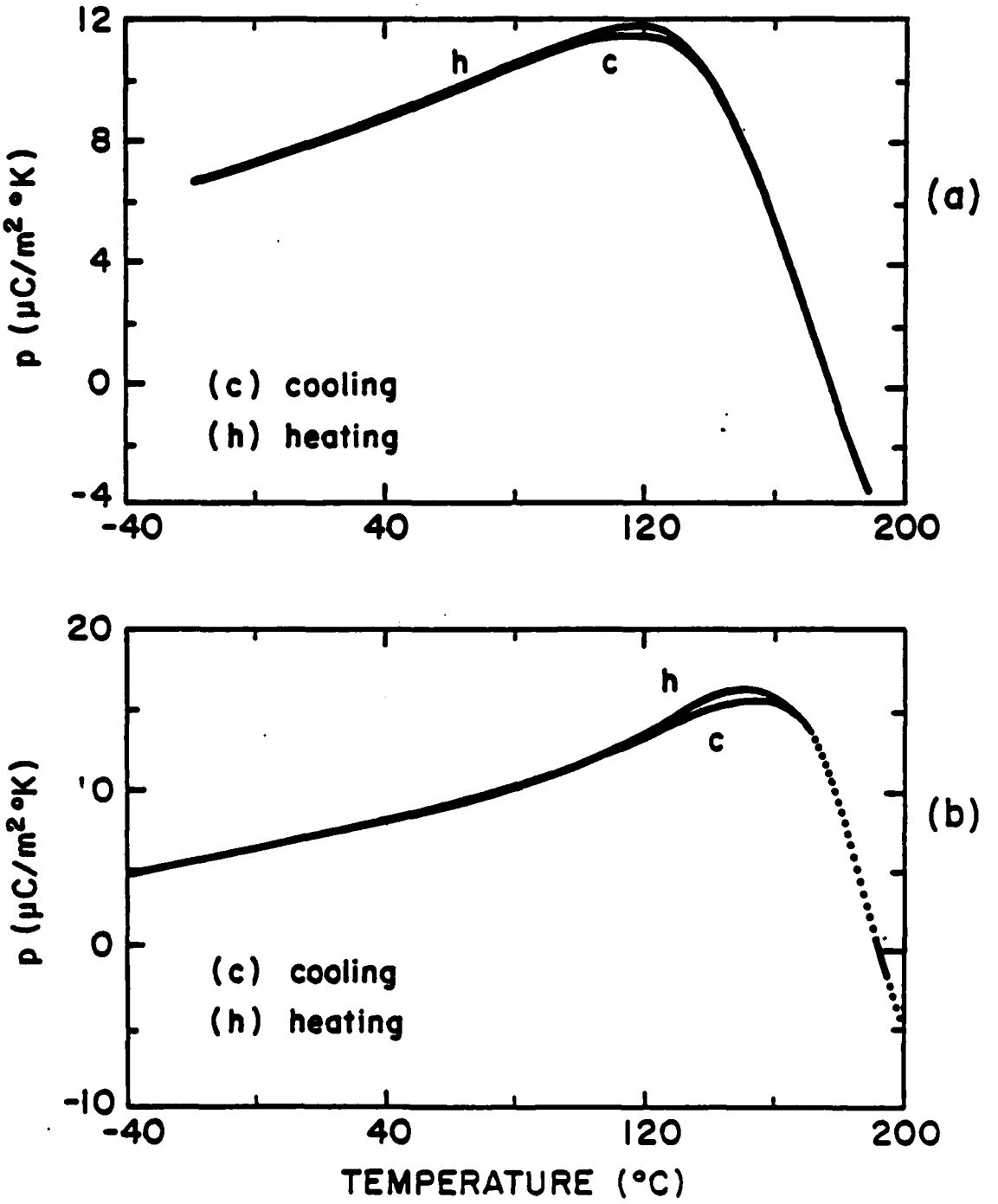
12
8
4
0
-4
h
c
(c) cooling
(h) heating
p (μC/m²°K)
-40
40
120
200
(a)
20
10
0
-10
h
c
(c) cooling
(h) heating
p (μC/m²°K)
-40
40
120
200
(b)
TEMPERATURE (°C)

fig 11

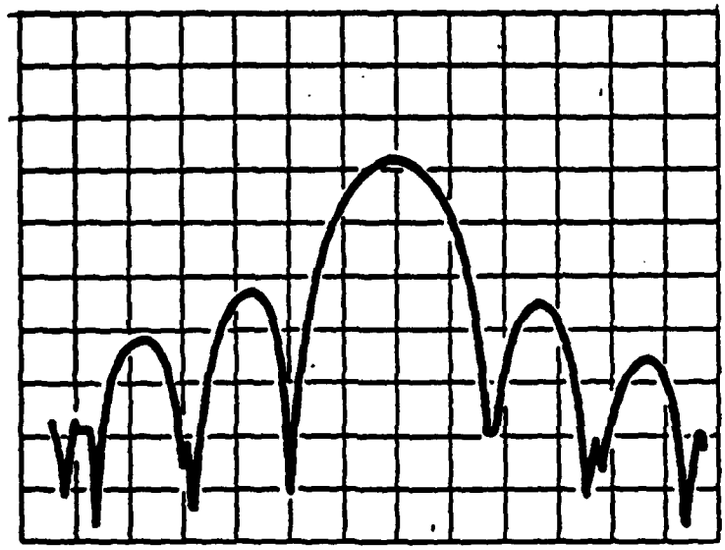

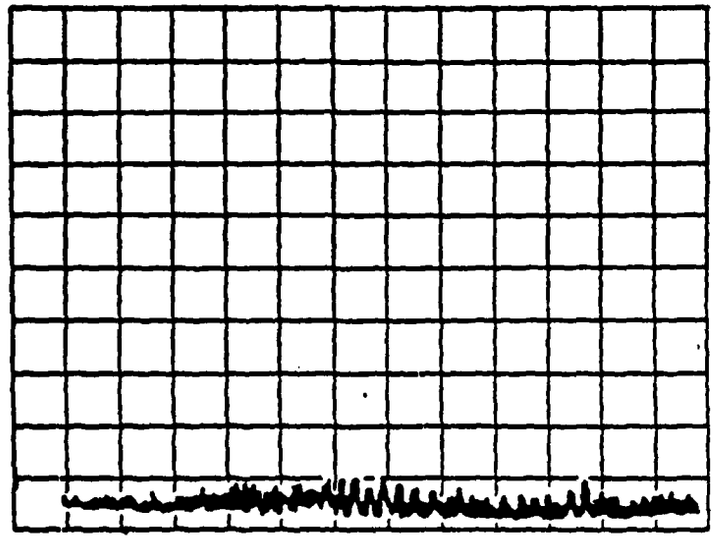

Fig 12

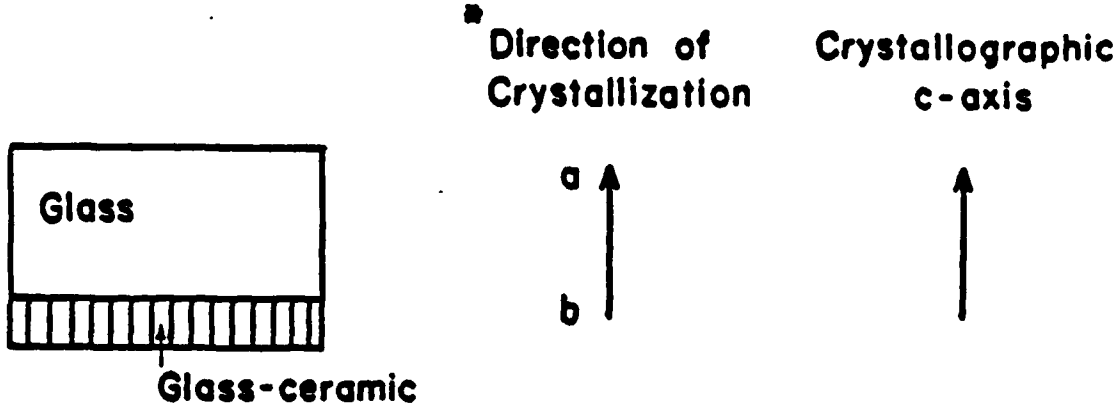

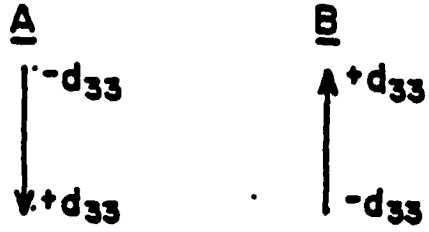

Two types of polar growth behavior

A	B
$Li_2O-B_2O_3$	$Li_2O-2SiO_2$
$Li_2O-SiO_2-B_2O_3$	Li_2O-SiO_2-ZnO
$Ba_2TiSi_2O_8$	$Li_2O-SiO_2-Fe_2O_3$
$Ba_2TiGe_2O_8$	
$Sr_2TiSi_2O_8$	

* b is the high temperature end of temperature gradient axis.

APPENDIX 2

New Glass Ceramics for Pyroelectric Devices

A. Halliyal, A.S. Bhalla, L.E. Cross and R.E. Newnham

(Submitted to J. Am. Cer. Soc.)

NEW GLASS CERAMICS FOR PYROELECTRIC DEVICES

A. Halliyal, A.S. Bhalla*, L.E. Cross* and R.E. Newnham*

Materials Research Laboratory
The Pennsylvania State University
University Park, PA 16802

ABSTRACT

Pyroelectric properties of a new family of materials - polar glass-ceramics are described in this paper. These glass-ceramics are prepared by heat treating a glass to convert it into a glass-ceramic consisting mainly of a grain oriented polar crystalline phase. The dielectric and pyroelectric properties of several compositions in the systems Li_2O-SiO_2-B_2O_3, BaO-SiO_2-TiO_2, and SrO-SiO_2-TiO_2 have been investigated to obtain glass ceramics with crystallites of $Li_2Si_2O_5$, $Li_2B_4O_7$, Li_2SiO_3, $Ba_2TiGe_2O_8$, $Ba_2TiSi_2O_8$ or $Sr_2TiSi_2O_8$ oriented along their polar c-axis. The pyroelectric figures of merit of polar glass-ceramics are discussed and compared with state-of-the-art pyroelectric materials. The figures of merit of polar glass-ceramics are approximately 40 to 60% of those of $LiTaO_3$.

I. INTRODUCTION

Recently a new technique for preparing glass-ceramics with oriented crystallites of a polar phase has been investigated extensively with the objective of fabricating inexpensive large area sensor elements for application in pyroelectric detectors and piezoelectric devices[1-4]. Using a suitable thermal processing, glass is converted into a glass-ceramic consisting of a grain oriented polar crystalline phase in a glass matrix. The macroscopic polarity thus developed gives rise to both piezoelectric and

*Member of the American Ceramic Society.

pyroelectric activity with markedly different properties from those of poled ferroelectric ceramics. Several glass forming polar materials have been prepared in polar glass-ceramic form and their piezoelectric and pyroelectric properties have been studied in our Laboratory[5]. Our earlier studies showed that polar glass-ceramics are promising candidate materials for piezoelectric resonators[3], surface acoustic wave (SAW) devices[6] and hydrophones[3]. The present paper is focussed on the pyroelectric properties of polar glass-ceramics. In the next section, a brief discussion of the properties and pyroelectric figures of merit of state-of-the-art materials is given. In subsequent sections, the preparation of polar glass-ceramics and an evaluation of their pyroelectric figures of merit are presented. The advantages and limitations of preparing pyroelectric elements by glass-ceramic route are discussed in the final section.

II. PYROELECTRIC MATERIALS

Pyroelectric effect is quite frequently used for the detection of infrared radiation. Even though the detectivity (D*) of pyroelectric materials are two to three orders of magnitude smaller than those of cooled photoconductive detectors, the advantage of operating at room temperature and lower cost makes the pyroelectric detectors more versatile. This has led to the extensive use of pyroelectric detectors for military and commercial applications such as in intruder alarms, forest fire mapping and thermal imaging devices (vidicons)[7]. The optimum property requirements for a pyroelectric target material have been reviewed in detail by a number of authors[8-12]. Properties of both single crystals such as triglycine sulfate (TGS), $LiTaO_3$, $Pb_5Ge_3O_{11}$, $Sr_{0.5}Ba_{0.5}Nb_2O_6$ and of ceramics such as $PbZr_{0.5}Ti_{0.5}O_3$, modified $PbTiO_3$ and $PbZrO_3$ have been evaluated for pyroelectric devices[11].

It is desirable, when comparing the properties of pyroelectric materials to define appropriate figures of merit for the particular application of interest. A few of the commonly used figures of merit[10,11] are listed in Table I. In general to achieve high detectivity, it is desirable to use a material which has a high pyroelectric coefficient and low dielectric constant, low dissipation factor, low density, low specific heat and low thermal diffusivity. Also the choice of material for a pyroelectric detector is not always straightforward, it depends on the size of the required detector and the intended frequency of operation. Environmental conditions (particularly temperature range), maximum incident power and cost must also be considered. The detecting element must be thin ($\simeq$30 μm) which means that the material should withstand the fabrication process and handling or should be suitable for preparing in the form of thin sheet. The dielectric and physical properties of important pyroelectric materials are given in Table II and their corresponding figures of merit are listed in Table III[11-12].

Triglycine sulfate [TGS = $(NH_2CH_2COOH)_3H_2SO_4$] is used widely because of its high figure of merit. However, it is water soluble and hygroscopic and rather fragile, and hence demands special precautions when it is being processed. The lower Curie temperature of TGS (49°C) is a major disadvantage. Some of these problems can be partially overcome by using alanine doped TGS or deuterated TGS. In spite of these problems, materials in the TGS family remain the favored materials for applications where sensitivity is of prime importance.

The figures of merit of lithium tantalate $LiTaO_3$ are lower than TGS because of its lower pyroelectric coefficient. It has advantages, however, of a very high Curie temperature and insolubility in water. Good quality single crystals of $LiTaO_3$ can be grown by the Czochralski technique, and hence it is

used widely for pyroelectric detectors. Recent work by Whatmore et al.[11,13] has shown that ceramics in the uranium doped $PbZrO_3$-$PbTiO_3$-$PbFeNbO_6$ system are very promising for pyroelectric detectors.

III. POLAR GLASS-CERAMICS

Large area targets are desirable in pyroelectric devices used in thermal imaging such as vidicons. It is difficult to grow large area single crystals or to prepare large area ceramics with uniform and reproducible microstructure and properties. In that respect polar glass-ceramic offer an attractive alternative technique to prepare large area pyroelectric targets. In the present work, glass-ceramics containing only polar but non-ferroelectric crystalline phases were considered in order to avoid the problems associated with poling and ageing encountered in ferroelectric materials. Another advantage of using non-ferroelectric materials is that they can be used at higher temperature unlike ferroelectric materials which lose their pyroelectric properties above the ferroelectric Curie temperature[5].

Glass Forming Systems

To aid in the identification of useful pyroelectrics, the properties of several polar materials were examined according to the following criteria. (1) The material should belong to one of the ten polar point groups. (2) It should form glass easily. (3) After processing, the crystallites in the glass-ceramics should show both crystallographic and polar orientation. (4) The glass-ceramic should have good physical integrity.

From several polar glass forming systems tested, six satisfied most of these requirements. The point group symmetry, dielectric, and pyroelectric properties of single crystals of these materials are listed in Table IV. The pyroelectric coefficients of these materials in general are low, compared to those of ferroelectric materials (listed in Table III), but their dielectric constants are also lower compared to those of ferroelectric materials.

AD-A171 409 FERROIC SHAPE MEMORY MATERIALS & PIEZO:PYRO-ELECTRIC ORIENTED RECRYSTALLI..(U) PENNSYLVANIA STATE UNIV UNIVERSITY PARK MATERIALS RESEARCH LA.. 2/2

UNCLASSIFIED R E NEWNHAM ET AL. JUL 86 ARO-18953.15-PH F/G 11/2 NL

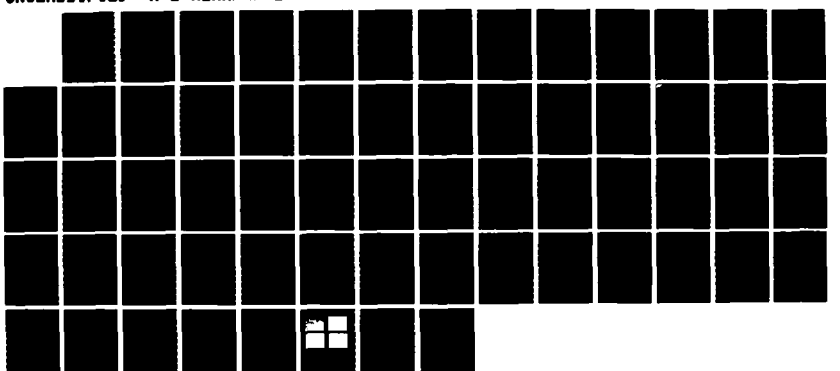

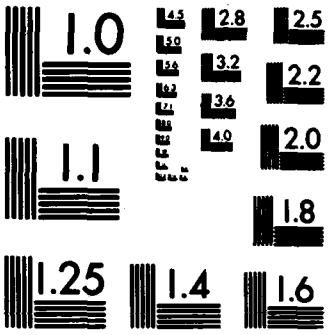

MICROCOPY RESOLUTION TEST CHART
NATIONAL BUREAU OF STANDARDS-1963-A

Pyroelectric properties of these materials listed in Table IV would indicate that these materials do have satisfactory values of the pyroelectric figures of merit.

IV. SAMPLE PREPARATION AND MEASUREMENTS

For the present study, systems listed in Table IV were selected. Because of problems associated with glass formation, crystallographic and polar orientation and mechanical strength of glass-ceramics, a wide range of composition within the system and various additives in small quantities were tested for each of the systems in order to obtain glass-ceramics with desired properties. Optimized compositions are listed in Table V.

Glasses were prepared by mixing reagent grade chemicals followed by melting in a platinum crucible. The temperatures at which glass compositions were melted are listed in Table V. The crystallization temperature of glasses were determined by differential thermal analysis (DTA) measurements. The temperatures where exothermic peaks were observed are shown in Table V. Glass-ceramic samples (approximately 1 cm in diameter) with oriented crystallites were prepared by recrystallizing the glasses in a strong temperature gradient at temperatures 50 to 100°C above the corresponding crystallization temperatures of the glasses. Additional details concerning the sample preparation technique can be found in References 1-5. X-ray diffraction and microstructure studies indicated that needle-like crystals grow from the surface into the bulk of the sample along the direction of temperature gradient. The crystalline phases in the samples were identified by powder x-ray diffraction patterns of glass-ceramics. For dielectric and pyroelectric measurements, samples of 1 cm in diameter and 0.5 to 1 mm thick were prepared in which 200-500 μm crystallites extended from one surface into the interior. The remainder of the glass-ceramic consisted of randomly

oriented crystallites. The samples were lightly polished with 3 μm alumina powder and electroded with sputtered gold film.

Dielectric constant and dissipation factors were measured over a wide range of temperature (-150 to 220°C) and frequency (10^2 to 10^7 Hz), using multifrequency LCR meters*, and a desk-top computer**.

A direct method (Byer and Roundy[18]), was used for measuring pyroelectric coefficients. The measurement was carried out using a desk-top computer with instrument control and data transfer provided by a multi-programmer interface+. The computer controlled the heating or cooling rate through the multiprogrammer and the interface. Pyroelectric current was measured with a picoammeter++. The typical heating or cooling rate was 3-4°/min. Pyroelectric coefficients were calculated in the temperature range -150° to 220°C in both heating and cooling cycles.

V. RESULTS AND DISCUSSION

The glass compositions listed in Table V are optimized compositions with respect to pyroelectric properties and mechanical strength. The crystalline phases for each composition are also listed in the table. All the crystalline phases except Li_2ZnSiO_4 belong to polar point groups. For glass-ceramics which contain crystalline phases, the measured properties represent an average of all the crystalline phases.

The physical and dielectric properties of glass-ceramics are listed in Table VI. The dielectric constant of glass-ceramics lie in the range 5 to 15, comparable to those of corresponding single crystals.

---

*Model 4274A and Model 4275A, Hewlett Packard, Palo Alto, CA.
**Model 9825A, Hewlett Packard, Palo Alto, CA.
+Model 59500A, Hewlett Packard, Palo Alto, CA.
++Model 4140B, Hewlett Packard, Palo Alto, CA.

The variation of pyroelectric coefficient p_3 with temperature for a few selected compositions is shown in Figures 1 and 2. The following trends in the pyroelectric properties are evident (Figures 1 and 2 and properties listed in Table VI and VII).

(1) The room temperature pyroelectric coefficients are in the range of 5 to 10 $\mu C/m^2 \cdot K$.

(2) For lithium borosilicate glass ceramics (Li_2O-B_2O_3-SiO_2), the sign of pyroelectric coefficient is negative and remains practically constant up to 100°C. Above 100°C, the pyroelectric current is masked by large thermal currents.

(3) For $Ba_2TiGe_2O_8$ glass-ceramics, the sign of p_3 is negative at room temperature and increases sharply at lower temperatures. The magnitude to p_3 is about 8 $\mu C/m^2 \cdot K$ at -140°C. There is a change in the sign p_3 at about 130°C. Above 130°C, p_3 is positive and increases with temperature.

(4) In glass-ceramics containing either $Ba_2TiSi_2O_8$ or $Sr_2TiSi_2O_8$ crystallites, the sign of p_3 is positive at room temperature and its magnitude increases slightly with temperature. The sign of p_3 becomes negative at about 180°C, and its magnitude increases with temperature.

Pyroelectric properties of $Ba_2TiGe_2O_8$[16], $Ba_2TiSi_2O_8$[17] and $Li_2B_4O_7$[15] single crystals have been studied extensively. It is difficult to grow defect free $Li_2Si_2O_5$ and $Sr_2TiSi_2O_8$[4] single crystals and there are no reports about the pyroelectric properties of these materials. It is clear that p_3 values of glass ceramics are about 80 to 90% of their respective single crystal values (Table VII). The characteristic variation of p_3 with temperature and the reversal of its sign in $Ba_2TiGe_2O_8$ (at 130°C) and in $Ba_2TiSi_2O_8$ (at 190°C) single crystals has been attributed to the changing balance between primary and secondary pyroelectric effect with temperature in these crystals[16,17].

The positive value of p_3 at room temperature in $Ba_2TiSi_2O_8$ and $Sr_2TiSi_2O_8$ may be due to the dominance of secondary pyroelectric effect. A detailed discussion of pyroelectric properties in these single crystals can be found in references 4, 16 and 17. The above argument also applies to glass-ceramics since the pyroelectric properties of glass-ceramics are due to the oriented cyrstallites of these phases.

The pyroelectric figures of merit of glass-ceramics and single crystals are given in Table VII. The figure of merit M_4 was not calculated because data on thermal diffusivity was not available. A comparison of the figures of merit of glass-ceramics with those of commonly used pyroelectric materials listed in Table III is given below.

The figure of merit M_1 is highest for lithium borosilicate glass-ceramics and is about one-third of $LiTaO_3$. For glass-ceramics in the fresnoite family M_1 is about one-fourth of $LiTaO_3$. The figure of merit M_2 of glass-ceramics is much lower than that of $LiTaO_3$ and other pyroelectric materials, because dielectric constant does not enter in the calculation of M_2. Lithium borosilicate glass-ceramics have higher M_3 (almost half of $LiTaO_3$) than fresnoite glass-ceramics because of their low density and dielectric constants. In the calculation of M_5, both the dielectric constant and tan δ are considered. Tan δ values are very high for lithium borosilicate glass-ceramics ($\simeq$0.05) whereas for fresnoite glass-ceramics tan δ values are very small ($<$0.001). For calculation of M_5, the highest value of tan δ (0.001) was taken for all fresnoite glass-ceramics. M_5 of lithium borosilicate glass-ceramics is very low because of high dielectric losses and those of fresnoite glass-ceramics are about 25% of $LiTaO_3$. Actual values of M_5 of fresnoite glass-ceramics will be slightly higher than the values listed in Table VII, if smaller tan δ values are taken for the calculation.

The pyroelectric figures of merit of most of the glass-ceramics are in the range 40 to 60% of those of $LiTaO_3$.

VI. ADVANTAGES AND LIMITATIONS OF THE TECHNIQUE

The present work demonstrates the possibility of using new polar glass-ceramics for pyroelectric devices. The pyroelectric figures of merit of glass-ceramics were shown to be about half of those currently used in pyroelectric devices. Further improvement in the figures of merit of glass-ceramics can be anticipated either by fine tuning the composition or by improved preparation techniques. Studies in our Laboratory have shown that an oriented region up to 500 μm in length in the glass-ceramic samples can be achieved even by isothermal recrystallization of glasses. This suggests the possibility of preparing large area targets by heating large glass sheets in a furnace. This technique can be applied only to materials which form glass easily. This, however, limits the choice of materials to silicates, germanates and borates if conventional glass melting techniques are followed. If alternative techniques for glass formation (e.g., sputtered glassy films, roller quenching, sol-gel method) are used, it may be possible to synthesize additional polar glass-ceramics.

VII. SUMMARY

The new technique of preparing pyroelectric elements by glass-ceramic route looks promising for preparing large area targets. Polar glass-ceramics from Li_2O-SiO_2-B_2O_3, BaO-GeO_2-TiO_2, BaO-SiO_2-TiO_2 and SrO-SiO_2-TiO_2 systems have been prepared and their dielectric and pyroelectric properties investigated. The pyroelectric figures of merit of glass-ceramics for different applications look promising. Several glass-ceramics showed figures of merit up to 60% of those obtained on $LiTaO_3$ single crystal. The present study demonstrates the possibility of using glass-ceramics and the feasibility of preparing large area sensor elements for pyroelectric devices.

References

1. A. Halliyal, A.S. Bhalla, R.E. Newnham, and L.E. Cross, "$Ba_2TiGe_2O_8$ and $Ba_2TiSi_2O_8$ Pyroelectric Glass-Ceramics," J. Mat. Sci., 16 [4], 1023-1028 (1981).
2. A. Halliyal, A.S. Bhalla, R.E. Newnham, and L.E. Cross, "Polar Glass-Ceramics," 38, 781-784 (1981).
3. A. Halliyal, A. Safari, A.S. Bhalla, R.E. Newnham, and L.E. Cross, "Grain Oriented Glass-Ceramics for Piezoelectric Devices," J. Amer. Ceram. Soc., 67 [5], 331-335 (1984).
4. A. Halliyal, A.S. Bhalla, L.E. Cross, and R.E. Newnham, "Dielectric, Piezoelectric and Pyroelectric Properties of $Sr_2TiSi_2O_8$ Polar Glass-Ceramic: A New Polar Material," J. Mat. Sci., 20 [8], 3745-3749 (1985).
5. A. Halliyal, "Study of the Piezoelectric and Pyroelectric Properties of Polar Glass-Ceramics," Ph.D. Thesis, The Pennsylvania State University (1984).
6. C.W. Lee, L.J. Bowen, J.M. Browne, A. Halliyal, A.S. Bhalla, and E. Yio, "Acoustic Wave Properties of Fresnoite Glass-Ceramics," Proc. IEEE Ultrasonic Symposium, pp. 285-289 (1984).
7. S.G. Porter, "A Brief Guide to Pyroelectric Detectors," Ferroelectrics, 33, 193-206 (1981).
8. E.H. Putley, Semiconductors and Semimetals, Vol. 5, 259-285, Academic Press, New York (1970).
9. S.T. Liu, "Pyroelectric Detectors and Materials," Proc. IEEE, 66 [1], 14-26 (1978).
10. S.T. Liu, "Critical Assessment of Pyroelectric Detectors," Ferroelectrics, 10, 83-89 (1976).

11. R.W. Whatmore, J.M. Herbert, and F.W. Ainger, "Recent Developments in Ferroelectrics for Infrared Detectors," Phys. Stat. Sol. (a), 61, 73-80 (1980).

12. J.M. Herbert, Ferroelectric Transducers and Sensors. Gordon and Breach Science Publishers, New York (1982).

13. R.W. Whatmore and A.J. Bell, "Pyroelectric Ceramics in the Lead Zirconate-Lead Titanate-Lead Iron Niobate System," Ferroelectrics, 35, 155-160 (1981).

14. S. Haussuhl, J. Liebertz, and S. Stah, "Single Crystal Growth and Pyroelectric, Dielectric, Piezoelectric, Elastic and Thermoelastic Properties of Orthorhombic Li_2SiO_3, Li_2GeO_3, and Na_2GeO_3," Crystals Research and Technology, 17 [4], 521-526 (1982).

15. A.S. Bhalla, L.E. Cross, and R.W. Whatmore. "Pyroelectric and Piezoelectric Properties of Lithium Tetraborate Single Crystal," Jpn. J. Appl. Phys. (accepted).

16. A. Halliyal, A.S. Bhalla, and L.E. Cross, "Phase Transitions, Dielectric, Piezoelectric and Pyroelectric Properties of Barium Titanium Germanate $Ba_2TiGe_2O_8$ Single Crystals," Ferroelectrics, 62, 3-9 (1985).

17. A. Halliyal, A.S. Bhalla, S.A. Markgraf, L.E. Cross, and R.E. Newnham, "Unusual Pyroelectric and Piezoelectric Properties of Fresnoite ($Ba_2TiSi_2O_8$) Single Crystals and Polar Glass-Ceramics," Ferroelectrics, 62, 27-38 (1985).

18. R.L. Byer and C.B. Roundy, "Pyroelectric Coefficient Direct Measurement Technique and Application to a NSEC Response Time Detector," Ferroelectrics, 3, 333-338 (1972).

Acknowledgements

It is a pleasure to thank our colleagues at the Materials Research Laboratory for their help in this work. This work was supported by the Army Research Office through contract #DAAG29-83-K-0062 and the National Science Foundation through contract #DMR-8010811.

List of Figures

Table I. Pyroelectric Material Figures of Merit.

Symbol	Expression	Units	Application
M_1	p/K	$C/m^2 \cdot K$	For a quick evaluation of material
M_2	$p/\rho c$	$p/\rho c$	current mode: a thin disc feeding current into a low impedance amplifier
M_3	$p/\rho cK$	Cm/J	voltage mode: a disc supplying voltage to a high impedance amplifier the inherent noise of which limits sensitivity of detector
M_4	$p/\rho cKD$	$C/m \cdot W$	for vidicons
M_5	$p/\rho c\ K^{1/2} \tan \delta^{1/2}$	Cm/J	voltage mode: for a high impedance amplifier when the pyroelectric element is the main source of noise

p = pyroelectric coefficient
K = Dielectric constant
$\tan \delta$ = Dissipation factor
ρ = Density
c = Specific heat per unit mass
c' = specific heat per unit volume ($=\rho c$)
D = thermal diffusivity

Table II. Dielectric and Physical Properties of Selected Pyroelectric Materials*.

Material	K (at 1 kHz)	tan δ (at 1 kHz)	c' J/cm^3•K	T_c •C	D (10^{-7} m^2/s)
Triglycine Sulfate (TGS) at 35°C	55	0.025	2.6	49	2.8
Deuterated Triglycine Sulfate (DTGS) at 40°C	43	0.020	2.4	61	2.9
$LiTaO_3$	54	0.0006	3.2	618	13.0
$Sr_{0.50}Ba_{0.5}Nb_2O_5$ (SBN)	380	0.003	2.1	121	—
PZFN (Hot Pressed Ceramic)**	240	0.003	2.5	250	--

*Mostly from Whatmore et al.[11].
**$PbZrO_3$ ceramics modified with Pb_2FeNbO_6.
K = Dielectric Constant.
c' = specific heat per unit volume.
tan δ = dielectric loss.
T_c = Curie temperature.
D = thermal diffusivity.

Table III. Pyroelectric Figures of Merit of Selected Materials*.

Material	p $\mu C/m^2 \cdot K$	p/K $\mu C/m^2 \cdot K$ M_1	p/c' 10^{-10} Cm/J M_2	p/c'K 10^{-12} Cm/J M_3	$\frac{p}{c'KD}$ 10^{-5} C/m·W M_4	$\frac{p}{c'\sqrt{K \tan \delta}}$ 10^{-10} Cm/J M_5
Triglycine Sulphate (TGS) at 35°C	600	10.91	2.32	4.23	1.51	1.98
Deuterated Triglycine Sulphate (DTGS) at 40°C	540	12.56	2.25	5.23	1.80	2.43
$LiTaO_3$	180	3.27	0.56	1.04	0.08	0.98
$Sr_{0.5}Ba_{0.5}Nb_2O_5$ (SBN)	650	1.71	3.10	0.81	—	2.90
PZFN (Hot Pressed) Ceramic)**	380	1.58	1.52	0.63	—	1.79

*Mostly from Whatmore, et al.[11].
**$PbZrO_3$ ceramics modified with Pb_2FeNbO_6.

Table IV. Dielectric and Pyroelectric Properties.

Material Single Crystal	Point Group	Density g/cc	K_3 1 kHz	tan δ 1 kHz	p $\mu C/m^2 \cdot K$	Ref.
$Li_2Si_2O_5$	mm2	—	—	—	—	
Li_2SiO_3	mm2	—	8.8*	0.01*	21.5	14
$Li_2B_4O_7$	4mm	2.45	10	2.0	-30	15
$Ba_2TiGe_2O_8$	mm2	4.84	11.4	<0.001	-4.0	16
$Ba_2TiSi_2O_8$	4mm	4.45	11.0	<0.001	+10.0	17
$Sr_2TiSi_2O_8$	4mm	—	—	—	—	

*50 kHz.

Table V. Glass Composition, Crystallization Temperatures and Crystalline Phases in Glass-Ceramics.

Composition	Glass Melting Temp. °C	Temp. of Crystallization °C	Crystalline Phases
Li_2O-$2SiO_2$-0.2ZnO	1350	580	$Li_2Si_2O_5$, Li_2ZnSiO_4
Li_2O-$1.8SiO_2$-$0.2B_2O_3$	1250	605, 680	$Li_2Si_2O_5$, $Li_2B_4O_7$, Li_2SiO_3
Li_2O-$1.7SiO_2$-$0.3B_2O_3$	1250	595, 670	$Li_2Si_2O_5$, $Li_2B_4O_7$, Li_2SiO_3
Li_2O-$1.6SiO_2$-$0.4B_2O_3$	1250	625, 665	$Li_2Si_2O_5$, $Li_2B_4O_7$, Li_2SiO_3
BaO-GeO_2-TiO_2	1400	800	$Ba_2TiGe_2O_8$
2BaO-$3SiO_2$-TiO_2	1450	930	$Ba_2TiSi_2O_8$
2BaO-0.15CaO-$2.9SiO_2$-TiO_2	1450	920	$Ba_2TiSi_2O_8$
1.6BaO-0.4CaO-$2.8SiO_2$-TiO_2	1450	930	$Ba_2TiSi_2O_8$
1.6BaO-0.4SrO-$3SiO_2$-0.2CaO-TiO_2	1450	930	$Ba_2TiSi_2O_8$
1.9BaO-0.1PbO-$3SiO_2$-TiO_2	1450	920	$Ba_2TiSi_2O_8$
2SrO-$3SiO_2$-TiO_2	1450	950	$Sr_2TiSi_2O_8$
1.8SrO-0.2BaO-$2.8SiO_2$0.1CaO-TiO_2	1450	940	$Sr_2TiSi_2O_8$

Table VI. Dielectric and Physical Properties of Glass-Ceramics.

Composition	Density g/cc	Specific Heat $J/cm^3 \cdot K$	K_3 1 kHz	tan δ 1 kHz
$Li_2O-2SiO_2-0.2ZnO$	2.47	2.36	6.5	0.008
$Li_2O-1.8SiO_2-0.2B_2O_3$	2.34	2.39	7.0	0.05
$Li_2O-1.7SiO_2-0.3B_2O_3$	2.32	—	7.5	0.05
$Li_2O-1.6SiO_2-0.4B_2O_3$	2.35	—	7.0	0.05
$BaO-GeO_2-TiO_2$	4.78		15	
$2BaO-3SiO_2-TiO_2$	4.01	2.04	9.0	0.001
$2BaO-0.15CaO-2.9SiO_2-TiO_2$	3.98	—	10	0.001
$1.6BaO-0.4CaO-2.8SiO_2-TiO_2$	—	—	10.5	0.001
$1.6\ BaO-0.4SrO-3SiO_2-0.2CaO-TiO_2$	3.87	—	9.8	0.001
$1.9BaO-0.1PbO-3SiO_2-TiO_2$	4.05	2.04	10.0	0.001
$2SrO-3SiO_2-TiO_2$	3.53	—	11.5	0.001
$1.8SrO-0.2BaO-2.8SiO_2-0.1CaO-TiO_2$	3.63	—	10.6	0.001

Table VII. Room Temperature Pyroelectric Figures of Merit of Glass-Ceramics.

Composition	p^* $\mu C/m^2 \cdot K$	p/K $\mu C/m^2 \cdot K$ M_1	p/c' $(10^{-12}$ Cm/J) M_2	$p/c'K$ $(10^{-12}$ Cm/J) M_3	$p/c'\sqrt{K \tan \delta}$ $(10^{-12}$ Cm/J) M_5
$Li_2O-2SiO_2-0.2ZnO$	-3.0	0.46	1.27	0.20	5.6
$Li_2O-1.8SiO_2-0.2B_2O_3$	-11.0	1.57	4.60	0.66	7.8
$Li_2O-1.7SiO_2-0.3B_2O_3$	-10.0	1.33	4.18	0.56	6.8
$Li_2O-1.6SiO_2-0.4B_2O_3$	-10.0	1.43	4.18	0.60	7.1
$BaO-GeO_2-TiO_2$	-2.0	0.13	0.98	0.07	8.0
$2BaO-3SiO_2-TiO_2$	+8.0	0.88	3.92	0.44	41.3
$1.9BaO-0.1PbO-3SiO_2-TiO_2$	+8.0	0.80	3.92	0.39	39.2
$2BaO-0.15CaO-2.9SiO_2-TiO_2$	+6.0	0.60	2.94	0.29	29.0
$1.6BaO-0.4CaO-2.8SiO_2-TiO_2$	+5.5	0.52	2.70	0.26	26.4
$1.6BaO-0.4SrO-3SiO_2-TiO_2-0.2CaO$	+4.5	0.46	2.21	0.23	22.3
$2SrO-3SiO_2-TiO_2$	+8.0	0.70	3.92	0.34	36.6
$1.8SrO-0.2BaO-2.8SiO_2-0.1CaO-TiO_2$	+7.0	0.66	3.343	0.32	33.3
$Li_2B_4O_7$ (Single Crystal)	-30.0	3.0	9.4	0.94	2.10
$Ba_2TiGe_2O_8$ (Single Crystal)	-4.0	0.35	1.97	0.17	18.4
$Ba_2TiSi_2O_8$ (Single Crystal)	+10.0	0.91	4.90	0.45	46.7

*Pyroelectric coefficient measured along c-axis (p_3).

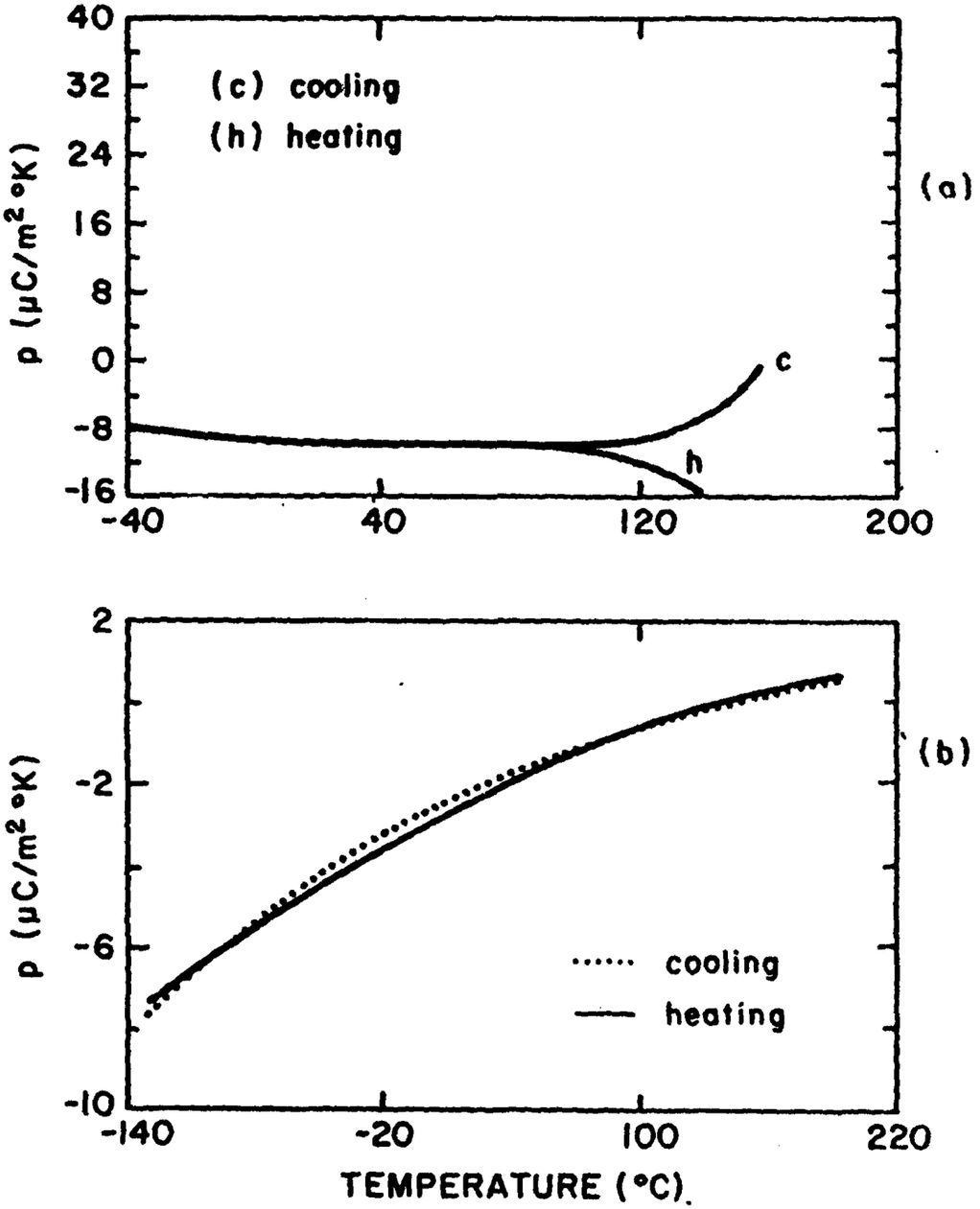
40
32
24
16
8
0
-8
-16
p (μC/m² °K)
(c) cooling
(h) heating
c
h
(a)
-40
40
120
200
2
-2
-6
-10
p (μC/m² °K)
cooling
heating
(b)
-140
-20
100
220
TEMPERATURE (°C)

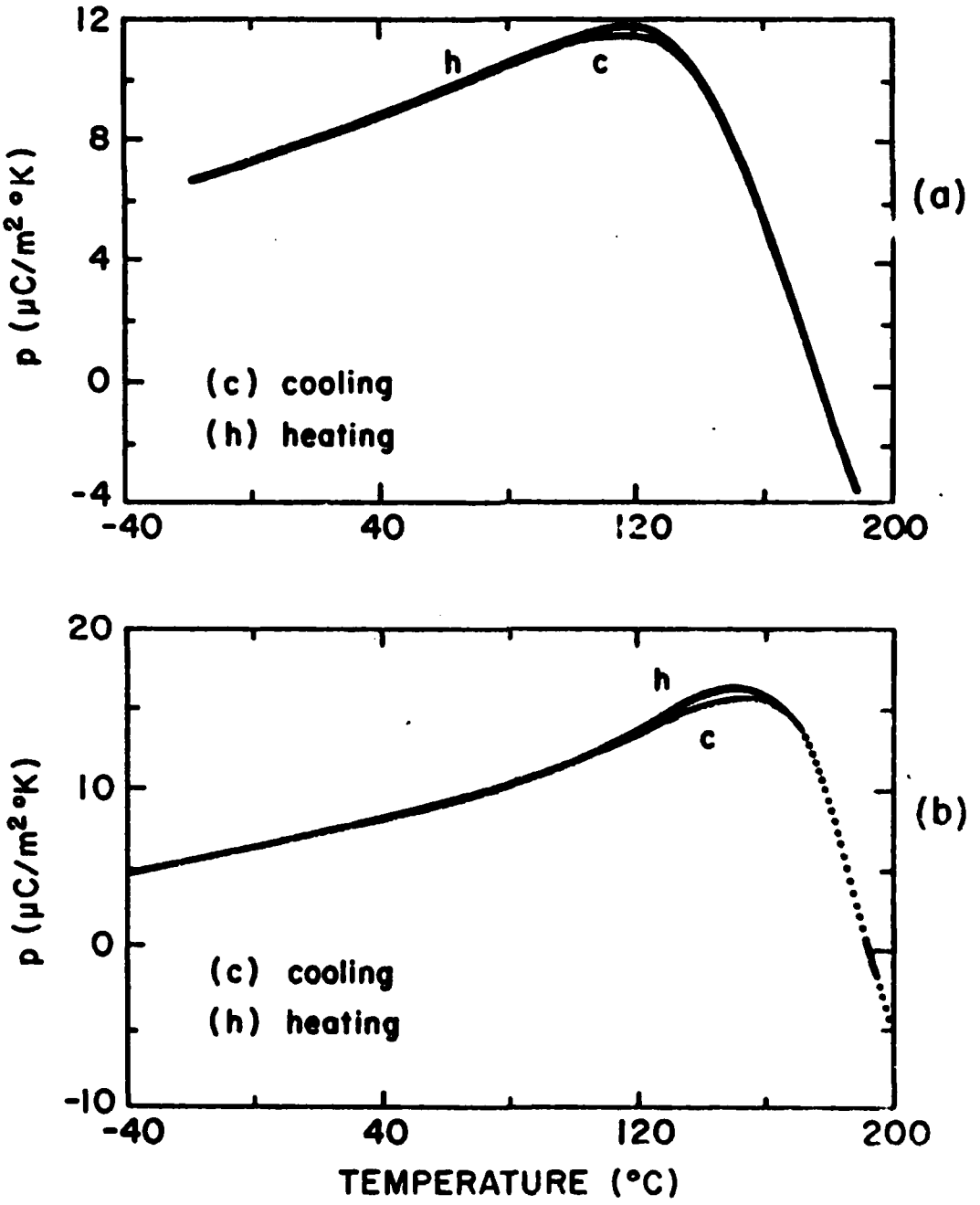
12
8
4
0
-4
p (μC/m² °K)
h
c
(c) cooling
(h) heating
-40
40
120
200
(a)
20
10
0
-10
p (μC/m² °K)
h
c
(c) cooling
(h) heating
-40
40
120
200
TEMPERATURE (°C)
(b)

APPENDIX 3

Unusual Pyroelectric and Piezoelectric Properties of Fresnoite ($Ba_2TiSi_2O_8$) Single Crystal and Polar Glass-Ceramics

A. Halliyal, A.S. Bhalla, S.A. Markgraf, L.E. Cross and R.E. Newnham

Ferroelectrics 62, 27 (1985)

Ferroelectrics, 1985, Vol. 62, pp. 27–38
0015-0193/85/6201–0027/$20.00/0

UNUSUAL PYROELECTRIC AND PIEZOELECTRIC PROPERTIES OF FRESNOITE ($Ba_2TiSi_2O_8$) SINGLE CRYSTAL AND POLAR GLASS-CERAMICS

A. HALLIYAL, A. S. BHALLA, S. A. MARKGRAF, L. E. CROSS and R. E. NEWNHAM

Materials Research Laboratory, The Pennsylvania State University, University Park, PA 16802 U.S.A.

(*Received October 17, 1984*)

The dielectric, piezoelectric and pyroelectric properties of fresnoite ($Ba_2TiSi_2O_8$) single crystal and polar glass-ceramics were studied in the temperature range −150 to 200°C. The sign of pyroelectric coefficient is positive at room temperature and becomes negative at 190°C. The dielectric constant, pyroelectric coefficient and planar coupling coefficient show a maximum value at 160°C and the frequency constant shows a minimum at the same temperature. The probable reasons for the anomaly in these properties are discussed.

INTRODUCTION

Fresnoite ($Ba_2TiSi_2O_8$) has a noncentrosymmetric tetragonal structure and belongs to the polar point group *4mm*. Single crystals of fresnoite have been grown successfully by the Czochralski method by several workers.[1,2] It has been shown that fresnoite has electromechanical coupling factors large enough for piezoelectric devices and that it is an interesting alternative substrate material for surface acoustic wave (SAW) devices.[1,3–5] The SAW characteristics of fresnoite are intermediate between those of $LiNbO_3$ and $LiTaO_3$. The pyroelectric coefficient of fresnoite is reported to be small and positive ($+10\ \mu C/m^2\ °K$). However, no detailed studies have been carried out regarding the temperature variation of piezoelectric and pyroelectric properties of fresnoite. It has also been shown that polar glass-ceramics with the fresnoite crystalline phase can be prepared by recrystallizing glasses of slightly modified compositions.[6,7] In these glass-ceramics, the polar texture results from needle-like fresnoite crystals growing from the glass surface during crystallization. The polar glass-ceramics showed piezoelectric and pyroelectric properties comparable to the single crystal properties.

In the present work, the dielectric, piezoelectric, and pyroelectric properties of fresnoite single crystal and glass-ceramics were studied in more detail. All of the above properties were studied as a function of temperature in the range −150 to 200°C.

EXPERIMENTAL PROCEDURE

Fresnoite crystals were grown by the Czochralski method from a stoichiometric melt. Crystals were grown in a platinum crucible on a ⟨001⟩ seed. Growth conditions were as follows: seed rotation speed 10–15 rpm; pulling speed 1.0 mm/hr, crucible rotation rate: 5 rpm. The resulting boules were colorless and transparent. *c* plates were cut from the boule and circular samples were prepared (5 mm dia, 0.5 mm thick). The major surfaces of the samples were coated with sputtered gold electrodes.

Glass samples containing one mole of excess silica ($2BaO \cdot 3SiO_2 \cdot TiO_2$) were prepared by mixing reagent grade chemicals and melting the batch in a platinum crucible. Glass-ceramic samples were prepared by crystallizing the glasses in a large temperature gradient normal to the surface of glass. The details of sample preparation technique can be found in References 6–8. Microstructure studies indicated that needle-like crystals grow from the surface into the bulk along the direction of temperature gradient. For measurements of all the properties, sections were cut normal to the temperature gradient and gold electrodes were sputtered on the major surfaces.

The dielectric constant and dissipation factors were measured at different frequencies using a capacitance bridge. Pyroelectric coefficients were determined by the

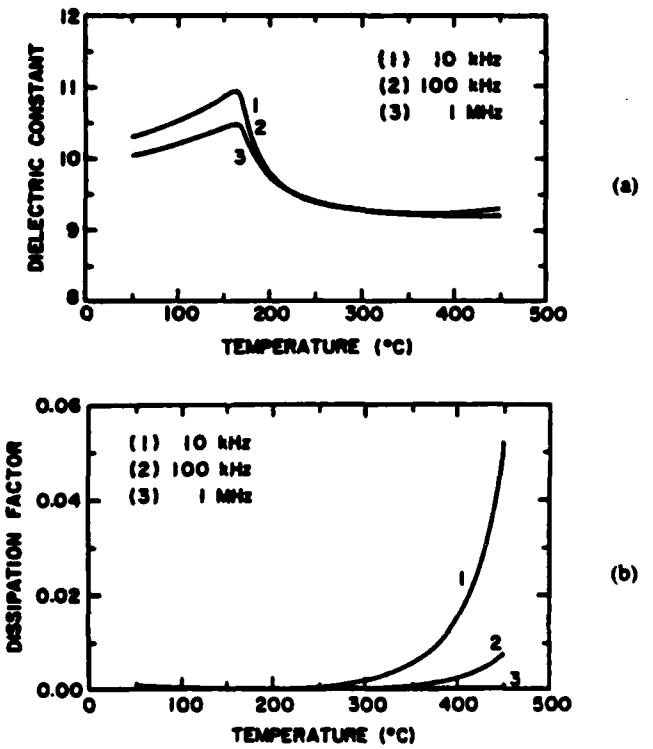

FIGURE 1 Dielectric constant (a) and dissipation factor (b) of $Ba_2TiSi_2O_8$ single crystal as a function of temperature and frequency.

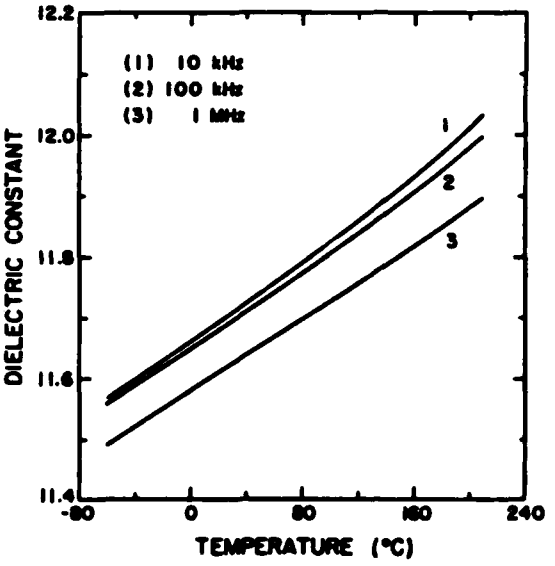

FIGURE 2 Dielectric constant of $2BaO\text{-}3SiO_2\text{-}TiO_2$ glass a function of temperature and frequency.

Byer–Roundy[9] technique. The heating and cooling rates employed were 4°C/min. The electromechanical properties were determined by standard resonance techniques. All the above properties were measured as a function of temperature in the range −150 to 200°C, both in heating and cooling cycles. Piezoelectric d_{33} coefficients were measured using a Berlincourt-d_{33} meter.

RESULTS

The dielectric constant and dissipation factor of fresnoite single crystals are shown in Figure 1. A broad peak was observed in the dielectric constant near 160°C and remained practically constant above 200°C. Surprisingly, no corresponding peak was observed in the dissipation factor curve. The dielectric losses increased at higher temperature, probably due to conduction losses. The dielectric constant of fresnoite glass (Figure 2) increases almost linearly with temperature without showing an anomaly in the temperature range −80 to 200°C. The dielectric spectrum of fresnoite glass-ceramic (Figure 3) is very similar to that of fresnoite single crystal, except that the dielectric constant peak occurs at 120°C instead of 160°C. In the glass-ceramic the only crystalline phase present was fresnoite, which indicates that the anomaly observed in the dielectric constant is an intrinsic property of fresnoite. The difference in the temperature of about 40° in the peak positions of dielectric constant of single crystal and glass-ceramics might be because of nonstoichiometric composition of glass-ceramics.

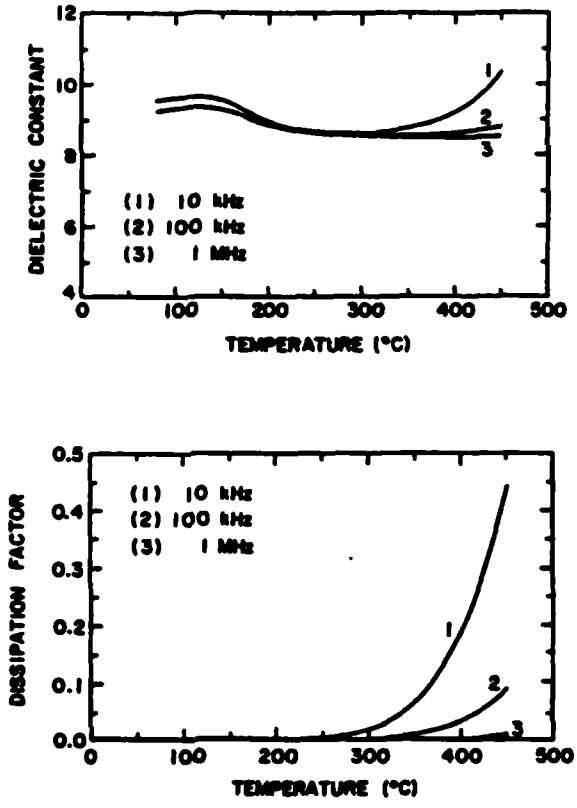

FIGURE 3 Dielectric constant (a) and dissipation factor (b) of $2BaO\text{-}3SiO_2\text{-}TiO_2$ glass-ceramic as a function of temperature and frequency.

The variation of pyroelectric coefficient p_3 of fresnoite single crystal as a function of temperature is shown in Figure 4. The pyroelectric coefficient is positive at room temperature and increases with temperature, reaching a maximum at 160°C. At still higher temperatures, p_3 decreases very quickly and becomes negative. A similar behavior is observed in glass-ceramics also (Figure 5). The variation of polarization (P) with temperature is shown in Figure 6, where P is arbitrarily taken as zero at −140°C. The polarization increases with temperature in accordance with the positive sign of p_3. A broad peak in polarization is observed at 160°C and beyond this temperature polarization decreases with temperature giving a negative pyroelectric coefficient.

The variation of planar mode frequency constant N_p and coupling coefficient k_p for single crystal and glass-ceramic are shown in Figures 7 and 8 respectively. For single crystal, the frequency constant decreases with temperature showing a minimum at 160°C and increasing sharply above 160°C. The coupling coefficient shows a maximum at 160°C. A similar behavior is observed in the case of glass-ceramics with the minimum in N_p occurring at 120°C. At the inflection point, the value of

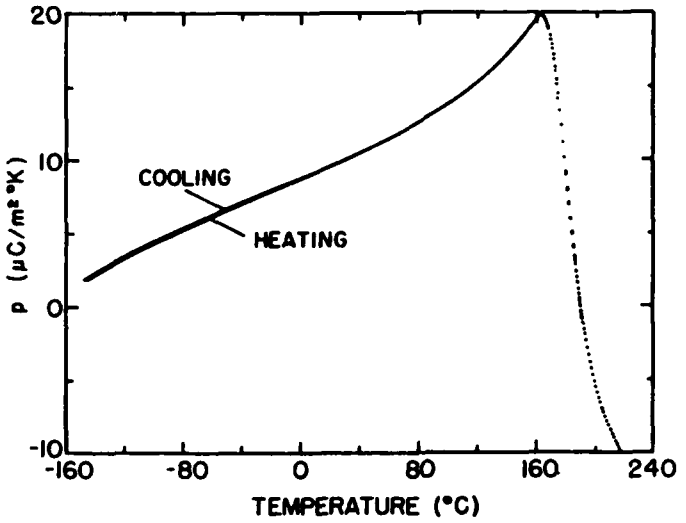

FIGURE 4 Variation of pyroelectric coefficient (p_3) of $Ba_2TiSi_2O_8$ single crystal as a function of temperature.

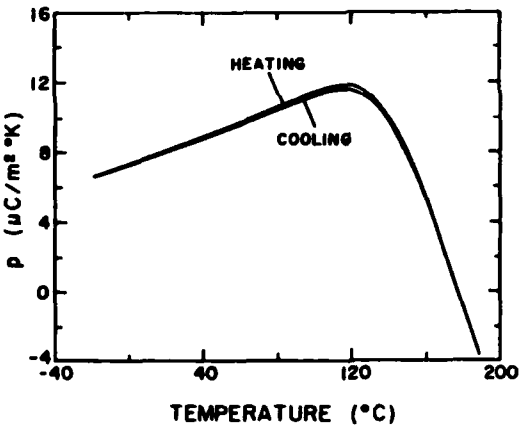

FIGURE 5 Pyroelectric coefficient as a function of temperature for $2BaO\text{-}3SiO_2\text{-}TiO_2$ glass-ceramics.

temperature coefficient of resonance (TCR), defined as

$$\text{TCR} = \frac{1}{f_r}\frac{\partial f_r}{\partial T} \tag{1}$$

is zero. Here, f_r is the resonance frequency at temperature T.

It should be noted that the minimum in N_p and the maximum in the pyroelectric coefficient and dielectric constant occur at the same temperature. The critical temperature where the anomaly in the above properties occurs is 160°C for single

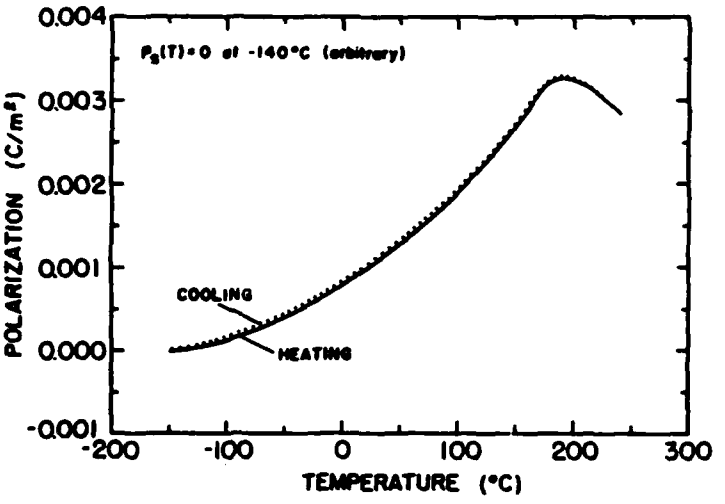

FIGURE 6 Polarization of $Ba_2TiSi_2O_8$ single crystal as a function of temperature.

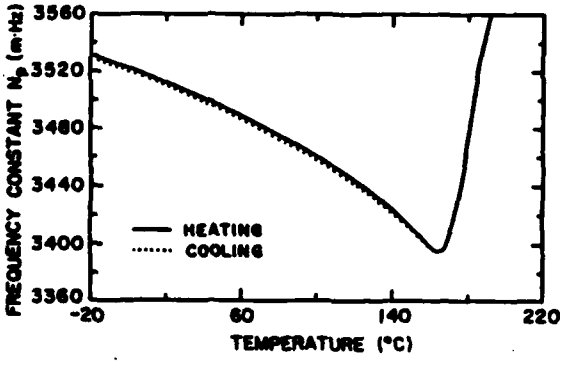

(a)

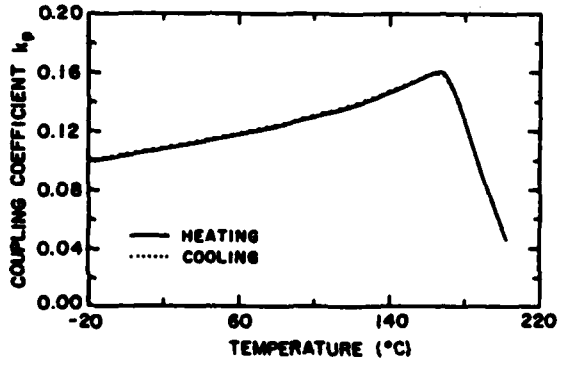

(b)

FIGURE 7 Frequency constant N_p (a) and electromechanical coupling k_p (b) of $Ba_2TiSi_2O_8$ single crystal as a function of temperature.

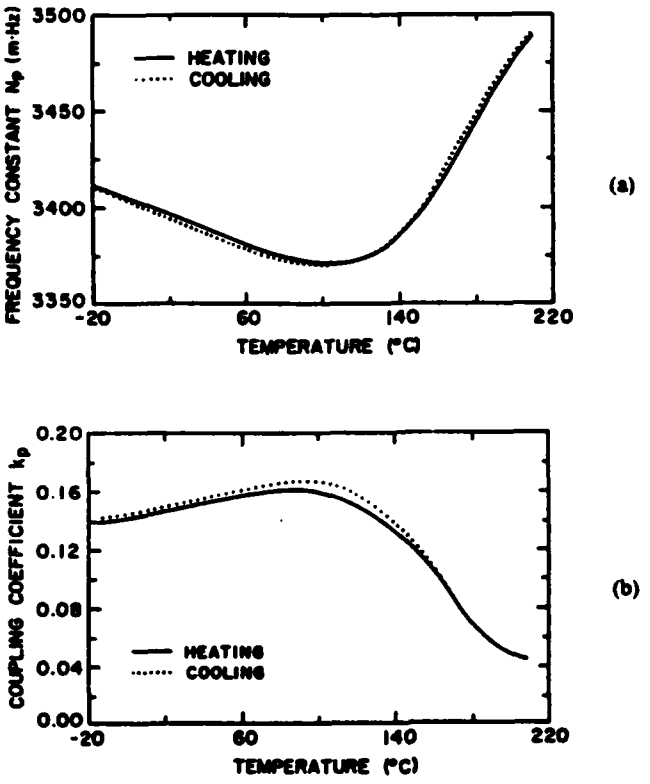

FIGURE 8 Frequency constant N_p (a) and electromechanical coupling coefficient k_p (b) of $2BaO\text{-}3SiO_2\text{-}TiO_2$ glass-ceramic.

crystal and 120°C for glass-ceramics. The room temperature properties of both single crystal and glass-ceramic are given in Table I.

DISCUSSION

The unusual features in the properties of both fresnoite single crystals and glass-ceramics can be summarized as follows:

(1) In both single crystal and glass-ceramics the sign of pyroelectric coefficient is positive at room temperature and becomes negative at about 190°C.

(2) A sharp peak in the dielectric constant, pyroelectric coefficient, and coupling coefficient are observed at 160°C in the case of single crystal and at 120°C in the case of glass-ceramics. A minimum is observed in resonance frequency at the same temperatures.

The difference in temperature between single crystal and glass-ceramics where the properties show an anomaly may be due to the nonstoichiometric composition of glass-ceramics. Hence all the properties of glass-ceramic described earlier reflect the properties of fresnoite crystalline phase.

TABLE I
Room temperature properties of fresnoite

Property	$Ba_2TiSi_2O_8$ Single crystal	$2BaO\text{-}3SiO_2\text{-}TiO_2$ Glass-ceramic
Density (gm/cc)	4.45	4.01
Dielectric constant		
K_{33} (1 kHz)	11.0	9.0
$\tan\delta$	<0.001	<0.001
Pyroelectric coefficient		
p_3 ($\mu C/m^2$ °K)	+10	+8
d_{33} (pC/N)	8	7
d_{31} (pC/N)	2.7	1.8
d_h (pC/N)	12.7	8.8
g_{33} (10^{-3} V m/N)	82	88
g_h (10^{-3} V m/N)	130	110
$d_h g_h$ (10^{-15} m^2/N)	1650	970
Frequency constants		
N_t (m · Hz)	2350	2250
N_p (m · Hz)	3500	3500
Electromechanical coupling coefficients		
k_t	0.25	0.25
k_p	0.12	0.14
Mechanical quality factor Q	3000	800
Temperature coefficient of resonance (ppm/°C)	100	100

The anomalies occurring in all the properties in fresnoite suggest the possibility of a structural phase transition near 160°C. In most ferroic crystals, structural phase transitions are invariably accompanied with anomalies in dielectric and related properties.

Several experiments were done in an attempt to detect a structural change in fresnoite near 160°C. X-ray diffractometer powder patterns were recorded at several temperatures from room temperature up to 400°C at intervals of 50°, using a high temperature x-ray diffractometer unit. No significant changes in either d spacings or intensities of different reflections could be detected. An analysis of the single crystal x-ray intensity data taken at 24° and 300°C did not indicate any change in the crystal symmetry or space group of the crystal. The results of the single crystal x-ray work will be published elsewhere.[10] Thus within their resolution limit, the above experiments failed to give any indication of a structural phase change in fresnoite. However, the possibility of a subtle structural change cannot be completely ruled out. If there is a phase transition near 160°C, it is clear that it is a polar to polar type of transition. However, it is not a ferroelectric or ferroelastic type of transition, since no ferroelectric or ferroelastic properties are observed in fresnoite below the transition.

If the possibility of a phase transition near 160°C is ruled out, it is somewhat difficult to explain the origin of all the anomalies which occur at exactly the same temperature, with practically no hysteresis. In a piezoelectric polar crystal, with reasonably high electromechanical coupling all the anomalies are coupled. The observed anomalies in the properties might have their origin in either elastic, dielectric or piezoelectric nature of the crystal, but because of the coupling between these properties, we can expect changes in all the properties.

The origin of the anomaly is probably not dielectric because the change in dielectric constant from 0° to 500°C is very small. For both single crystal and glass-ceramics, the planar and thickness mode resonance frequencies were in the range 0.4 to 0.6 MHz and 4 to 6 MHz respectively. Hence the dispersion observed in the dielectric constant (Figures 1 and 3) is probably due to the mechanical resonances. To verify whether the dielectric anomaly still remains in clamped crystal, the dielectric constant was measured at 10 MHz, which is above all major resonances. A similar peak in dielectric constant was observed near 160°C, for 10 MHz measurement also. Since the anomaly in the dielectric constant was observed in clamped crystals also, the origin of the anomalies in all the properties is probably not piezoelectric. The most probable cause for the anomaly in all the properties seems to be the anomalous behavior of a few of the elastic constants near 160°C. Because of the coupling between elastic and piezoelectric properties, we might expect anomaly in the piezoelectric properties also. Measurement of the temperature dependence of all the elastic constants and thermal expansion coefficients from room temperature up to 250°C is certainly necessary to confirm the above argument.

The reversal of sign in pyroelectric coefficient is a rare phenomenon and can occur without a structural phase transition. A number of materials show a sign reversal, going from positive to negative (or vice versa) at a certain temperature: $Li_2SO_4 \cdot H_2O$.[11] $Ba(NO_3)_2$.[12] $Ba_2TiGe_2O_8$[13] and $(NH_4)_2SO_4$.[14] The reason for the sign reversal of pyroelectric coefficient in many of these materials thought to be the cancellation of primary and secondary pyroelectric effects as discussed below. The magnitude and sign of secondary pyroelectric coefficient at a particular temperature can be calculated by knowing the elastic, piezoelectric and thermal expansion coefficients of the material at that temperature. Thus because of the coupling between these properties, anomalous changes in elastic or piezoelectric properties can lead to anomalies in pyroelectric properties also. A simple calculation of the sign and magnitude of secondary pyroelectric coefficient in fresnoite can be made is described below.

The pyroelectric coefficient (p) of a material under constant stress and electric field is defined by the relation

$$p = \left(\frac{\partial P_s}{\partial T}\right)_{E,\sigma} \tag{2}$$

where P_s is the spontaneous polarization, T is the temperature, E the electric field and σ the stress. The measured pyroelectric coefficient (at constant stress) is the sum of two terms given by

$$p_i^\sigma = p_i^\varepsilon + d_{ijk}^T C_{jklm}^{T,E} \alpha_{lm}^\sigma \tag{3}$$

where p_i^σ is the total pyroelectric effect measured at constant stress and p_i^ε the pyroelectric effect at constant strain is called the primary effect. The second term is the pyroelectric contribution due to the deformation of the crystal via the expansion coefficient and the piezoelectric terms. d_{ijk}^T represents the piezoelectric tensor at constant temperature, $C_{jklm}^{T,E}$ is the elastic stiffness coefficient at constant temperature and electric field and α_{lm}^σ is the thermal expansion coefficient at constant stress. All terms in the previous equation are at constant electric field.

In ferroelectric pyroelectrics the primary effect is large and negative, because the spontaneous polarization decreases with increasing temperature. The secondary effect is considerably smaller and may have either sign depending on the values of coefficients. Thus in ferroelectric materials, the experimentally observed pyroelectric coefficients are dominated by the primary effect and are negative. In nonferroelectric materials there is no simple way to predict the sign and magnitude of primary and secondary pyroelectric effects. In practice, the total pyroelectric effect can be measured and the secondary effect calculated from the coefficients d, α and C.

For the point group 4 mm of $Ba_2TiSi_2O_8$, the secondary pyroelectric coefficient is given by the following equation.[15]

$$p_{sec} = 2d_{31}(C_{11}\alpha_1 + C_{12}\alpha_1 + C_{13}\alpha_3) + d_{33}(2C_{13}\alpha_1 + C_{33}\alpha_3) \qquad (4)$$

For $Ba_2TiSi_2O_8$ single crystals all the piezoelectric and elastic constants are known. The sign of d_{31} is positive in this material. When calculations are made using Equation (4), we obtain $p_{sec} = +16.5\ \mu C/m^2\ °K$.

In Equation (3), if at a particular temperature the primary and secondary parts are equal in magnitude but opposite in sign, the pyroelectric coefficient at constant stress p_i^σ will be zero. This kind of behaviour has been reported in $Li_2SO_4 \cdot H_2O$.[11] In this material the secondary effect is positive at all temperatures whereas the primary effect is positive only above 158°K. A sign change in the pyroelectric coefficient occurs at 106°K because of the cancellation of primary and secondary parts. In addition, the pyroelectric coefficient exhibits a broad extremum at 50°K.

In the case of $Ba_2TiSi_2O_8$ crystal, the pyroelectric coefficient is positive in the temperature range $-150°$ to $+190°C$, indicating that p_{sec} is larger than $p_{primary}$ in this temperature range. The pyroelectric coefficient goes through a maximum at about 160°C and changes its sign from positive to negative at about 190°C which implies that the primary effect dominates. A calculation of $p_{primary}$ and p_{sec} at different temperatures can be done if we know the temperature variation of all the elastic, piezoelectric and thermal expansion coefficients of fresnoite near the anomaly.

APPLICATION IN PYROELECTRIC AND PIEZOELECTRIC DEVICES

The room temperature dielectric, piezoelectric and pyroelectric properties of fresnoite are listed in Table I. In this section a brief evaluation of the properties of fresnoite is given for pyroelectric detectors and hydrophones.

To determine the usefulness of a pyroelectric material for a specific application, different figures of merit are used which combine the pyroelectric, dielectric and thermal properties of the material.[16,17] The commonly used figures of merit are defined below.

$M_1 = p/K$ for a quick evaluation of the material

$M_2 = p/\rho cK$ for a fast response detector

$$M_3 = \frac{p}{\rho cK^{1/2} \tan\delta^{1/2}} \text{ for vidicon}$$

TABLE II

Room temperature pyroelectric figures of merit

Property	$Ba_2TiSi_2O_8$[a] Single crystal at 25°C	$Ba_2TiSi_2O_8$[a] Single crystal at 160°C	$2BaO\text{-}3SiO_2\text{-}TiO_2$ Glass-ceramic	$LiTaO_3$ single crystal
p_3 ($\mu C/m^2$ °K)	+10	+20	+8	−180
M_1 ($\mu C/m^2$ °K)	0.95	1.82	0.88	3.27
M_2 (10^{-12} C m/J)	0.46	0.9	0.44	1.04
M_3 (10^{-12} C m/J)	46.7	92	41.3	98

[a] For calculation, the values for density and specific heat were assumed to be the same at 25°C and 160°C.

In the above equations, p is the pyroelectric coefficient, K is the dielectric constant, ρ is the density, c is the volume specific heat and $\tan\delta$ is the dielectric loss. The values of M_1, M_2, and M_3 of both fresnoite single crystal and glass-ceramics are listed in Table II, along with the values for $LiTaO_3$ which is at present most widely used pyroelectric material. From the table it can be seen that at room temperature the figures of merit of fresnoite are about 25 to 30% of the corresponding values of $LiTaO_3$. The transition at 160°C is highly reproducible with practically no hysteresis. The nonhysteresis behavior near the transition is a very useful feature in the high temperature pyroelectric point detector application. The values of figures of merit M_1, M_2, and M_3 of fresnoite at 160°C are comparable with those of $LiTaO_3$. Since fresnoite is a nonferroelectric polar material, there will not be any problems of depoling which is a limitation with most of the ferroelectric materials. Fresnoite is a promising material for high temperature pyroelectric detectors.

The measured values of the dielectric constant, d_{33}, and g_h of fresnoite single crystal and glass-ceramics are listed in Table I, along with the calculated values of g_{33}, d_h and $d_h g_h$. The values of g_h and the product of $d_h g_h$ of fresnoite are comparable to PVF_2 and much higher than lead zirconate titanate (PZT) ceramics. Although the values of d_{33} and d_h of fresnoite are comparatively low, the magnitudes of g_{33} and g_h are high because of their low dielectric constant. The values of g_h remains practically constant up to a pressure of 35 MPa. Hence fresnoite can be an excellent candidate material for several piezoelectric devices like hydrophones. A more detailed discussion of the advantages of using fresnoite in piezoelectric devices can be seen in Reference 18.

ACKNOWLEDGMENTS

We thank all our colleagues in the ferroelectrics group at MRL for their help in this work. This work was supported by the Army Research Office through Contract #DAAG29-80-C-0008 and the National Science Foundation Grant No. DMR-8303906.

REFERENCES

1. M. Kimura, Y. Fujino and T. Kawamura, *Appl. Phys. Lett.*, **29**, 227 (1976).
2. S. Haussuhl, J. Eckstein, K. Reicher and F. Wallarafen, *J. Cryst. Growth*, **40**, 200 (1977).
3. M. Kimura, *J. Appl. Phys.*, **48**, 2850 (1977).

4. H. Yamauchi, *J. Appl. Phys.*, **49**, 6162 (1978).
5. J. Meingailis, J. F. Vetelino, A. Jhunjunwala, T. B. Reed, R. E. Fahey and E. Stein, *Appl. Phys. Lett.*, **32**, 203 (1978).
6. A. Halliyal, A. S. Bhalla, R. E. Newnham and L. E. Cross, *J. Mater. Sci.*, **16**, 1023 (1981).
7. A. Halliyal, A. S. Bhalla, R. E. Newnham, *Mat. Res. Bull.*, **18**, 1007 (1983).
8. G. J. Gardopee, R. E. Newnham and A. S. Bhalla, *Ferroelectrics*, **33**, 155 (1981).
9. R. L. Byer and C. B. Roundy, *Ferroelectrics*, **3**, 333 (1972).
10. S. A. Markgraf, *et al.* (to be published).
11. S. B. Lang, *Phys. Rev.*, **B4**, 3603 (1970).
12. V. V. Gladkii and I. S. Zheludev, *Sov. Phys. Cryst.*, **10**, 63 (1965).
13. H. Schmid, P. Genequand, H. Tippmann, G. Pouilly and H. Guedu, *J. Mater. Sci.*, **13**, 2257 (1978).
14. N. Yamada, *J. Phys. Soc. Jap.*, **46**, 561 (1979).
15. A. S. Bhalla and R. E. Newnham, *Phys. Stat. Sol.* (*a*)., **58**, K19 (1980).
16. E. H. Putley, in *Semiconductors and semimetals*, Vol. 5, Ed. by R. D. Willardson and A. C. Beer, Academic Press, NY, page 259 (1981).
17. S. G. Porter, *Ferroelectrics*, **33**, 193 (1981).
18. A. Halliyal, A. Safari, A. S. Bhalla, R. E. Newnham and L. E. Cross, *J. Am. Cer. Soc.*, **67**, 331 (1984).

APPENDIX 4

X-Ray Structure Refinement and Pyroelectric Investigation of Fresnoite, $Ba_2TiSi_2O_8$

S.A. Markgraf, A. Halliyal, A.S. Bhalla, R.E. Newnham and C.T. Prewitt

Ferroelectrics 62, 17 (1985)

Ferroelectrics, 1985, Vol. 62, pp. 17–26
0015-0193/85/6201–0017/$15.00/0

X-RAY STRUCTURE REFINEMENT AND PYROELECTRIC INVESTIGATION OF FRESNOITE, $Ba_2TiSi_2O_8$

S. A. MARKGRAF, A. HALLIYAL, A. S. BHALLA and R. E. NEWNHAM

Materials Research Laboratory, The Pennsylvania State University, University Park, PA 16802 USA

and

C. T. PREWITT

Department of Earth and Space Sciences, SUNY at Stony Brook, Stony Brook, NY 11794 USA

(*Received October 17, 1984*)

Crystal structure parameters have been refined from single crystal x-ray intensity data collected on $Ba_2TiSi_2O_8$ at 24 and 300°C. Anisotropic refinements in space group *P4bm* yielded residuals of 0.035 and 0.042 at 24 and 300°C, respectively. Pyroelectric measurements give a room temperature pyroelectric coefficient of $+10\ \mu C\ m^{-2}\ K^{-1}$. A structural mechanism for the pyroelectric effect is discussed in terms of large oxygen displacements. A sign reversal in the pyroelectric coefficient occurs at 160°C, perhaps caused by the cancellation of primary and secondary effects.

INTRODUCTION

Fresnoite, $Ba_2TiSi_2O_8$ is a non-centrosymmetric tetragonal crystal in space group *P4bm*. It has received attention recently for its pyroelectric, piezoelectric, and surface acoustic wave properties.[1-5] In addition, the possibility of making polar glass-ceramics by the recrystallization of a glass of this composition has been demonstrated successfully.[6] During the polar glass-ceramic study, it was observed that fresnoite glass-ceramics show a sharp sign reversal in the pyroelectric coefficient at 160°C. Single crystals also show the effect, and several other electrical properties show anomalies at 160°C (dielectric constant, K, frequency constant, N_p, electromechanical coupling, k_p).[7] High temperature x-ray powder diffraction data, DTA, and specific heat measurements gave no indication of a phase transition. If a structural distortion was responsible for the sharp sign reversal in the pyroelectric coefficient it must be small in magnitude. The structure of fresnoite was solved by Moore and Louisnathan[8] and Masse *et al.*[9] Due to the recent technological interest in $Ba_2TiSi_2O_8$, and the unusual pyroelectric behavior, it seemed worthwhile to re-investigate the crystal structure of fresnoite, both at room temperature and above 160°C.

TABLE I

Crystallographic data for fresnoite. Estimated Standard Deviation are given in parentheses. (This convention is followed in all tables.)

Space Group	$P4bm$ ($z = 2$)		
Lattice Parameters	a(Å)	c(Å)	*Volume* (Å^3)
Temp (°C)			
24	8.527(1)	5.2104(9)	378.8(1)
300	8.542(1)	5.219(1)	380.8(1)
500	8.550(2)	5.235(2)	382.6(2)
24 (after heating)	8.528(1)	5.210(1)	378.8(1)
S (Standard Deviation of an observation of unit weight)	$S = 2.48$ at 24°C		
	$S = 2.78$ at 300°C		
Expansion Coefficients			
$\bar{\alpha}_c$	9.9×10^{-6}°C^{-1} (this study)		
	10.3×10^{-6}°C^{-1} (Ref. 2)		
	9.3×10^{-6}°C^{-1} (Ref. 3)		
$\bar{\alpha}_a$	5.7×10^{-6}°C^{-1} (this study)		
	9.8×10^{-6}°C^{-1} (Ref. 2)		
	8.7×10^{-6}°C^{-1} (Ref. 3)		

EXPERIMENTAL

Fresnoite crystals were grown on a ⟨001⟩ seed by the Czochralski method from a stoichiometric melt. Growth conditions were as follows: seed rotation speed of 10–15 rpm; pulling speed of 1.0 mm/hr; crucible rotation of 5 rpm. The resulting boules were colorless and transparent.

A c plate was cut from a boule, crushed, and a small fragment was chosen for x-ray investigation. An attempt was made to grind the fragment into a sphere, but proved unsuccessful. The crystal had many faces, all with rounded corners. Approximate dimensions were $140 \times 100 \times 60$ μm. Precession photography showed sharp, rounded spots, with no evidence of twinning.

Integrated intensity data were measured with an automated Picker four-circle diffractometer operating with graphite-monochromated Mo$K\alpha$ radiation. Reflections within a quadrant of reciprocal space containing the positive and negative polar axes, with radius of $(\sin\theta)/\lambda = 0.70$ Å^{-1}, were collected at 24 (1176 reflections) and 300°C (1180 reflections). Heating in-situ was accomplished with the heater described by Brown *et al.*[10] The error in temperature was ±20°C. Unit cell parameters were calculated at 24, 300, 500°C and again at 24°C after heating, through least-squares method on 24 reflections within the range $39° \leq 2\theta \leq 55°$. As the technique does not quantify possible centering and/or orientation errors, the reported standard deviations for the lattice parameters may be low (Table I).

All intensities were corrected for Lorentz and polarization factors and converted to structure factors. Since the crystal was very complex in shape, an accurate measurement of it for absorption was not possible. Therefore no absorption correction was made. A reflection was deleted if $I_{obs} < 2\sigma_I$, where σ_I is based on counting

statistics, or if the variation of a form exceeded 4σ, where σ is the standard deviation of the population. The latter is a rather stringent criterion, yet only leads to the rejection of approximately 25 symmetry-averaged reflections per data set. Most of these rejected reflections were relatively intense and at low $(\sin\theta)/\lambda$, where absorption effects would be strongest.

The structure was refined with the program RFINE IV[11] using starting parameters taken from Moore and Louisnathan.[8] Atomic scattering factor curves were taken from the International Tables for X-ray Crystallography, Vol. IV,[12] as were corrections for anomalous dispersion. Strong extinction was not a serious problem, hence a correction was considered unnecessary.

RESULTS AND DISCUSSIONS

Lattice parameters and crystallographic data at various temperatures are given in Table I. Anisotropic refinements in *P4bm* on 579 (24°C) and 575 (300°C) symmetry-averaged reflections converged in three cycles. The structural features are the same as those reported by Moore and Louisnathan[8] and Masse *et al.*,[9] consisting of Si_2O_7 groups linked to square pyramidal TiO_5 members, producing layers parallel to

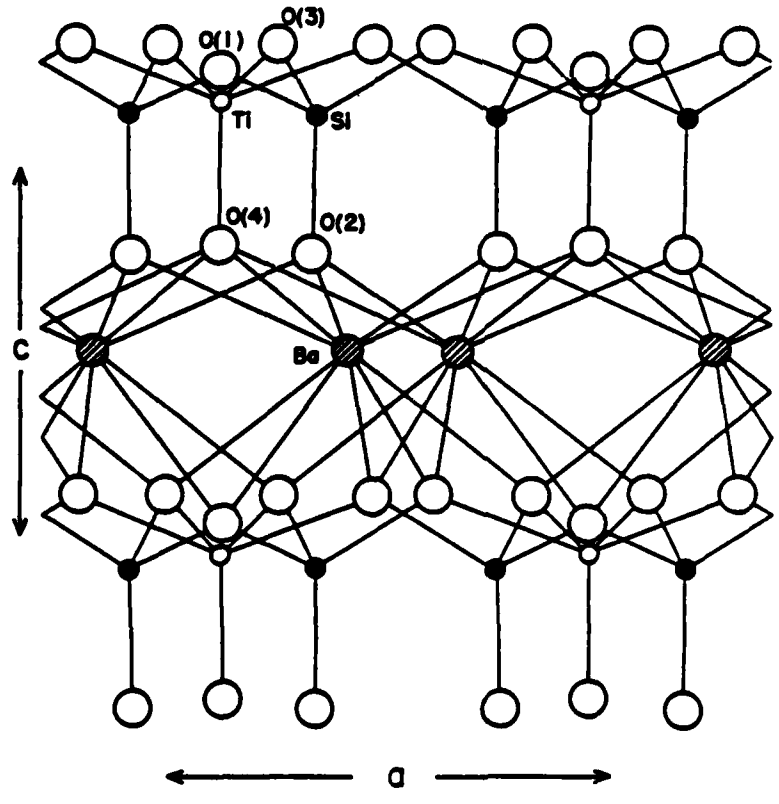

FIGURE 1 Crystal structure of fresnoite, after Moore and Louisnathan.[8]

TABLE II

Measured and calculated structure factors for selected Bijvoet pairs for $Ba_2TiSi_2O_8$

hkl	$\lvert F_{obs}\rvert$	σ_F	$\lvert F^{+}_{calc}\rvert$[a]	$\lvert F^{-}_{calc}\rvert$	$\frac{F_{c,hkl}}{F_{c,\bar{h}\bar{k}\bar{l}}}$	$\frac{F_{o,hkl}}{F_{o,\bar{h}\bar{k}\bar{l}}}$
127	58.434	1.371	59.076	58.902	(+)1.008	:0.924
$12\bar{7}$	63.253	1.455	58.615	59.350	(−)0.992	
536	39.848	1.044	40.433	40.252	(+)1.009	:0.950
$53\bar{6}$	41.951	1.080	40.056	40.673	(−)0.990	
665	51.253	1.242	52.786	53.689	(+)0.991	:0.934
$66\bar{5}$	54.871	1.318	53.240	53.226	(−)1.009	
10, 1, 4	59.731	1.401	61.259	61.390	(+)1.003	:0.987
10, 1, $\bar{4}$	60.497	1.421	61.086	61.549	(−)0.997	
783	39.831	1.061	40.009	40.616	(+)0.991	:0.974
$78\bar{3}$	40.902	1.075	40.380	40.244	(−)1.009	
11, 2, 2	29.339	0.965	30.523	29.559	(+)1.037	:0.968
11, 2, $\bar{2}$	30.303	0.976	29.447	30.641	(−)0.965	
5, 10, 1	35.842	0.989	34.867	35.116	(+)0.997	:1.029
5, 10, $\bar{1}$	34.824	0.982	34.966	35.015	(−)1.002	
11, 2, 1	17.569	1.099	16.746	17.246	(+)0.978	:0.967
11, 2, $\bar{1}$	18.161	1.068	17.128	16.875	(−)1.022	
10, 5, 2	49.144	1.200	52.009	51.292	(+)1.020	:0.946
10, 5, $\bar{2}$	51.927	1.247	51.002	52.326	(−)0.980	
953	22.848	1.007	21.673	23.500	(+)0.929	:1.018
$95\bar{3}$	22.451	0.991	23.339	21.826	(−)1.077	
934	40.705	1.071	41.091	41.806	(+)0.988	:0.975
$93\bar{4}$	41.733	1.086	41.582	41.321	(−)1.012	
815	39.228	1.041	38.837	38.925	(+)1.002	:0.986
$81\bar{5}$	39.772	1.041	38.762	39.007	(−)0.998	
266	27.783	0.990	26.022	31.734	(+)0.985	:0.905
$26\bar{6}$	30.698	0.980	26.411	31.229	(−)1.016	
137	27.446	0.990	25.233	27.293	(+)0.936	:1.002
$13\bar{7}$	27.395	0.985	26.965	25.584	(−)1.067	

[a] $\lvert F^{+}_{calc}\rvert$ is based on refinements with a positive z value; $\lvert F^{-}_{calc}\rvert$ from the refinement with negative z coordinates.

{001}. The Ba^{2+} cation, in ten-fold coordination, connects the layers (Figure 1). As with any polar space group, it is possible to determine the absolute configuration of the crystal structure through analysis of Bijvoet pairs. In addition, the respective R factors of each model may be used in a Hamilton significance test.[13] Table II contains 14 Bijvoet pairs with $2\theta \geq 55°$ taken from the 24°C data set. There is a clear preference for the z (negative) model, although five of the fourteen pairs do not agree with this model. However, all five are within a single standard deviation (σ_F).

TABLE III

Positional parameters, displacements and equivalent isotropic temperature factors, B_{eq} (Å^2) for $Ba_2TiSi_2O_8$

		Positional Parameters		Displacement[a]	B_{eq}	
		24°C	300°C	$\Delta \times 10^{-4}$	24°C	300°C
Ba	x	0.32701(3)	0.32708(4)	0.7(5)	0.99(1)	1.41(1)
	y	0.82701(3)	0.82708(4)	0.7(5)		
	z	0.0	0.0	—		
Ti	x	0.0	0.0	—	0.70(4)	0.90(5)
	y	0.0	0.0	—		
	z	−0.5354(5)	−0.5355(6)	1(8)		
Si	x	0.1280(2)	0.1280(2)	0(3)	0.70(3)	0.82(4)
	y	0.6280(2)	0.6280(2)	0(3)		
	z	−0.5129(8)	−0.5133(10)	4(13)		
O(1)	x	0.0	0.0	—	1.44(16)	1.68(19)
	y	0.5	0.5	—		
	z	−0.6293(19)	−0.6284(23)	−9(30)		
O(2)	x	0.1259(5)	0.1261(6)	2(8)	1.01(11)	1.29(13)
	y	0.6259(5)	0.6261(6)	2(8)		
	z	−0.2051(12)	−0.2078(15)	27(19)		
O(3)	x	0.2924(6)	0.2924(7)	0(9)	1.84(13)	1.77(15)
	y	0.5772(8)	0.5774(8)	2(11)		
	z	−0.6429(11)	−0.6436(13)	7(17)		
O(4)	x	0.0	0.0	—	1.82(18)	2.46(23)
	y	0.0	0.0	—		
	z	−0.2096(20)	−0.2134(26)	38(33)		

[a]Est. Std. Dev. of the form $(\sigma_{24}^2 + \sigma_{300}^2)^{1/2}$.

Examination of the R factors for the two models also shows a preference for the z (negative) model. With z (positive): $Rw = 0.047$, and $R = 0.040$, where $R = \Sigma(||F_o| - |F_c||)/\Sigma|F_o|$ and $Rw = [\Sigma w(|F_o| - |F_c|)^2/(\Sigma wF_o^2)]^{1/2}$. The weighting term, w, is defined as $1/\sigma_F^2$, where σ_F is calculated from the counting statistics. Taking z (negative) yields: $Rw = 0.040$ and $R = 0.035$. To see if this difference is significant at the 0.5 percent confidence level Hamilton's tables[13] give $R = 1.004$. The conclusion is that there is a high probability that the difference is significant. Analysis of the 300°C data yields similar results: z (positive), $Rw = 0.053$, $R = 0.045$, z (negative): $Rw = 0.047$, $R = 0.042$. All atomic coordinates, thermal parameters, interatomic distances, etc. are therefore taken from the z (negative) refinements.

Data, and the estimated standard deviations, from the 24 and 300°C refinements are given in Tables III to VI. Positional parameters and equivalent isotropic temperature factors are given in Table III. Interatomic distances and angles are listed in Table IV. Table V contains the anisotropic temperature factors. Final observed and calculated structure factors are listed in Table VI†. Mean thermal

†Table 6 is available from the authors at the Materials Research Laboratory

TABLE IV

Interatomic distances (Å) and angles (°) for $Ba_2TiSi_2O_8$

	24°C	300°C
Ba-O(1)	2.843(7)	2.850(8)
Ba-O(2)	2.650(5)	2.659(6)
Ba-O(2')	2.793(5)	2.804(6)
Ba-O(3)	2.844(6)	2.846(7)
Ba-O(3')	3.008(6)	3.012(7)
Ba-O(4)	3.338(3)	3.351(5)
Ti-O(3)	1.970(6)	1.975(6)
Ti-O(4)	1.698(11)	1.681(14)
O(3)-O(4)	2.944(10)	2.937(12)
O(3)-O(3')	2.671(8)	2.677(9)
Si-O(1)	1.658(4)	1.658(5)
Si-O(2)	1.604(8)	1.595(10)
Si-O(3)	1.616(6)	1.619(7)
O(1)-O(2)	2.681(10)	2.672(12)
O(3)-O(2)	2.719(8)	2.713(10)
O(1)-O(3)	2.579(6)	2.585(6)
O(4)-Ti-O(3)	106.52(18)	106.59(21)
O(3)-Ti-O(3')	146.96(37)	146.81(42)
Si-O(3)-Ti	138.57(39)	138.45(44)
Si-O(1)-Si	137.09(69)	137.52(82)
O(2)-Si-O(1)	110.58(39)	110.44(46)
O(2)-Si-O(3)	115.09(25)	115.15(27)

expansion coefficients were calculated from the unit cell parameters with the equation $\bar{\alpha}_X = X_{24}^{-1}(X_T - X_{24})/(T - 24)$, where X is the parameter in question, T is temperature, and $(X_T - X_{24})/(T - 24)$ is the slope of X vs. temperature determined from linear regression. Results for $\bar{\alpha}_c$, 9.9×10^{-6} °C^{-1}, are in good agreement with other workers, whereas $\bar{\alpha}_a$, 5.7×10^{-6} °C^{-1}, is slightly lower than found previously[2,3] (Table I).

Atomic coordinates and interatomic distances and angles agree with the earlier values of Moore and Louisnathan,[8] although the present values are more precise. Previous structure refinements disagreed in the Ti–O interatomic distances, with Masse *et al.* reporting that both Ti–O interatomic distances are approximately 2.00 Å, and Moore and Louisnathan reporting a short bond, 1.634 Å, and a longer one, 2.00 Å. The current structure refinement yields results in agreement with the latter (Table IV). Fresnoite is one of the few titanates that luminesces efficiently at room temperature, and the explanation for this has centered on the short Ti–O interatomic distance within the TiO_5 group.[14]

STRUCTURAL MODEL FOR PYROELECTRICITY

The pyroelectric coefficient of a material in general is described as the sum of the primary and secondary effects[15]

$$(p_3)_T = (p_3)_{\text{prim}} + (d_{3j}\alpha_i c_{ji})_{\text{sec}} \qquad i, j = 1, \ldots 6$$

TABLE V

Anisotropic temperature factors ($Å^2$) for $Ba_2TiSi_2O_8$[a]

24°C	β_{11}	β_{22}	β_{33}	β_{12}	β_{13}	β_{23}
Ba	0.00364(5)	0.00364(5)	0.0079(2)	−0.00178(4)	0.0003(1)	0.0003(1)
Ti	0.0023(1)	0.0023(1)	0.0069(10)	—	—	—
Si	0.0024(1)	0.0024(1)	0.0064(7)	0.0002(2)	0.0003(5)	0.0003(5)
O(1)	0.0062(9)	0.0062(9)	0.006(3)	−0.0031(11)	—	—
O(2)	0.0038(5)	0.0038(5)	0.007(2)	−0.0017(7)	−0.0002(8)	−0.0002(8)
O(3)	0.0030(6)	0.011(1)	0.013(2)	0.0038(6)	0.0015(9)	0.0029(10)
O(4)	0.0076(10)	0.0076(10)	0.009(3)	—	—	—
300°C						
Ba	0.00507(6)	0.00507(6)	0.0116(2)	−0.00222(5)	0.0001(1)	0.0001(1)
Ti	0.0027(2)	0.0027(2)	0.010(1)	—	—	—
Si	0.0025(2)	0.0025(2)	0.0091(8)	0.0000(2)	0.0003(5)	0.0003(5)
O(1)	0.0066(10)	0.0066(10)	0.011(3)	−0.0031(14)	—	—
O(2)	0.0051(6)	0.0051(6)	0.008(2)	−0.0018(9)	0.0001(9)	0.0001(9)
O(3)	0.0032(7)	0.0086(10)	0.017(2)	0.0024(7)	0.001(1)	0.001(1)
O(4)	0.010(1)	0.010(1)	0.014(4)	—	—	—

[a] Of the form: $\exp\{-(\beta_{11}h^2 + \beta_{22}k^2 + \beta_{33}l^2 + 2\beta_{12}hk + 2\beta_{13}hl + 2\beta_{23}kl)\}$.

where $(p_3)_{\text{prim}} = (\partial P/\partial T)_\epsilon$ is the pyroelectric coefficient under constant strain, d the piezoelectric constant, α the thermal expansion coefficients and c_{ji} the stiffness coefficients of a crystal.

Pyroelectric coefficients of single crystals of fresnoite were measured by a direct Byer–Roundy method[16] (with a heating and cooling rate of 4°/minute) in a temperature range of −150 to 220°C (Figure 2). The magnitude of the pyroelectric coefficient at room temperature is 10 $\mu C\ m^{-2}\ K^{-1}$; this value includes both primary and secondary pyroelectric effects. Bhalla and Newnham,[17] using the published values for the piezoelectric, compliance and thermal expansion coefficients, have calculated the secondary effect in fresnoite to be +16.5 $\mu C\ m^{-2}\ K^{-1}$, setting the primary effect at −6.5 $\mu C\ m^{-2}\ K^{-1}$.

It is possible to calculate a pyroelectric coefficient based on a point-charge model with the equation

$$p_3 = \Delta P/\Delta T = \left(ec \left| \sum_i v_i n_i \Delta z_i \right| \right) \Big/ V \Delta T$$

where e is the elementary charge, c the unit cell parameter, v_i the valence of the ith ion, n_i the number of equivalent positions for the ith ion, Δz_i the displacement of the z coordinate between the two temperatures of the ith ion, V the room temperature volume of the unit cell, ΔT the temperature range. Table III lists the atomic displacements, along with an estimated standard deviation, calculated from the refinements at 24 and 300°C. The most striking shift in the atomic coordinates is found in the O(2) Δz, 27×10^{-4}, and O(4) Δz, 38×10^{-4}, positions. Using these two displacements a pyroelectric coefficient of 30 $\mu C\ m^{-2}\ K^{-1}$ is calculated. This is greater than the room temperature value, but the calculated value is an average quantity for the temperature range 24–300°C. Also, the calculation ignores the other, rather small displacements, nor does it consider electron redistribution.

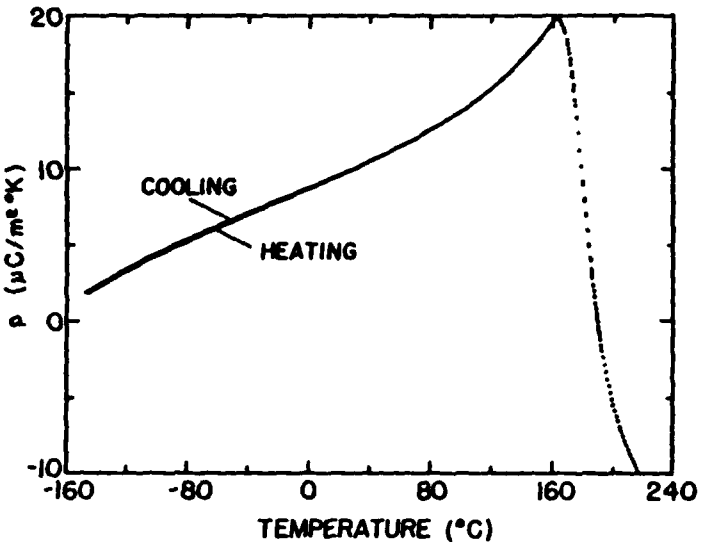

FIGURE 2 Variation of pyroelectric coefficient (p_3) of $Ba_2TiSi_2O_8$ single crystal as a function of temperature.

Tourmaline, another silicate mineral exhibiting pyroelectricity, has been studied in a similar manner.[18] Interpretation of the structural mechanism for pyroelectricity rested on an anomalously large oxygen displacement of 0.0051. Using this feature, along with large anisotropic temperature factors for the oxygen, Donnay[18] points out the agreement with Boguslawski's theory[19] for pyroelectricity. In Boguslawski's analysis of pyroelectricity, the effect is caused by large anharmonic thermal vibrations.

Abrahams *et al.*[20] have developed a model for the pyroelectric effect in tourmaline. Using a technique similar to a normal probability plot, Abrahams and coworkers state that the large oxygen displacement found by Donnay is of low statistical significance. They find that the largest significant displacement for any z coordinate is the $\Delta z = 0.0005$ displacement for Al. A model for tourmaline was then proposed in which an average cation displacement of $5\text{–}10 \times 10^{-4}$ Å along the polar axis produced the observed pyroelectric coefficient.

The similarity in the Δz displacements of the oxygen atoms in fresnoite and tourmaline is obvious. Anisotropic temperature factors for the O(2) and O(4) atoms in fresnoite are not anomalously large. Anharmonicity does not appear to be critical, unless the large errors in the positional parameters are evidence of such. A normal probability plot is not possible on the fresnoite data, and so a direct correction to the estimated standard deviations cannot be calculated. If, however, the $\sqrt{2}$ underestimation in σ found in the IUCr single-crystal project[21] is applied, the significance of the oxygen displacement is lessened. Still, no displacement is more significant than the O(2) and O(4) shift. It is possible to calculate a pyroelectric coefficient of approximately 19 $\mu C\ m^{-2}\ K^{-1}$ based on cation displacements of $5\text{–}10 \times 10^{-4}$. It is difficult to ascertain which displacement is causing the pyroelectricity in fresnoite, and the data does not lead to a conclusive answer.

In ferroelectric materials, the total pyroelectric coefficient is large and negative. Calculated secondary coefficients are relatively small, often positive, making the primary pyroelectric coefficient negative and large. In contrast, for non-ferroelectric polar crystals the total pyroelectric coefficient is more often dominated by the secondary effect, and both are commonly positive.[17] Another, albeit rare, feature of pyroelectric crystals is the reversal of the pyroelectric sign. If the crystal does not undergo a temperature related phase transition that induces a center of symmetry, the spontaneous polarization may increase or decrease with temperature. Several compounds show a sign reversal in the pyroelectric coefficients, going from positive to negative (or vice versa) at a certain temperature: $Li_2SO_4 \cdot H_2O$;[22] $Ba(NO_3)_2$;[23] $Ba_2TiGe_2O_8$;[24] $Ba_2TiSi_2O_8$; $Rb_2Cd_2(SO_4)_3$[25] and $(NH_4)_2(SO_4)$.[26] Often the explanation for the sign reversal centers on the cancellation of primary and secondary pyroelectric effects. In fresnoite this appears to be the case. The structure does not undergo a phase transition at 160°C. Moreover, the reversal in the sign of the pyroelectric coefficient is reproducible between heating and cooling cycles, thus ruling out the possibility of thermal conduction. What is surpising about the reversal is its sharpness; most other reversals show a gradual slope when crossing the zero point. An example is the first sign reversal in fresnoite at -180°C.[27] The pyroelectric coefficient sign reversals at lower temperatures are commonly due to the secondary effect gradually becoming smaller with decreasing temperature. In the case of fresnoite, the high temperature pyroelectric coefficient reversal has a unique signature, and anomalies occur at 160°C in all the piezoelectric properties. It is possible that the large oxygen displacements change a few elastic constants enough to cause the pyroelectric sign reversal. The germanium analog of fresnoite, $Ba_2TiGe_2O_8$, undergoes a ferroelastic transition at 810°C.[28] It is therefore conceivable that $Ba_2TiSi_2O_8$ may have slight anomalies in the elastic constants.

ACKNOWLEDGMENTS

We wish to thank Ken Baldwin and Don Swanson for assistance in the x-ray part of the study. This work was supported by the Army Research Office through DAAG29-80-C-0008 and NSF Grant DMR-8303906.

REFERENCES

1. M. Kimura, Y. Fujino and T. Kawamura, *Appl. Phys. Lett.*, **29**, 227 (1976).
2. M. Kimura, *J. Appl. Phys.*, **48**, 2850 (1977).
3. S. Haussühl, J. Eckstein, K. Recker and F. Wallrafen, *J. Crystal Growth*, **40**, 200 (1977).
4. J. Meingailis, J. F. Vetelino, A. Jhunjhunwala, T. B. Reed, R. E. Fahey and E. Stern, *Appl. Phys. Lett.*, **32**, 203 (1978).
5. H. Yamauchi, *J. Appl. Phys.*, **49**, 6162 (1978).
6. A. Halliyal, A. S. Bhalla, R. E. Newnham and L. E. Cross, *J. Mat. Sci.*, **16**, 1023 (1981).
7. A. Halliyal *et al.* (to be published).
8. P. B. Moore and S. J. Louisnathan, *Z. Krist.*, **130**, 438 (1969).
9. R. Masse, J.-C. Grenier and A. Durif, *Bull. Soc. franc. Mineral. Cristallogr.*, **90**, 20 (1967).
10. G. E. Brown, S. Sueno and C. T. Prewitt, *Am. Mineral.*, **58**, 698 (1973).
11. L. W. Finger and E. Prince, *U.S.N.B.S. Tech. Note*, **854** (1975).
12. J. A. Ibers and W. C. Hamilton, Eds., International Tables for X-Ray Crystallography, Vol. IV. Revised and Supplementary Tables. Kynoch Press, Birmingham (1974).
13. W. C. Hamilton, *Acta Cryst.*, **18**, 502 (1965).
14. G. Blasse, *J. Inorg. Nucl. Chem.*, **41**, 639 (1979).
15. J. F. Nye, Physical Properties of Crystals (Oxford University Press, Oxford, 1979).

16. R. L. Byer and C B. Roundy, *Ferroelectrics*, **3**, 333 (1972).
17. A. S. Bhalla and R. E. Newnham, *Phys. Stat. Sol. (a)*, **58**, K19 (1980).
18. G. Donnay, *Acta Cryst.*, **A33**, 927 (1977).
19. S. von Boguslawski, *Phys. Z.*, **15**, 283, 569, 805 (1914).
20. S. C. Abrahams, F. Lissalde and J. L. Bernstein, *J. Appl. Cryst.*, **12**, 104 (1979).
21. W. C. Hamilton and S. C. Abrahams, *Acta Cryst.*, **A26**, 18 (1970).
22. S. B. Lang, *Phys. Rev. B*, **4**, 3603 (1971).
23. V. V. Gladkii and I. S. Zheudev, *Sov. Phys. Cryst.*, **10**, 63 (1965).
24. H. Schmid, P. Genequand, H. Tippmann, G. Pouilly and H. Guedu, *J. Mat. Sci.*, **13**, 2257 (1978).
25. N. Yamada, *J. Phys. Soc. Jpn.*, **46**, 561 (1979).
26. H. G. Unruh and U. Rudiger, *J. Phys. (France)*, **33**, 77 (1972).
27. A. S. Bhalla (unpublished work).
28. M. Kimura, K. Utsumi and S. Nanantsu, *J. Appl. Phys.*, **47**, 2249 (1976).

APPENDIX 5

Dielectric, Piezoelectric and Pyroelectric Properties of $Sr_2TiSi_2O_8$ Polar Glass-Ceramic: A New Polar Material

A. Halliyal, A.S. Bhalla, L.E. Cross, R. E. Newnham

J. Mat. Sci 20, 3745-3749 (1985)

JOURNAL OF MATERIALS SCIENCE 20 (1985) 3745–3749

Dielectric, piezoelectric and pyroelectric properties of $Sr_2TiSi_2O_8$ polar glass–ceramic: a new polar material

A. HALLIYAL, A. S. BHALLA, L. E. CROSS, R. E. NEWNHAM
Materials Research Laboratory, The Pennsylvania State University, University Park, PA 16802, USA

Polar $Sr_2TiSi_2O_8$ glass–ceramics were prepared by recrystallizing glasses in a steep temperature gradient. The dielectric, piezoelectric and pyroelectric properties were studied as a function of temperature in the temperature range −150 to 200° C. The sign of the pyroelectric coefficient is positive at room temperature and is attributed to the dominance of the secondary pyroelectric effect over the primary effect. Anomalies were observed in the dielectric, pyroelectric and piezoelectric properties and a large hysteresis was observed in all these properties. Probable causes for the anomalies are discussed.

1. Introduction

Fresnoite ($Ba_2TiSi_2O_8$, hereafter designated BTS) is a polar but non-ferroelectric crystal with *tetragonal space group P4bm. Single crystals of* fresnoite have been grown successfully by the Czochralski technique by several workers [1–3]. Fresnoite has been shown to be a promising substrate material for surface acoustic wave (SAW) devices [1–5]. Its SAW properties are intermediate between those of $LiNbO_3$ and $LiTaO_3$. For fresnoite z-cuts with wave propagation along the [1 1 0] direction, the electromechanical coupling factor k_s^2 is 1.5% and the temperature coefficient of delay (TCD) is 50 ppm.

Recently, Ito and co-workers [6, 7] have shown that the TCD of fresnoite can be greatly lowered through the partial substitution of strontium for barium. Crystals of composition $(Ba_{2-x}Sr_x)TiSi_2O_8$ with uniform strontium concentration can be grown by edge-defined film-fed growth (EFG), for the compositions ranging from $x = 0$ to 0.8. It was found to be difficult to grow crystals of homogeneous composition by the Czochralski technique [7]. The strontium concentration in a Czochralski-grown crystal varies according to the normal freezing distribution. Z-cut crystals with strontium concentration of $x = 0.8$ give a TCD value of 20 ppm with practically no reduction in the value of k_s^2, and look to be very useful for SAW devices.

In compositions with $x \geq 1.0$, $SrTiO_3$ and $SrSiO_3$ also crystallize along with fresnoite, making it impossible to grow pure strontium titanium silicate ($Sr_2TiSi_2O_8$, hereafter designated STS) single crystals by the usual crystal growing techniques. However, X-ray diffraction studies on ceramic samples have shown that all compositions with $x = 0$ to 2.0 prepared by conventional ceramic processing techniques give single-phase fresnoite-type structure. The crystal symmetry of STS is the same as that of BTS. However, there are no measurements reported for the piezoelectric and pyroelectric properties of STS because of the difficulties in single-crystal growth. Moreover, since STS is a non-ferroelectric material, it is not possible to reorient the polar axes in individual crystallites and hence randomly axed ceramic samples will be of no use in studying the piezoelectric and pyroelectric properties.

In our earlier work it has been demonstrated that polar glass–ceramics with the fresnoite

0022–2461/85 $03.00 + .12

structure can be prepared by recrystallizing glasses of slightly modified fresnoite compositions [8–11]. In these glass–ceramics, the polar texture results from needle-like crystals growing from the glass surface during crystallization. These fresnoite polar glass–ceramics showed piezoelectric and pyroelectric properties comparable to the single-crystal properties.

In the present study, polar STS glass–ceramics were prepared from glasses of non-stoichiometric composition. The dielectric, piezoelectric and pyroelectric properties of STS glass–ceramics were studied as a function of temperature in the temperature range −150° C to 200° C. Since our previous studies have shown that the properties of BTS single crystals and polar glass–ceramics are very similar [11], we expect that the properties of STS glass–ceramics reported in the present paper might be very similar to the single-crystal properties.

2. Experimental details

Glass samples were prepared by mixing reagent-grade chemicals followed by melting in a platinum crucible at 1400 to 1450° C. The melt was retained in the furnace for 4 to 6 h for fining and homogenization. The fined glass melt was air quenched by pouring it into graphite moulds to form cylinders of approximately 0.8 to 1 cm in diameter and 1 to 1.5 cm in length. Initially, an attempt was made to prepare glasses of stoichiometric STS composition. It was not possible to obtain clear glasses with uniform composition because of phase separation in the melt. Addition of excess silica to the composition helped to eliminate the phase separation problem. Glass samples containing one mole of excess silica (composition: $2SrO–3SiO_2–TiO_2$) were prepared for the present study. Glass–ceramic samples with polar texture were prepared by crystallizing the glasses in a temperature gradient as described elsewhere [8–11]. Microstructure studies indicated that needle-like crystals grow from the surface into the bulk along the direction of temperature gradient. X-ray powder diffraction patterns of glass–ceramic samples showed that the only crystalline phase in glass–ceramics was STS. Property measurements were carried out on sections (8 mm diameter and 0.5 mm thick) cut normal to the temperature gradient and with gold electrodes sputtered on the major surfaces.

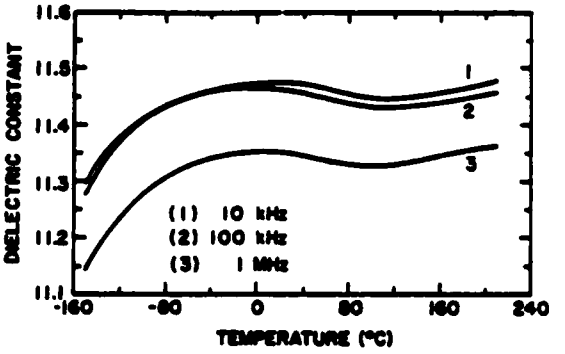

Figure 1 Dielectric constant of $2SrO–3SiO_2–TiO_2$ glass–ceramic as a function of temperature and frequency, over temperature range −150 to 200° C.

The dielectric constant and dissipation factors were measured at different frequencies using a capacitance bridge, and pyroelectric coefficients were measured by the Byer–Roundy [12] technique. The heating and cooling rates employed were 4° C min^{-1}. The electromechanical properties were determined by standard resonance techniques. All the above properties were measured as a function of temperature in both heating and cooling cycles. The hydrostatic voltage coefficient g_h was measured by a dynamic method described by Safari [13].

3. Results

The dielectric constant and dissipation factor of STS glass–ceramic are shown in Figs. 1 to 3. Broad peaks in dielectric constant were observed near 20 and 200° C. Below −20° C, the dielectric constant slowly decreased with decreasing temperature. There was an increase in dielectric

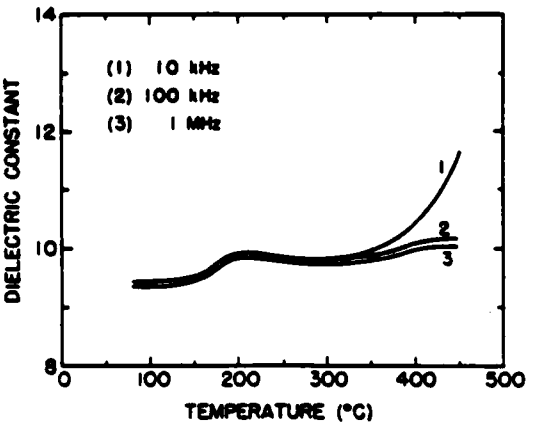

Figure 2 Dielectric constant of $2SrO–3SiO_2–TiO_2$ glass–ceramic as a function of temperature and frequency, over temperature range 80 to 450° C.

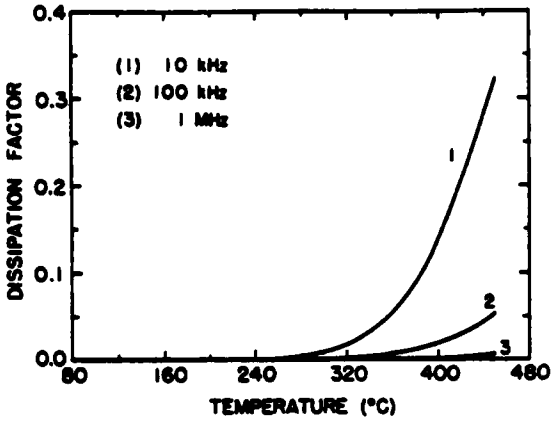

Figure 3 Dissipation factor of $2SrO-3SiO_2-TiO_2$ glass–ceramic as a function of temperature and frequency.

TABLE I Room-temperature properties of $2SrO-3SiO_2-TiO_2$ glass–ceramics

Density (g cm^{-3})	3.55
Dielectric constant K_{33}, at 1 kHz	11.5
Dissipation factor	< 0.001
Pyroelectric coefficient p_3 (μC m^{-2} K^{-1})	+ 7.5
d_{33}(pC N^{-1})	14
d_{31}(pC N^{-1})	1.6
d_h(pC N^{-1})	8.7
g_{33}(10^{-3} V m N^{-1})	138
g_h(10^{-3} V m N^{-1})	85
$d_h g_h$(10^{-15} m^2 N^{-1})	740
Frequency constant N_t (m Hz)	2550
Frequency constant N_p (m Hz)	3300
k_t	0.08
k_p	0.10
Mechanical quality factor Q	700
Temperature coefficient of resonance (ppm °C^{-1})	50

constant and dissipation factor at higher temperatures, probably because of conduction. The dissipation factor curve was featureless up to 250° C and the losses were very low (< 0.001).

The variation of pyroelectric coefficient p_3 as a function of temperature is shown in Fig. 4. The pyroelectric coefficient p_3 is positive at room temperature and shows a very broad peak at about −20° C. An anomaly is observed in p_3 at about 120° C. A large hysteresis was observed between heating and cooling cycles above −10° C and this was particularly absent below −10° C. This behaviour in $p_3(T)$ was confirmed by repeating the heating and cooling measurement twice. Plots of $p_3(T)$ recorded during the two heating cycles were exactly the same, as were the plots for the two cooling cycles.

The variation of frequency constant N_p and electromechanical coupling factor k_p are shown in Figs. 5 and 6. Frequency constant N_p showed a minimum at about 150° C in the cooling cycles and at about 200° C in the heating cycles. A large hysteresis similar to the one in pyroelectric coefficient measurement was observed between heating and cooling cycles in N_p and k_p. At the inflection point the value of temperature coefficient of resonance (TCR), defined as

$$\text{TCR} = \frac{1}{f_r}\frac{\partial f_r}{\partial T} \qquad (1)$$

is zero. Here, f_r is the resonance frequency at temperature T. The minimum in N_p during the heating cycle and the small anomaly in the dielectric constant occur at the same temperature (~200° C). The room-temperature properties of STS glass–ceramics are listed in Table I.

4. Discussion

In our previous study on BTS single crystals and

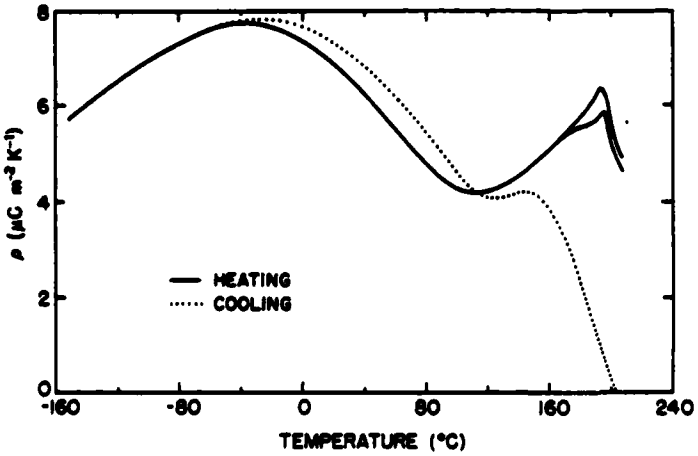

Figure 4 Variation of pyroelectric coefficient with temperature for $2SrO-3SiO_2-TiO_2$ glass–ceramic.

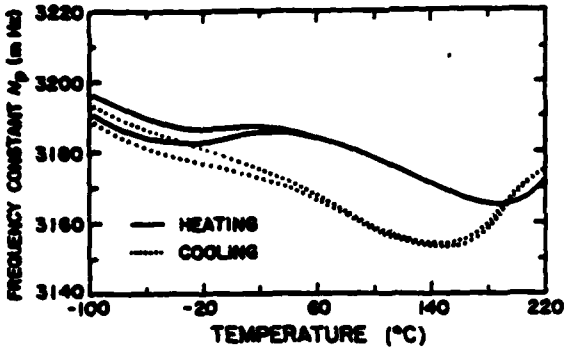

Figure 5 Temperature dependence of frequency constant N_p of $2SrO-3SiO_2-TiO_2$ glass–ceramic.

glass–ceramics [11], it was clear that all the properties of glass–ceramics containing one mole of excess silica (composition: $2BaO-3SiO_2-TiO_2$) were very similar to those of BTS single crystals. In the case of STS glass–ceramics (composition: $2SrO-3SiO_2-TiO_2$) we can also expect the properties of glass–ceramics to be similar to the properties of STS single crystals. In addition, we can expect the same anomalies in the dielectric, piezoelectric and pyroelectric properties of single crystals also.

The unusual features in all the properties of STS glass–ceramics suggest the possibility of a structural phase transition, since in most of the ferroelectric crystals structural changes are accompanied by anomalies in dielectric and related properties. In the absence of data about the properties of STS single crytals, it may be fruitful to compare the properties of STS glass–ceramics with those of BTS single crystals which show similar anomalies in properties [11]. In BTS single crystals, the sign of the pyroelectric coefficient is positive at room temperature and becomes negative at about 190° C. Sharp peaks in K_{33}, p_3 and k_p are observed at 160° C and a minimum is observed in resonance frequency at the same temperature. A single-crystal X-ray study [14] did not indicate any phase transition in BTS. The origin of the anomaly in the dielectric and related properties of BTS is thought to be related to anomalous behaviour of some of the elastic constants near 160° C [11], and, because of the coupling between elastic and other properties, this could also lead to anomalies in the piezoelectric and pyroelectric properties.

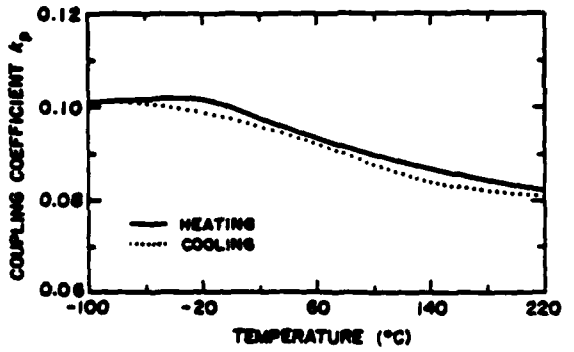

Figure 6 Variation of planar coupling coefficient k_p with temperature for $2SrO-3SiO_2-TiO_2$ glass–ceramic.

A comparison of the properties of BTS single crystals and STS glass–ceramics indicates that it is highly unlikely that there is a phase transition in STS in the temperature range −150° C to 200° C. In STS also the reason for the anomaly in all the properties might be anomalous behaviour of some of the elastic constants. However, a detailed measurement of the temperature dependence of all the elastic constants and thermal expansion coefficients is necessary to support the above assumption.

The pyroelectric coefficient p_3 of STS is positive in the temperature range −150° C to 200° C and shows a peak value of about 8 $\mu C\,m^{-2}\,K^{-1}$ at about −20° C. In BTS also, p_3 is positive at room temperature and the reason for this is that the secondary component of p_3 (p_{sec}) is larger than the primary component of p_3 (p_{prim}) at room temperature [15]. The calculated value of p_{sec} in BTS is about 16.5 $\mu C\,m^{-2}\,K^{-1}$. Unfortunately it is not possible to separate the primary and secondary effects in STS as the full family of elastic, piezoelectric and thermal expansion constants required to assess the secondary effect have not yet been measured.

In the case of both BTS single crystals and glass–ceramics, all the properties were exactly the same in both heating and cooling cycles and the anomalies occurred at the same temperature without any hysteresis [11]. In STS glass–ceramic, there is a large hysteresis in piezoelectric and pyroelectric properties and the anomalies occur at slightly different temperatures in heating and cooling cycles. The reason for this hysteresis in STS is not clear at present. Measurement of dielectric constant and pyroelectric coefficient with an applied bias electric field might help in understanding the origin of this unusually large hysteresis.

5. Summary

The present study demonstrates the usefulness of preparing polar materials by the glass–ceramic route. For several non-ferroelectric materials, which are difficult to prepare in single-crystal form and can be prepared easily as glasses, the polar glass–ceramic technique described in the present work can be used to assess the piezoelectric and pyroelectric effects in the crystalline phase. Ceramic samples of such materials will not be useful for studying the above properties since they cannot be poled by an external electric field. If it is possible to prepare glasses of the required material with minor modification in the composition, the technique of preparing glass–ceramics with oriented polar texture provides an alternative method to study the properties of such materials. In the case of $Sr_2TiSi_2O_8$ it was possible for the first time to obtain reliable data on both pyroelectric and piezoelectric properties, by the glass–ceramic technique.

Acknowledgements

We thank all our colleagues in the ferroelectrics group at MRL for their help in this work. This work was supported by the Army Research Office through Contract No. DAAG29-80-C-0008 and the National Science Foundation Grant No. DMR-8303906.

References

1. M. KIMURA, Y. FUJINO and T. KAWAMURA, *Appl. Phys. Lett.* **29**, (1976) 227.
2. M. KIMURA, *J. Appl. Phys.* **48**, (1977) 2850.
3. S. HAUSSUHL, J. ECKSTEIN, K. REICHER and F. WALLARAFEN, *J. Cryst. Growth* **40** (1977) 200.
4. H. YAMAUCHI, *J. Appl. Phys.* **49** (1978) 6162.
5. J. MELNGAILIS, J. F. VEACLINO, A. THUNJUNWALA, T. B. REED, R. E. FAHEY and E. STERN, *Appl. Phys. Lett.* **32** (1978) 203.
6. Y. ITO, K. NAGATSUMA and S. ASHIDA, *ibid.* **36** (1980) 894.
7. *Idem. Jap. J. Appl. Phys.* **20** (1981) 163.
8. A. HALLIYAL, A. S. BHALLA, R. E. NEWNHAM and L. E. CROSS, *J. Mater. Sci.* **16** (1981) 1023.
9. A. HALLIYAL, A. S. BHALLA and R. E. NEWNHAM, *Mater. Res. Bull.* **18** (1983) 1007.
10. A. HALLIYAL, A. SAFARI, A. S. BHALLA, R. E. NEWNHAM and L. E. CROSS, *J. Amer. Ceram. Soc.* **67** (1984) 331.
11. A. HALLIYAL, S. A. MARKGRAF, A. S. BHALLA, L. E. CROSS and R. E. NEWNHAM, *Ferroelectrics* in press.
12. R. L. BYER and C. B. ROUNDY, *Ferroelectrics* **3** (1972) 333.
13. A. SAFARI, PhD Thesis, The Pennsylvania State University, 1983.
14. S. A. MARKGRAF, A. HALLIYAL, A. S. BHALLA, R. E. NEWNHAM and C. T. PREWITT, *Ferroelectrics* in press.
15. A. S. BHALLA and R. E. NEWNHAM, *Phys. Status Solidi a* **58** (1980) K19.

Received 18 October
and accepted 22 November 1984

APPENDIX 6

Phase Transitions, Dielectric, Piezoelectric and Pyroelectric Properties of Barium Titanium Germanate $Ba_2TiGe_2O_8$ Single Crystals

A. Halliyal, A.S. Bhalla and L.E. Cross

Ferroelectrics 62, 3 (1985)

Ferroelectrics, 1985, Vol. 62, pp. 3–9
0015-0193/85/6201–0003/$15.00/0

PHASE TRANSITIONS, DIELECTRIC, PIEZOELECTRIC AND PYROELECTRIC PROPERTIES OF BARIUM TITANIUM GERMANATE $Ba_2TiGe_2O_8$ SINGLE CRYSTALS

A. HALLIYAL, A. S. BHALLA, and L. E. CROSS

Materials Research Laboratory, The Pennsylvania State University, University Park, PA 16802

(Received September 23, 1984; in final form December 10, 1984)

Measurement of the dielectric permittivity ϵ_{33}, the pyroelectric coefficient p_3 and the piezoelectric planar coupling k_p and frequency constant N_p in single crystal $Ba_2TiGe_2O_8$ show clear evidence of a heretofore unobserved first order phase change which occurs at $-50°C$ on cooling and near 0°C on heating. The balance of evidence suggests that the transition is to a reorientable but irreversible ferroelectric phase, involving a tilt of the prototypic polar c axis. The inversion of the sign of the pyroelectric effect reported earlier near 135°C is confirmed and is attributed to the changing balance between primary and secondary components in the pyroelectric coefficient.

INTRODUCTION

Barium titanium germanate ($Ba_2TiGe_2O_8$—hereafter designated BTG) was identified by Masse and Durif,[1] and also by Blasse[2] as having a structure similar to that of the mineral fresnoite $Ba_2TiSi_2O_8$ which has tetragonal $4mm$ symmetry. Single crystals of BTG have been grown both by Bridgman and Czochralski techniques.[3,4] Kimura *et al.*[3] have determined the crystal symmetry at room temperature to be orthorhombic $mm2$, with a peculiar long b-axis spacing which is reportedly $11 \times a_0$ (lattice constants: $a = 12.30$ Å, $b = 135.2$ Å, $c = 10.70$ Å). However, x-ray single domain data of Schmid and co-workers indicate orthorhombic symmetry ($a_{o.r.} \cong b_{o.r.} a_{tetr.}\sqrt{2} = 12.27$ Å, $c_{o.r.} = 5.35$ Å), whereas x-ray powder diffraction studies by Masse,[1] Guha,[5] and Gabalica–Robert and Tarte[16] reveal only the tetragonal pseudosymmetry ($a = 8.684 \pm 0.007$ Å, $c = 5.365 \pm 0.005$ Å[1]; $a = 8.68$ Å, $b = 5.37$ Å[5]; $a = 8.677(12)$ Å, $c = 5.364(10)$ Å[16]).

Kimura *et al.*[6] have also reported a solid state phase transition in BTG at 810°C, which they indicate reduces the point symmetry from $4mm$ to $mm2$ on cooling leading to a mimetically twinned ferroelastic structure. They confirmed ferroelasticity in the lower temperature phase by observing stress detwinning at 700°C under a uniaxial stress of 100 kg/cm^2. Disappearance of twin domains due to the application of stress implies the exchange of crystallographic axis a and b in some domains, with the appearance of the crystallographic b axis (which is the long axis) orthogonal to the compressive stress direction. By considering the possible ferroelastic species of $4mm$ prototype symmetry, the above workers pointed out the most probable ferroelastic species as $4mmFmm2$. It has also been reported that BTG has a large

electromechanical coupling factor in the thickness shear mode[3] ($k_{15} = 0.27$ and $k_{24} = 0.31$) and a small pyroelectric coefficient[4] ($p_3 = -4\ \mu C/m^2\ °K$) which reverses its sign at about 135°C. The pyroelectric coefficient increases sharply below room temperature, but in the above study, measurements were not carried out below 0°C. Measurements of the D-E relation and the temperature dependence of the dielectric constant did not indicate BTG to be ferroelectric for field applied along (*c*)[3] in the temperature range from −180 to 1200°C. No detailed studies have been reported on the temperature variation of piezoelectric properties.

The present work was undertaken to examine the dielectric, piezoelectric and pyroelectric properties of BTG single crystals in more detail. The above properties were studied as a function of temperature in the temperature range −150 to 200°C. The present studies indicated the occurrence of a new abrupt phase transition at about −25°C, which has not been reported earlier. In this paper, the probable reasons for the sign reversal of the pyroelectric coefficient at 135°C are discussed. The properties near the low temperature phase transition are examined in detail and the possible ferroic species resulting from this transition are considered.

CRYSTAL GROWTH AND MEASUREMENTS

Crystals for the present study were grown by the Czochralski pulling method from stoichiometric melts contained in a platinum crucible. Growth conditions were as follows: seed rotation speed 20 rpm; initial pulling rate 10 mm/hr; final pulling rate 2 mm/hr. Crystal boules of size 8–10 mm dia × 10–15 mm length were obtained by the above procedure. The resulting boules were colorless and transparent. *c*-plates were cut from the boule and circular samples of 5 mm dia and 0.5 mm thick were prepared. The major surfaces of the samples were coated with sputtered gold electrodes.

The dielectric constant and dissipation factors were measured at different frequencies using a capacitance bridge. Pyroelectric coefficients were determined by the Byer–Roundy[7] technique. The heating and cooling rates employed were 4°C/min. The electromechanical properties were determined by standard resonance techniques. All the above properties were measured as a function of temperature in both heating and cooling cycles. Piezoelectric d_{33} coefficients were measured using a Berlincourt—d_{33} meter. The hydrostatic voltage coefficient g_h was measured by a dynamic method described in Ref. 8.

RESULTS

The variation of the dielectric constant of a BTG single crystal with temperature, measured at 100 Hz, is shown in Figure 1. There is a small but abrupt jump in the dielectric constant in both heating and cooling cycles. The jump occurs at approximately −50°C in the cooling cycle and at 0° in the heating cycle. Surprisingly, no corresponding peaks were observed in the dissipation factor curve. The dissipation factor was less than 0.001 in the temperature range −140 to 200°C. The temperature dependence of the pyroelectric coefficient p_3 is shown in Figure 2. p_3 is negative at

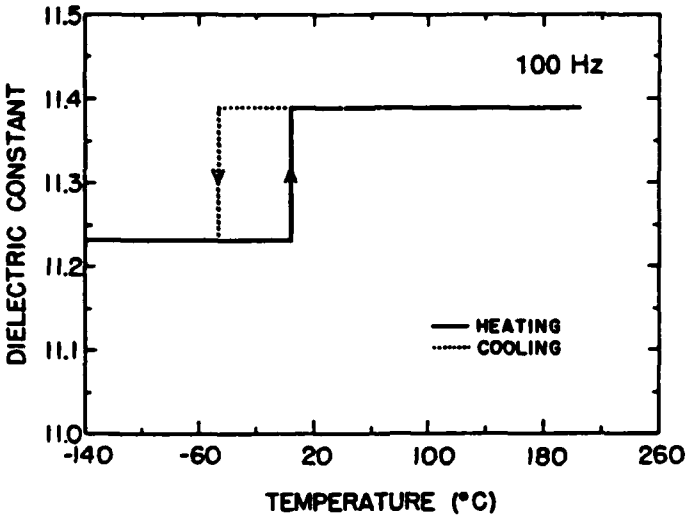

FIGURE 1 Dielectric constant of $Ba_2TiGe_2O_8$ single crystal as a function of temperature.

low temperature and decreases in magnitude with increasing temperature, crossing zero at 135°C. Above 135°C, the sign of p_3 is positive and increases slightly with temperature (similar results were reported by Schmid *et al.*[4]). Very strong peaks were observed in p_3 in both heating and cooling cycles at the same temperature where there were discontinuities in the dielectric constant. The peak value of the pyroelectric coefficient at about -50°C was about $-120\ \mu C/m^2$ °K. The variation

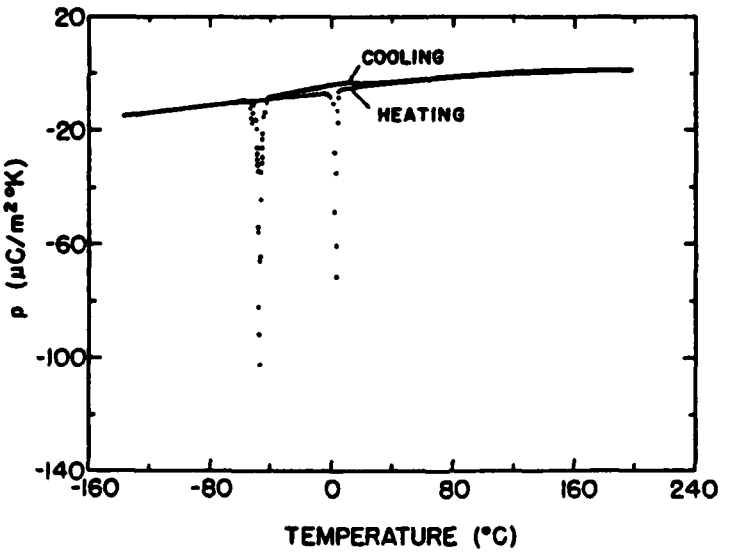

FIGURE 2 Variation of pyroelectric coefficient (p_3) of $Ba_2TiGe_2O_8$ single crystal as a function of temperature.

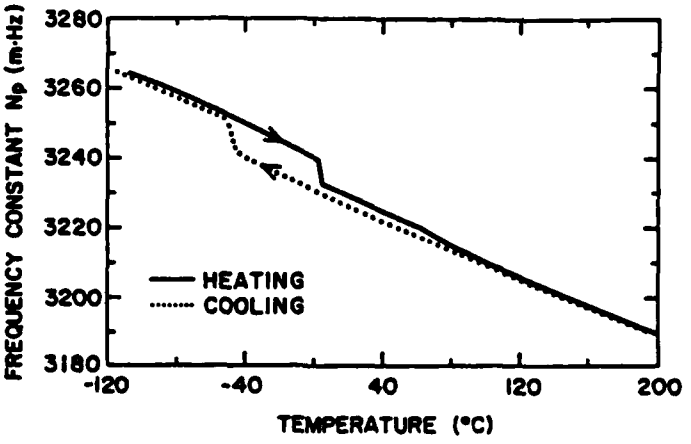

FIGURE 3 Frequency constant N_p of $Ba_2TiGe_2O_8$ single crystal as a function of temperature.

of planar frequency constants N_p and electromechanical coupling factor k_p are shown in Figures 3 and 4. Discontinuities were observed in both heating and cooling cycles, similar to the discontinuity in dielectric constant curve. It was clear that the discontinuities observed in the dielectric and piezoelectric properties were very small in comparison to the strong peaks observed in the pyroelectric coefficient curve. The reproducibility of the discontinuity in the above properties was tested by making measurements on several samples and by repeating the measurements several times on the same samples. The discontinuity in the above properties could be observed everytime with similar hysteresis. The room temperature properties of BTG are listed in Table I.

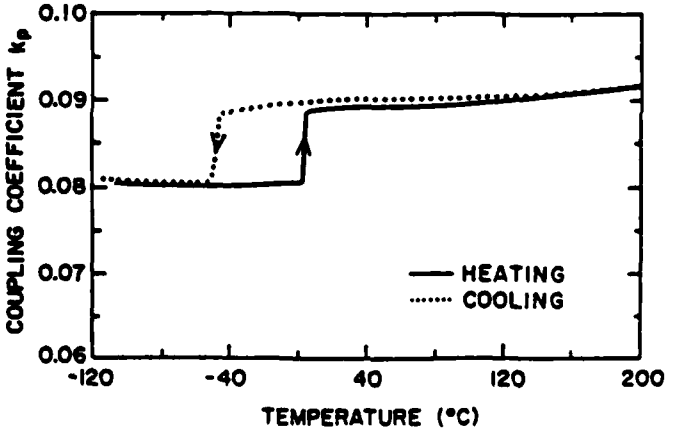

FIGURE 4 Electromechanical coupling coefficient k_p of $Ba_2TiGe_2O_8$ single crystal as a function of temperature.

TABLE I

Room temperature properties of $Ba_2TiGe_2O_8$[a]

Density (gm/cc)	4.84
K_{33} (1 k · Hz)	11.4
$\tan\delta$ (1 k · Hz)	< 0.001
Pyroelectric coefficient p_3 ($\mu C/m^2$ °K)	−4.0
d_{33} (pC/N)	8.0
d_{31} (pC/N)	2.0
d_h (pC/N)	12.1
g_{33} (10^{-3} Vm/N)	80
g_h (10^{-3} Vm/N)	120
$d_h g_h$ (10^{-15} Vm/N)	1450
Frequency constant N_t (m · Hz)	2150
Frequency constant N_p (m · Hz)	3200
k_p	0.09
Q (radial)	6000
TCR (ppm/°C)	60

[a]Data from the present study.

DISCUSSION

Unusual features in the properties of BTG crystals revealed in these studies may be summarized as follows:

(1) The pyroelectric coefficient p_3 which is negative at room temperature passes through zero at ~ 135°C and becomes positive at higher temperature.

(2) The sharp and intense peaks in p_3 at − 50° on cooling and at 0°C on heating suggest a first order phase change which involves a dicontinuous change of the polar magnitude p_3 in the crystal.

(3) The smaller but abrupt changes in ϵ_{33}, k_p and N_p at the same temperatures confirm that a phase change occurs.

To discuss the results intelligently, it is first necessary to determine the symmetries in the different phases. Best evidence would suggest that BTG is orthorhombic at room temperature in the ferroelastic species $4mmFmm2$ (Aizu[9,10]). Optical evidence of twins with the appropriate wall orientations in our crystals, taken together with the biaxial conoscopic figure in the high temperature phase would tend to confirm this mm2 assignment.

Additional species which are accessible from $4mm$ are $4mmFm$, $4mmF2$, and $4mmF1$ (Table II). Of these $4mmF2$ is ferroelastic, but $4mmFm$ and $4mmF1$ are both ferroelastic and divertable but irreversible ferroelectrics. Since the unique 2-fold axis of $mm2$ is preserved in the ferroelastic species it is unlikely that a major change of magnitude of P_3 would be involved in the change $mm2 \rightarrow 2$. For the species 1 and m, however, P_3 must tilt away from the 2-fold axis so that a first order change would give a finite step in P_3 and the large charge release observed. It may be noted that neither change will give rise to reversible polarity and ferroelectricity for the E field along the c axis E_3, but only for fields orthogonal to the original c axis.

Unequivocal evidence to distinguish m and 1 from 2 can be obtained by optical measurements on crystal sections parallel to the c axis, and these measurements are now in progress.

TABLE II

Ferroic species for prototype symmetries $4mm$ and $mm2$

Prototype symmetry	Possible aizu species	Property
$4mm$	$4mmF1$ $4mmFm$	Ferroelectric and Ferroelastic
	$4mmF2$ $4mmFmm2$	Ferroelastic but not Ferroelectric
$mm2$	$mm2F1$ $mm2Fm$	Ferroelectric and Ferroelastic
	$mm2F2$	Ferroelastic but not Ferroelectric

We believe that the balance of evidence suggests that BTG may be a divertable but irreversible ferroelectric at temperatures below $-50°C$ with symmetry in point group 1 or m.

For the pyroelectric sign change, there is no evidence of phase change near 135°C and we believe that the change is due to a competition between primary and secondary components of p_3, as in $Li_2SO_4 \cdot H_2O$,[11] $Ba(NO_2)_2 \cdot H_2O$,[12] $Ba_2TiSi_2O_8$[13] and $(NH_4)_2SO_4$[14]. Unfortunately, it is not yet possible to separate primary and secondary effects in BTG as the full family of elastic, piezoelectric and thermal expansion constants required to assess the secondary effect has not yet been measured.

If as in fresnoite, $Ba_2TiSi_2O_8$, the secondary effect p_{sec} is positive,[15] then in BTG the primary effect must be negative and must dominate at lower temperatures. This would not be inconsistent with a low temperature phase in which P is tilted from the c axis. Since the tilt angle will be in the nature of an order parameter for this phase, it will decrease with increasing temperature, reducing the normal decrease of P and thus the normally negative p_3 primary.

We speculate that at 135°C the secondary and primary pyroelectric coefficients are equal and that above this temperature, the secondary effect dominates, but more detailed measurements are needed to verify this hypothesis.

ACKNOWLEDGMENTS

We thank all our colleagues in the ferroelectrics group at MRL for their help in this work. This work was supported by the Army Research Office through Contract =DAAG29-80-C-0008 and the National Science Foundation Grant No. DMR-8303906.

REFERENCES

1. R. Masse and A. Durif, *Bull. Soc. Fr. Min. Cryst.*, **90**, 407 (1967).
2. G. Blasse, *J. Inorg. Nucl. Chem.*, **30**, 2283 (1968).
3. M. Kimura, K. Doi, S. Nanamatsu and T. Kawamura, *Appl. Phys. Lett.*, **23**, 531 (1973).
4. H. Schmid, P. Genequand, H. Tippmann, G. Pouilly and H. Guedu, *J. Mat. Sci.*, **13**, 2257 (1978).

5. J. P. Guha, *J. Amer. Ceram. Soc.*, **60**, 246 (1977).
6. M. Kimura, K. Utsumi and S. Nanamatsu, *J. Appl. Phys.*, **47**, 2249 (1976).
7. R. L. Byer and C. B. Roundy, *Ferroelectrics*, **3**, 333 (1972).
8. A. Safari, Ph.D. Thesis, The Pennsylvania State University (1983).
9. K. Aizu, *Phys. Rev. B*, **2**, 754 (1970).
10. K. Aizu, *Phys. Rev.*, **146**, 423 (1966).
11. S. B. Lang, *Phys. Rev. B*, **4**, 3603 (1970).
12. V. V. Gladkii and I. S. Zheludev, *Sov. Phys. Cryst.*, **10**, 50 (1965).
13. A. Halliyal, *et al.*, *Ferroelectrics* (to be published).
14. N. Yamada, *J. Phys. Soc. Jpn.*, **46**, 561 (1974).
15. A. S. Bhalla and R. E. Newnham, *Phys. Stat. Sol. (a)*, **58**, K19 (1980).
16. M. Gabelica-Robert and P. Tarte, *Phys. Chem. Minerals*, **7**, 26 (1981).

APPENDIX 7

Piezoelectric Properties and Microstructure of Glass-Ceramics in the BaO-SrO-SiO_2-TiO_2 System

E.E. Ylo III, M. Wheeler, A. Halliyal,
A.S. Bhalla and R.E. Newnham

(To be published in IEEE Proc. of International Symposium on Application of Ferroelectrics, Bethlehem, 1986)

A. Halliyal

PIEZOELECTRIC PROPERTIES AND MICROSTRUCTURE OF GLASS-CERAMICS IN THE BaO-SrO-SiO$_2$-TiO$_2$ SYSTEM

E.E. Ylo III, M. Wheeler, A. Halliyal, A.S. Bhalla, and R.E. Newnham

Materials Research Laboratory, The Pennsylvania State University, University Park, PA 16802 USA

Abstract

Previous studies have shown that fresnoite ($Ba_2TiSi_2O_8$) glass-ceramics with oriented crystallites are promising candidate materials for pyroelectric detectors and surface acoustic wave devices. A detailed investigation of the properties and microstructure of glass-ceramics in the $Ba_{2-x}Sr_xTiSi_2O_8$ solid solution has been carried out. Glasses of several compositions were prepared and recrystallized through a heating schedule to produce an oriented region of crystallites perpendicular to the surface, 100-500μm in depth. The microstructure of the glass-ceramics was examined by scanning electron microscopy. Their dielectric and piezoelectric properties were studied.

1. Introduction

In the recent past, a new technique for preparing glass-ceramics with oriented crystallites of a polar phase has been investigated with the objective of fabricating inexpensive, large area sensor elements for application in pyroelectric detectors and piezoelectric devices[1-4]. Through a suitable thermal process, glass is converted to a glass-ceramic consisting of a grain-oriented polar crystalline phase in a glassy matrix. The macroscopic polarity thus developed gives rise to both piezoelectric and pyroelectric activity with markedly different properties from those of poled ferroelectric ceramics. Earlier studies have shown that these glass-ceramics are promising materials for piezoelectric resonators[2], hydrophones[5,6], pyroelectric devices[7], and surface acoustic wave (SAW) substrates[6].

Several glass-forming polar materials have been prepared in glass-ceramic form. Some of the systems studied include Li_2O-SiO_2, Li_2O-SiO_2-B_2O_3, BaO-SiO_2-TiO_2, BaO-GeO_2-TiO_2, and SrO-SiO_2-TiO_2. Among the crystalline phases recrystallized from the glasses are $Li_2Si_2O_5$, $Li_2B_4O_7$, $Ba_2TiSi_2O_8$, $Sr_2TiSi_2O_8$, and $Ba_2TiGe_2O_8$. One or more of these polar phases are obtained in the glass-ceramic, depending on the composition of the glass. The compositions of the glasses were optimized by compositional variations to obtain glass-ceramics with good physical properties[2,5].

Fresnoite ($Ba_2TiSi_2O_8$) single crystals are promising as SAW substrates, with its SAW properties intermediate between those of $LiNbO_3$ and $LiTaO_3$[9,10]. Modified fresnoite glass-ceramics have also been shown to be viable candidate materials for hydrophones[5,6] and SAW devices[6].

Recently, Ito and coworkers[11,12] have shown that the temperature coefficient of delay (TCD) of fresnoite single crystals can be lowered through the partial substitution of strontium for barium. Crystals of composition $(Ba_{2-x}Sr_x)TiSi_2O_8$ with uniform Sr concentration can be grown by edge-defined film-fed growth (EFG), for the compositions ranging from x= 0 to 0.8. Z-cut crystals with a strontium concentration of x= 0.8 gave a TCD value of 20 ppm/°C with practically no reduction in the SAW coupling coefficient(k_s^2), and look to be very useful for SAW devices.

In compositions with x≥ 1.0, $SrSiO_3$ and $SrTiO_3$ also crystallize along with the fresnoite phase, making it impossible to grow pure strontium titanate silicate single crystals by the usual crystal growing techniques. However, x-ray diffraction studies on

ceramic samples indicated that all compositions with x= 0 to 2.0 prepared by conventional ceramic processing techniques give single-phase fresnoite-type structure. The results indicated that Sr substituted for Ba, and a complete solid solution for the ceramics occurred.

In the present work, polar glass-ceramics in the $Ba_2TiSi_2O_8$-$Sr_2TiSi_2O_8$ solid solution system were prepared by recrystallizing the glasses. The microstructure, dielectric, and piezoelectric properties of these glass-ceramics are presented in this paper. Surface acoustic wave properties will be reported later.

2. Experimental Details

Glasses of compositions (2-x)BaO-xSrO-0.15CaO-2.9SiO_2-TiO_2 with x= 0.0, 0.2, 0.6, 1.0, 1.4, 1.8, 2.0 were prepared. Reagent grade $BaCO_3$, $SrCO_3$, $CaCO_3$, $SiO_2 \cdot nH_2O$, and TiO_2 were mixed by ball milling in an alcohol medium, and the mixture was dried. The batch was then melted in a platinum crucible in a globar furnace at 1430°C for 6-10 hours. The glass was poured into a graphite mold to form pellets about 1 cm in diameter and 7 cm thick. Glass samples were annealed at 500°C, well below the nucleation temperature to avoid bulk nucleation.

The typical heat-treatment cycle employed for crystallizing glasses is shown in Figure 1. The temperature was increased up to 500°C slowly and held there for one hour to avoid thermal shock. Then the temperature was raised to the crystallization temperature (950°C) quickly to minimize bulk nucleation. Glasses were crystallized at 950°C for two hours and cooled to 800°C, where they were held for six hours to anneal the glass-ceramics. The glass-ceramics were then slowly cooled to room temperature.

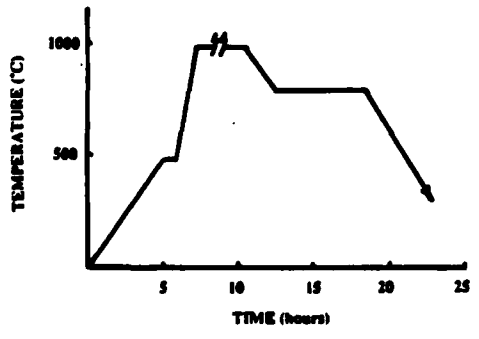

FIGURE 1 Recrystallization schedule for Ba-Sr fresnoite glass-ceramics.

To examine the microstructure of the glass-ceramics, samples were polished and etched with 2% HF solution to reveal the oriented growth of crystallites. The samples were then studied using a scanning electron microscope.

For dielectric and piezoelectric measurements, samples in the form of circular disks, having dimensions of about 10 mm in diameter and 0.5 mm thick, were prepared by sectioning the oriented portion of the glass-ceramics. Gold electrodes were sputtered on the polished surfaces. The dielectric constants were calculated by measuring the capacitance of the samples using an LCR bridge*. The piezoelectric constant d_{33} parallel to the crystal growth direction was measured with a d_{33}-meter**. Electromechanical coupling factor was measured by the gain-bandwidth method as described by Holland and EerNisse[13].

3. Results and Discussion

SEM micrographs of selected glass-ceramic samples are shown in Figure 2. The length of the crystallites in the oriented region varied between 100 to 500 μm, with the length being less in glass-ceramics containing higher Sr concentration. Also, a slight curvature in the growth of the crystallites was observed in Sr-rich glass-ceramics.

The variation of the dielectric and piezoelectric properties of glass-ceramics with mole fraction of SrO is shown in Figures 3-6. The dielectric constant, K_{33}, is in the range 10 to 16, with the dissipation factor remaining very low near 0.1 %. As for the piezoelectric d_{33} coefficient, the range is 4 to 16 pC/N, with the composition 0.2BaO-1.8SrO-0.15CaO-2.9SiO_2-TiO_2 showing the highest d_{33}. This composition has a high piezoelectric g_{33} voltage coefficient (110 x 10^{-3} Vm/N) compared to PZT ceramics because of its low dielectric constant. The planar coupling coefficient, k_p, decreases with SrO whereas the planar frequency constant, N_p, is about 3500 m-Hz for all compositions.

* Hewlett-Packard 4274A LCR Meter
**Berlincourt d_{33}-meter, Channel Products (Model CPDT 3300)

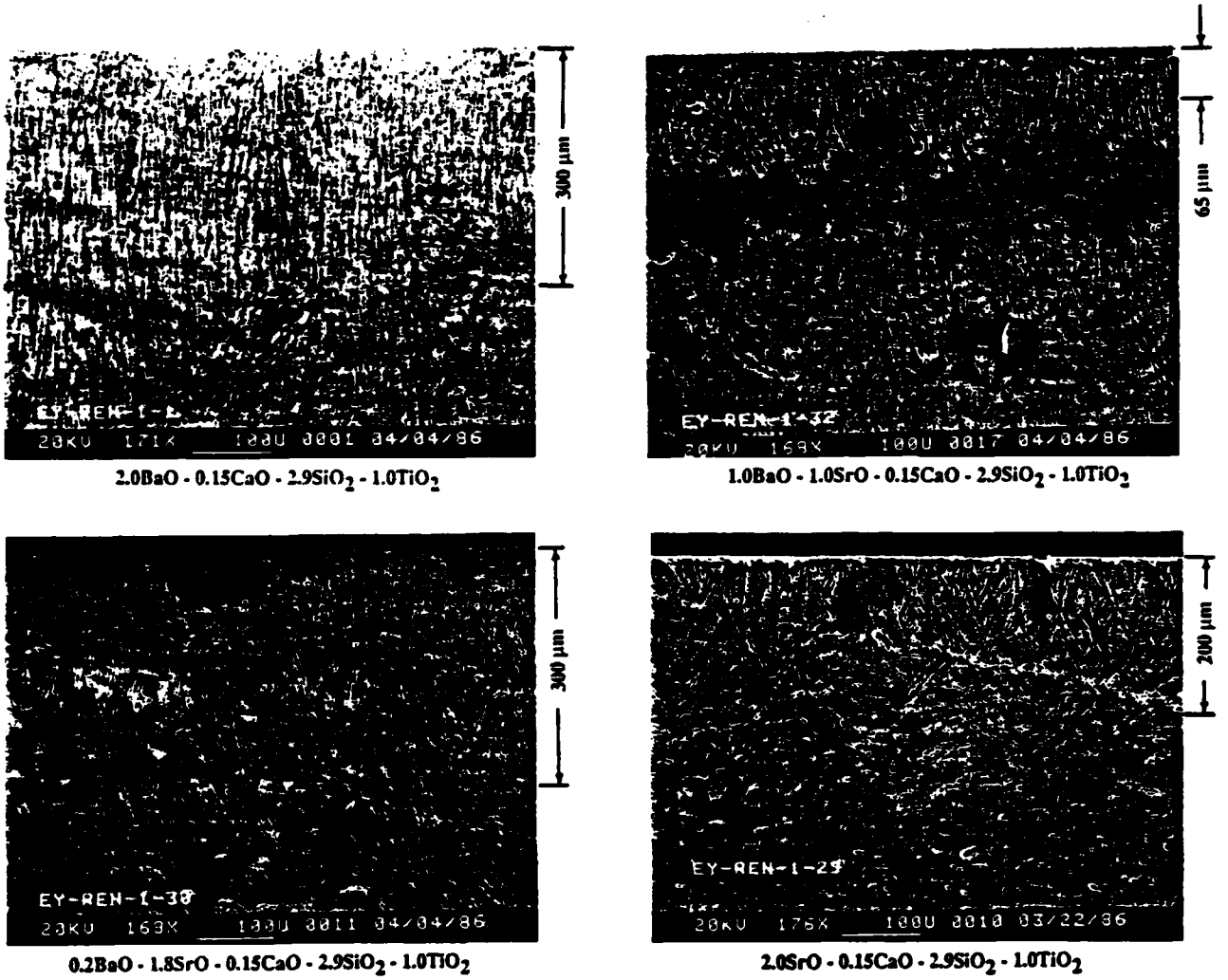

FIGURE 2 SEM micrographs of the oriented region in Ba-Sr fresnoite glass-ceramics.

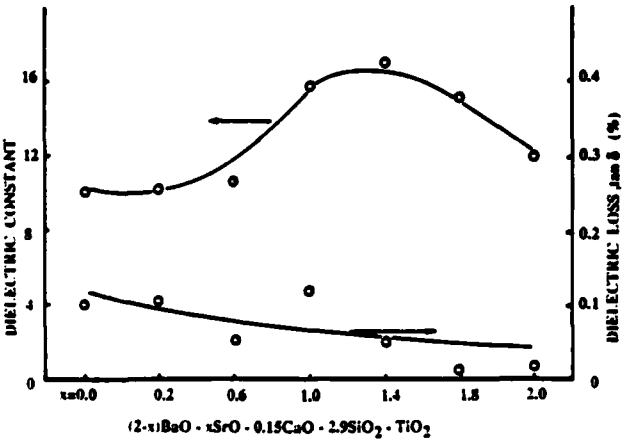

FIGURE 3 The dielectric constant, K_{33}, and the dissipation factor for Ba-Sr fresnoite glass-ceramics (1 kHz, room temperature).

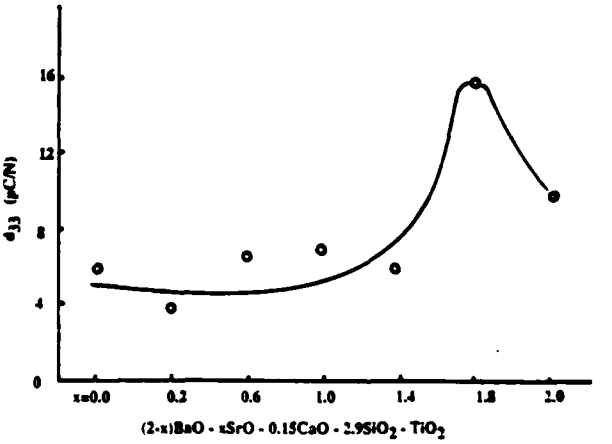

FIGURE 4 The piezoelectric constant, d_{33}, for Ba-Sr fresnoite glass-ceramics.

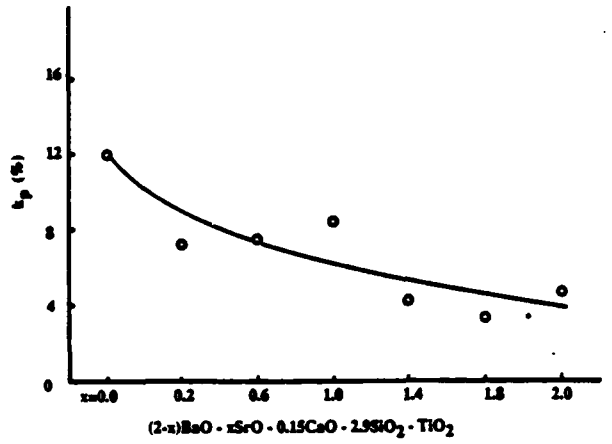

FIGURE 5 The planar coupling coefficient, k_p, for Ba-Sr fresnoite glass-ceramics.

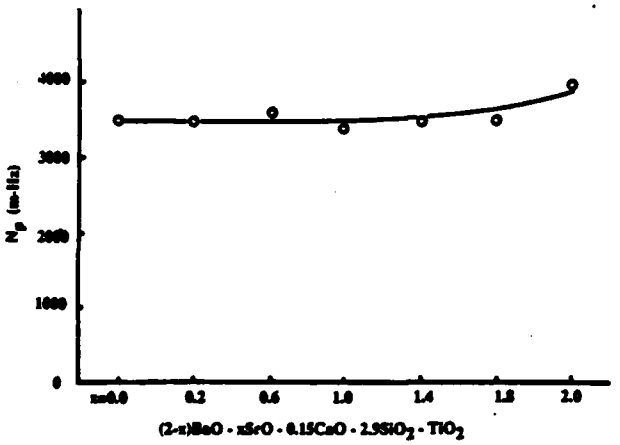

FIGURE 6 The planar frequency constant, N_p, for Ba-Sr fresnoite glass-ceramics.

From the present study, it is clear that we can prepare polar glass-ceramics in the fresnoite system, by replacing Ba with Sr, in the entire solid solution range. Although the length of the oriented crystallites and the planar coupling coefficient decrease with the addition of Sr, the piezoelectric d_{33} coefficient increases.

The surface acoustic wave properties of fresnoite glass-ceramics of composition 2.0BaO-0.15CaO-2.9SiO2-TiO2 have been reported[8]. This composition showed a SAW coupling coefficient of 1.1 % and a temperature coefficient of delay of 60 ppm/°C. In $Ba_{2-x}Sr_xTiSi_2O_8$ single crystals, a decrease in the TCD has been observed with the addition of Sr. We can expect a similar behavior in the modified fresnoite glass-ceramics. The surface acoustic wave properties of polar glass-ceramics in the Ba-Sr fresnoite system will be reported in the future.

4. Summary

Glass-ceramics in the $Ba_{2-x}Sr_xTiSi_2O_8$ solid solution have been prepared. The length of the oriented regior ranged between 100 to 500μm; glass-ceramics with higher Sr concentration had crystallites that exhibited curvature. The piezoelectric d_{33} coefficients were in the range 6 to 16 pC/N, and the planar coupling coefficients were in the range 12 to 6 %. The composition 0.2BaO-1.8SrO-0.15CaO-2.9SiO2-TiO2 showed a high piezoelectric g_{33} voltage coefficient (110×10^{-3} Vm/N). These glass-ceramics are useful for SAW devices.

Acknowledgments

This work was supported by the National Science Foundation Grant DMR-8303906.

REFERENCES

1. G.J. Gardopee, R.E. Newnham, and A.S. Bhalla, Ferroelectrics 33, 155 (1981).
2. A. Halliyal, A.S. Bhalla, and R.E. Newnham, and L.E. Cross, IEEE Ultrasonics Symposium, 315 (1981).
3. A. Halliyal, A.S. Bhalla, and R.E. Newnham, L.E. Cross, and T.R. Gururaja, J. Mater. Sci. 17, 295 (1982).
4. A. Halliyal, A.S. Bhalla, and R.E. Newnham, Mat. Res. Bull. 18, 1007 (1983).
5. A. Halliyal, A. Safari, A.S. Bhalla, R.E. Newnham, and L.E. Cross, J. Am. Ceram. Soc. 67, 331(1984).
6. R.Y. Ting, A. Halliyal, and A.S. Bhalla, Appl. Phys. Lett. 44, 852 (1984).
7. A. Halliyal, A.S. Bhalla, L.E. Cross, and R.E. Newnham, J. Am. Cer. Soc. (submitted).
8. C.W. Lee, L.J. Bowen, J.M. Browne, A. Halliyal, A.S. Bhalla, and E. Ylo,III, Proc. IEEE Ultrasonic Symposium, 285 (1984).
9. H. Yamauchi, J. Appl. Phys. 49, 6162 (1978).
10. J. Melngailis, J.F. Veaclino, A. Thunjunwala, T.B. Reed, R.E. Fahey, and E. Stern, Appl. Phys. Lett. 32, 203 (1978).
11. Y. Ito, K. Nagatsuma, and S. Ashida, Appl. Phys. Lett. 36, 894 (1980).
12. Y. Ito, K. Nagatsuma, and S. Ashida, Jap. J. Appl. Phys. 20, 163 (1981).
13. R. Holland and E.P. EerNisse, Trans. on Sonics and Ultrasonics 16, 173 (1969).

END

DTIC

9-86